AD-A012 292

POBAL-S, THE ANALYSIS AND DESIGN OF A HIGH ALTITUDE AIRSHIP

Jack D. Beemer, et al

Raven Industries, Incorporated

Prepared for:

Air Force Cambridge Research Laboratories

15 February 1975

AD-A012292

AFCRL-TR-75-0120

POBAL-S, THE ANALYSIS AND DESIGN OF A HIGH ALTITUDE AIRSHIP

Jack D. Beemer
Roger R. Parsons
Loren L. Rueter
Paul A. Seuferer
LaDell R. Swiden

Raven Industries, Incorporated
205 East Sixth Street
Sioux Falls, South Dakota 57101

15 February 1975

Final Report for Period October 1972 - March 1975

Approved for public release; distribution unlimited

AIR FORCE CAMBRIDGE RESEARCH LABORATORIES
AIR FORCE SYSTEMS COMMAND
UNITED STATES AIR FORCE
HANSCOM AFB, MASSACHUSETTS 01731

Unclassified
Security Classification

AD-A012 292

DOCUMENT CONTROL DATA - R & D

(Security classification of title, body of abstract and indexing annotation must be entered when the overall report is classified)

1. ORIGINATING ACTIVITY (Corporate author) Raven Industries, Incorporated 205 East Sixth Street Sioux Falls, South Dakota 57101	2a. REPORT SECURITY CLASSIFICATION Unclassified 2b. GROUP

3. REPORT TITLE

POBAL-S, THE ANALYSIS AND DESIGN OF A HIGH ALTITUDE AIRSHIP

4. DESCRIPTIVE NOTES (Type of report and inclusive dates)
Scientific Final for Period October 1972 - March 1975

5. AUTHOR(S) (First name, middle initial, last name)
Jack D. Beemer (principal author), Roger R. Parsons, Loren L. Rueter, Paul A. Seuferer, LaDell R. Swiden

6. REPORT DATE 15 February 1975	7a. TOTAL NO. OF PAGES 184	7b. NO. OF REFS 23
8a. CONTRACT OR GRANT NO. F19628-73-C-0076 b. PROJECT NO. 6665-10-01 c. 62101F d. 686665	9a. ORIGINATOR'S REPORT NUMBER(S) R-0275006 9b. OTHER REPORT NO(S) (Any other numbers that may be assigned this report) AFCRL-TR-75-0120	

10. DISTRIBUTION STATEMENT

Approved for public release; distribution unlimited.

11. SUPPLEMENTARY NOTES	12. SPONSORING MILITARY ACTIVITY Air Force Cambridge Research Lab. Hanscom AFB, Massachusetts 01731 Contract Monitor: Arthur O. Korn/LCB

13. ABSTRACT

An engineering analysis and development effort has been executed to design a superpressure airship, POBAL-S, capable of station keeping at an altitude of 21 kilometers for a duration of 7 days while supporting a payload weighing 890 newtons and requiring 500 watts of electrical power. A detailed parametric trade-off between various power sources and other design choices was performed. The computer program used to accomplish this analysis is described and many results are presented. The system concept which resulted was a fuel cell powered, propeller driven airship controlled by an on-board autopilot with basic commands telemetered from a ground control station. Design of the balloon, power train, gimbaled propeller assembly, and electronic/electrical systems is presented. Flight operations for launch and recovery are discussed.

PRICES SUBJECT TO CHANGE

DD FORM 1 NOV 65 1473

Unclassified
Security Classification

Unclassified
Security Classification

14. KEY WORDS	LINK A		LINK B		LINK C	
	ROLE	WT	ROLE	WT	ROLE	WT
Airship						
Balloon						
Balloon film material						
Powered balloon						
Power sources						
Remotely piloted vehicle						
Superpressure balloon						

Security Classification

CONTENTS

CONTENTS

FIGURES

Page

FIGURES

1. INTRODUCTION

Considerable effort has been expended during the last several years in the development of unmanned high altitude station keeping vehicles. Such vehicles are airborne platforms capable of loitering above a specific location or geographic area on the earth while maintaining a high altitude. These vehicles have applications encompassing military, civil, and scientific uses. Examples of vehicle concepts include drones, RPV's (Remotely Piloted Vehicles), flying wings, microwave beamed power vehicles, synchronous stationary satellites (not airborne), free floating balloons, tethered balloons, and powered balloons. This report is intended to concentrate on powered balloons. A brief discussion of balloon concepts follows.

Many studies of tethering balloons at altitudes in excess of 18,000 meters (60,000 feet) have been performed. The primary problem associated with this concept is the procurement of a lightweight, high strength tether cable which would make such a system design feasible. Present developments are centered on the use of Kevlar fibers for a dielectric cable. The high cable tensions and system performance characteristics are extremely difficult to predict because of the great changes in the relative wind conditions imposed on such a system. Thus, the primary disadvantage of the tethered balloon concept is the required direct link between the balloon and the ground.

Three types of free floating balloon systems have been studied. One study addressed the problem of setting up and maintaining a network of superpressure balloons such that from a statistical standpoint one of the balloons would be within a specified area for a certain percentage of the time.[1] The actual study looked more closely at the problem of a communications network instead of a down-looking reconnaissance type balloon, but the problems are similar. The disadvantage of this type of system is the obviously high number of balloons required and initial costs which would be incurred. Once the network is developed, then an on-going balloon replenishment program could be set up to maintain the network. One of the main advantages of this type of system is the simplicity of the individual vehicles.

[1]Winker, J. A., High Altitude Relay Platform System, Report No. 0669011, Raven Industries, Inc. Final Report, Contract 4691, Task Order 18. 15 May 1969.

The second type of free floating balloon concept utilizes a balloon floating in the stratosphere between 15 kilometer (50,000 feet) and 21 kilometer (70,000 feet) where easterly winds would prevail during much of the year.[2] To attain a loitering capability a reefable parachute would be lowered to a level where westerly winds would exist. In this way the parachute would act as a variable drag device such that a force balance between the balloon and the parachute would be attained so that no horizontal motion would exist. This type of system is entirely dependent upon proper wind conditions existing. This drastically reduces the operational capabilities of the system because of the dependence of the system upon the specific wind conditions. Thus such a system can only be used for a few months of each year.

The third type of station keeping free floating balloon is a concept which has actually been demonstrated and used.[3,4,5] This involves ballasting and valving to attain a reasonable degree of altitude changing and altitude control so that wind directions and speeds could be altered. This type of station keeping concept has been rather limited in duration because the mission generally needs to be terminated shortly after all the ballast is used up. Other limitations of this concept include its dependence upon proper wind conditions existing and of being able to find these advantageous wind fields.

---

[2]Bourke, Edgan R. II, "Addenum To Presentation On a Unique Approach to Balloon Station Keeping", Raytheon Company. Presented at Earth Observations From Balloons Symposium, American Society of Photogrammetry. Published by Raytheon Company. 7 February 1969.

[3]Nolan, George F., High Altitude Minimum Wind Fields and and Balloon Applications, AFCRL 64-843, Air Force Cambridge Research Laboratories, 1964.

[4]Nolan, George F., A Study of Mesoscale Features of Summertime Minimum Wind Fields in the Lower Stratosphere, AFCRL 67-0601, Air Force Cambridge Research Laboratories, 1967.

[5]Nolan, George F., "Meteorological Considerations for Tethered and Hovering Free Balloons", Air Force Cambridge Research Laboratories. Symposium Proceedings, Earth Observations From Balloons, American Society of Photogrammetry. February 1969.

The work performed under this contract was to result in a design of a superpressure airship capable of an airspeed of 8.18 meter/second (15.9 knot) at an altitude of approximately 21 kilometer (70,000 feet) for a 7 day duration with a payload weighing 890 newton (200 pounds) requiring 500 watts of power continuously.* A major task under this POBAL-S program focused on the specific system design. The completeness of the design was limited by the availability of funds.

Prior to entering into a specific design of a selected system type, a parametric investigation of various system concepts was performed.[6] The various power sources which were investigated included internal combustion engines, fuel cells, batteries, and solar cells.

The system concept which was chosen utilized a fuel cell as the power source. The parametric analysis revealed that the fuel cell powered system would be cost effective and reliable as a demonstration vehicle capable of meeting the performance specifications.

---

*Originally the speed requirement was 10.3 m/s (20 kn) and no power was to be allocated to the payload. During the course of the contract the speed requirement was reduced to 8.18 m/s (15.9 kn) and the payload power requirement was defined as 500 W continuous power. The effort reported on in Section 4.0 uses the original speed and payload power requirements. The design discussed in Section 5.0 uses the newer requirements.

[6]Beemer, Jack D., et al., POBAL-S, R & D Design Evaluation Report, Part I, System Concept Choice, Report No. 0273001, Raven Industries, Inc. Air Force Cambridge Research Laboratories Contract No. F19628-73-C-0076. 23 February 1973.

2. DEVELOPMENT OF HIGH ALTITUDE POWER BALLOONS

The first serious study of the high altitude station keeping powered balloon concept was performed by General Mills, Inc. during the late 1950's.[7] This study described a powered airship which was to carry a payload of 440 to 1320 N (100 to 300 lb) to an altitude of 18 to 24.5 km (60,000 to 80,000 ft) for a duration of 1 to 8 hours. The Mechanical Division of General Mills, subsequently absorbed by Litton Industries, carried out a considerable amount of additional analysis after its Lighter-Than-Air Concepts Study was published. In 1967 Litton discontinued ballooning activities.

Since the first efforts performed by General Mills there was little actual work done until after 1965. At this time Goodyear Aerospace Corporation began work in this subject area which resulted in a report entitled An Investigation of Powered, Lighter-Than-Air Vehicles.[8] This work was performed under the sponsorship of the Air Force Cambridge Research Laboratories. Two basic concepts were studied in this report. The first was an aerodynamically shaped airship which could be flown to and from the 21 km (70,000 ft) design altitude, and the second was a natural shape balloon which only operated at the design altitude. For the second concept at termination of the mission the payload and power plant were to be parachuted back to earth.

The first hardware constructed and used in the manner of a high altitude station keeping vehicle was fabricated by Goodyear Aerospace Corporation.[9] The propulsion system consisted basically of a propeller at one end of a gondola and a rudder at the other. The gondola orientation, or heading, and the rudder position were telemetered to the ground along with other monitored flight information. The rudder position was changed by radio command to make the gondola point in the proper direction. This system was not demonstrated to be

[7] Anderson, A. A., et al., Lighter-Than-Air Concepts Study, Report No. 1765, General Mills, Inc. Final Report, Contract 1589 (07). 1 September 1957. Revised, March 1960.

[8] Vorachek, Jerome J., Investigation of Powered Lighter-Than-Air Vehicles, GER 14076, Goodyear Aerospace Corporation. AFCRL-68-0626, Final Report, Air Force Cambridge Research Laboratories, Contract No. F19628-67-C-0047. 27 November 1968.

[9] High Altitude Powered Balloon Test Program, Report No. BB-2304, Goodyear Aerospace Corporation. November 1968.

controllable. It was likely that it was not controllable because of aerodynamic considerations and because an autopilot was not incorporated into the system.

The next effort pertinent to high altitude station keeping vehicles was performed by Raven Industries during 1969 and 1970.[10] This was the High Platform II program under which the first high altitude, solar powered, autopiloted airship was successfully demonstrated. The main purpose of this program was to actually demonstrate, at a moderate cost, that a practical high altitude (21 km or 70,000 ft altitude), long duration, station keeping vehicle could be built.

The High Platform II vehicle itself was only a sun seeking vehicle and had a cadmium sulfide solar cell array placed on the balloon envelope such that when the vehicle was oriented toward the sun enough power would be supplied to propel the balloon at a design speed of 10.3m/s (20 kn). Also, the vehicle could only be used for daytime operation since batteries, which would have been necessary for nighttime operation, were not a part of this system. This superpressure balloon was configured with a propeller suspended underneath it on a gondola and was controlled with both moving and stationary horizontal and vertical statilizing surfaces. High Platform II was flown in May of 1970.

The next activity which was initiated was the High Platform III Design Study performed by Raven Industries.[11] This was a paper study contract which resulted in a final report describing a preliminary design for a system having a four month operating duration at an altitude of 25.5 km (85,000 ft) with a capability of maintaining a continuous 7.7 m/s (15 kn) air speed. This paper study also generated a limited amount of parametric trade-off analysis information. Of particular importance, this analysis revealed that there was no advantage to utilizing altitude control to minimize the stress levels in the envelope by driving the vehicle up or down with a positive or negative angle of attack respectively.

---

[10]Beemer, Jack D., et al., High Platform II, Report No. R-0870025, Raven Industries, Inc., Final report, Contract 4691, Task Order 22. 14 August 1970.

[11]Beemer, J.D., et al., High Platform III Design Study, Report No. 0871005, Raven Industries, Inc., Final Report, Contract 5831. 31 August 1971.

The airship designed under the High Platform III Design Study had a volume of 17,000 m^3 (600,000 ft^3). The envelope length was 94 m (309 ft) and had a fineness ratio of 5.0. It was to be powered with cadmium sulfide solar panels which furnished the necessary electrical power to an electric motor driving a gimbaled propeller which was mounted on the tail of the airship. The horizontal and vertical stabilizing surfaces were to be pressurized with air and the envelope itself was fabricated from a biaxially oriented nylon film. One of the unproven assumptions used in the design of High Platform III was that a pulse charging technique could be used to increase the number of charging cycles available from the battery. Another assumption was that the nylon film would in fact be developed into a successful superpressure balloon material. The High Platform III Design Study was completed in August 1971.

Shortly after the High Platform III Design Study was completed, the Air Force Cambridge Research Laboratories issued an RFP for a free balloon propulsion system. The basic goal of the system was to keep an 880 N (200 lb) payload on station at a nominal altitude of 18 km (60,000 ft) for a 24 hour duration. The method of accomplishing this was to utilize altitude control on the balloon such that it could be propelled through a minimum wind field. Goodyear Aerospace Corporation was awarded the contract under this effort.[12] In September, 1972, the Goodyear free balloon propulsion system was flown from Holloman Air Force Base. The system consisted of a natural shape balloon from which a battery powered, electric motor driven propeller was suspended. This system was to have a 24 hour duration, 12 hours of which was to be under powered flight. The nominal thrust required by the propeller was 445 N (100 lb). Due to mechanical failure, the flight of this system was terminated with less than 6 hours of powered flight. During this time it was demonstrated that although the concept was feasible, problems of instability were present.

Because of the sensitivity of station keeping vehicle size, mass, and power requirements for various mission parameters, it was felt necessary to have a general overview of the concept of superpressure high altitude station keeping

---

[12] Vorachek, Jerome J., Edward W. McGraw, John W. Bezbatchenko, Development of a Free Balloon Propulsion System, Goodyear Aerospace Corporation. AFCRL TR-73-0128, Final Report, Air Force Cambridge Research Laboratories, Contract No. F19628-72-C-0072. April 1973.

airships. Thus, the Study of High Altitude Station Keeping Vehicles was performed by Raven Industries.[1] This resulted in a final report in March, 1973. It was under this study contract that the HASKV computer program was written to parametrically analyze various system concepts. Also, a vehicle capable of operating at 21 km (70,000 ft) for a few months duration with an average speed of 10.3 m/s (20 kn) carrying a 880 N (200 lb) payload was designed, and the results were presented in the final report.

Under the Study of High Altitude Station Keeping Vehicles Raven Industries utilized its own in-house expertise in electonic systems, superpressure balloon technology, and mechanical hardware design. However, an extensive literature search and subsequent vendor contact effort was spent to gain knowledge of the primary power sources and electric motor. More than seventy companies and organizations active in thermal electric generators, solar cells, fuel cells, batteries, turbine engines, reciprocating engines, and rotary piston engines were solicited for information pertinent to the study. With the information thus gained, it was possible to enter into a parametric analysis in which all vehicle components could be parametrically defined. The parametric work performed showed very clearly the great advantages of using a superpressure balloon material stronger than polyester film and the necessity of using solar power for such extended mission durations.

It was during this latter study contract that the POBAL-S project was begun. The remainder of this report summarizes the work performed under the POBAL-S program and presents the design of the POBAL-S airship.

[1] Beemer, Jack D., et al., Study of High Altitude Station Keeping Vehicles, Report No. 0373003, Raven Industries, Inc., Advanced Research Projects Agency Order No. 1983 Final Report. 15 March 1973.

3. REVIEW OF CONCEPT DESIGNS

This section of the report discusses the various aspects of the balloon system design. The intent is to provide a simplified description of the system components. This will be beneficial in understanding the vehicle design and will aid in understanding the computer program. The readers attention is called to Section 5. of this report for a more detailed description of the fuel cell powered airship. The types of vehicle concepts which were studied are shown in Figure 3.1.

3.1 Balloon Vehicle

For the aerodynamic shaped balloon systems, only balloon designs utilizing conventional high altitude superpressure spherical balloon technology were considered in the parametric analysis. This type of balloon has normally been constructed from polyester film laminates. The purpose of lamination is to prevent helium leakage due to pin holing, while the polyester film itself has very low permeability to helium and very high strength characteristics. The use of such materials allows the balloon envelope to be pressurized to a level such that at nighttime, when the radiation conditions may result in the balloon temperature being less than ambient temperature, the balloon will still be superpressured. If the pressure in the balloon goes below ambient pressure, the balloon will go slack and descend in altitude. Typically the duration of superpressure balloons is measured in terms of months, and several balloons have flown well in excess of 400 days. These long durations can be accomplished because it is not required that ballast be used to retain altitude throughout the nighttime.

Variations in material types, density, and acceptable stress levels have been considered in the parametric analysis. Ideas which have been considered include the use of high strength fibers laminated between layers of the balloon film to increase the film strength-to-weight ratio and applying to the film a thermochromic coating which exhibits transitional optical absorption and reflectance characteristics which could possibly help control the supertemperature. These approaches are not believed to be feasible for use with this type of balloon. Technological improvements in superpressure balloon materials will likely be accomplished in the near future, but the higher stressing limits which have been studied parametrically should encompass such improvements.

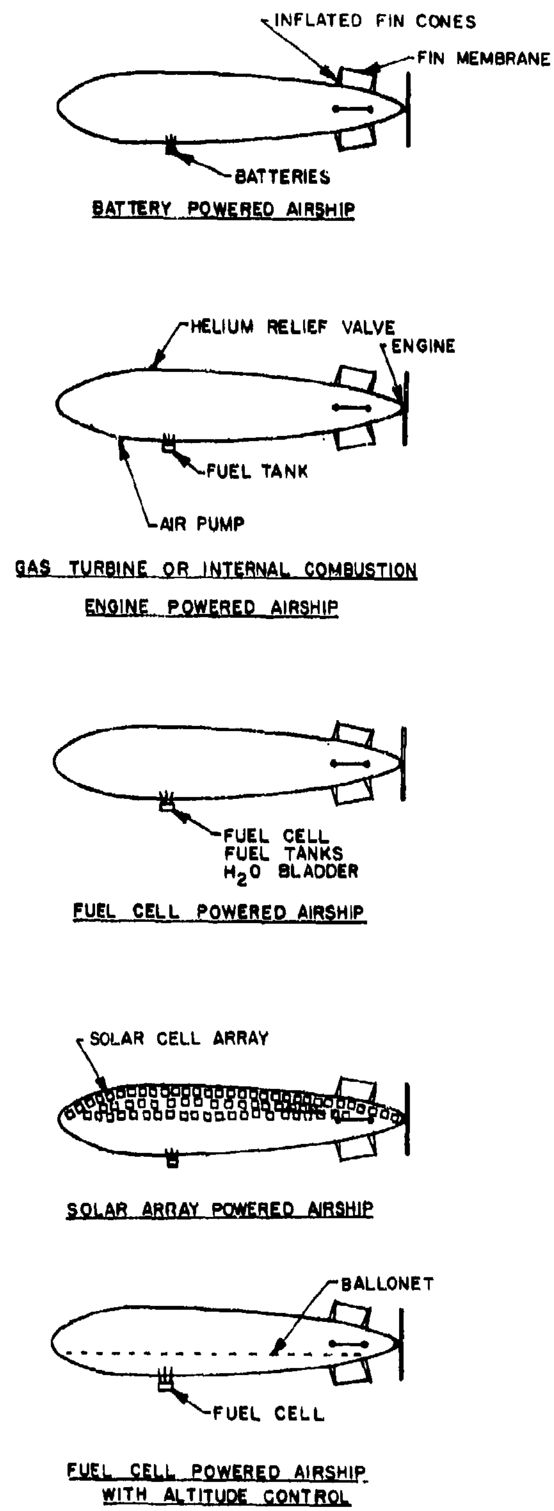

Figure 3.1 Vehicle concepts analyzed.

The balloon vehicle itself is defined to include the envelope, the fins or stabilizing surfaces and any attachment hardware. The basic shape is assumed to be that of a Navy Class C airship with a fineness ratio of 5.0. Other fineness ratios have been investigated and it has been determined that near-optimum system design will occur within the range of fineness ratios of 5.0 to 7.0.[11,14]

The stabilizing surfaces are assumed to be constructed from air pressurized conical shaped beams (two for each surface) with an impermeable membrane stretched between. (Refer to Figure 5.1 for a detailed sketch of the system.) The beams would be pressurized by use of a very small, low power consumption air compressor. In this way the integrity of the primary envelope is retained and minimal departure from conventional superpressure balloon technology is accomplished.

3.2 Airship Propulsion and Control

The propulsion and gimbal assembly includes the motor or engine for propulsion and the mechanical hardware required to pitch and yaw the propeller. (Refer to Figures 5.3, 5.4, 5.17.) The actual thrust is derived by use of a propeller. The gimbaling mechanism itself is designed using roll nuts and screws powered by small electric motors to provide two-degree freedom of movement for the propeller. The control of the airship is thus accomplished by changing the propeller position by electronic signals provided by an autopilot so that the vehicle will remain within acceptable limits in pitch and yaw. A very important component of the system is the speed reducer which allows the propeller to operate at much slower angular velocity than does the motor or engine powering it. Experience has shown that belt drive systems are highly efficient and acceptable for the use as contemplated here.

3.3 Power Source

The primary variation between system concepts was in the power source used to drive the propeller. In the parametric study the solar cell array, fuel cell, gas turbine, internal combustion engine, batteries, and advantageous wind fields were analyzed. Two of these sources, the solar cell array

[14] Rueter, Loren L., "Drag Analysis for POBAL-S & HASKV High Altitude Airships", informal paper, Raven Industries, Inc., 10 October 1972.

and the advantageous wind fields, utilize ambient energy sources. All other types analyzed either burned fuel or generated their own emf (electromotive force). The solar cell array, fuel cell, and gas turbine powered concepts received the most attention in the analysis. Wankel and Diesel engines were the only two internal combustion engines studied, and parametrically they are quite similar to the gas turbine in concept.

The concept of using only primary batteries for power has been analyzed; and, as anticipated, because of system size it does not appear feasible except for very short duration missions. The advantages of such a concept lie in the simplicity of the design since all that is required is the batteries, mounted somewhere in front of the system center of gravity, with power cables running back to an electric motor.

The gas turbine and internal combustion engine concepts are very similar. These power sources would actually be mounted on the gimbal arrangement and gimbaled as with the electric motor for the electrical type systems. The fuel would be located near the front of the airship so that horizontal stability could be attained. Under this scheme it would not be possible to save the consumed fuel, and consequently a ballonet or pumping and valving scheme must be integrated into the system. The advantage of this type of system as compared to the fuel cell system is that the fuel can be stored in conventional type tanks. Considerations in final system design would have to be given to pumping the fuel from the storage area to the combustion chambers.

The fuel cell powered concept is similar to the solar powered concept in that it provides electrical power to a gimbaled motor/propeller arrangement. The water generated by the fuel cell would be stored and not disposed of. The advantages of storing the water is that the system mass remains constant during operation. Thus, the floating altitude and static trim angle of the airship will not change during the flight. Also, this allows the fuel to be located at that position along the balloon which is required to attain horizontal equilibrium when the system is shut down. The fuel cell concept also requires that the additional heat generated by the fuel cell be radiated. It may be possible to make use of this waste heat in controlling negative supertemperatures, but if one were to shut the system down at night then this heat would not be present. Thus, the system would have to be designed as if this capability were non-existent.

For the solar powered concept, the panels of cells, which are integrated to make the array, are placed on the surface of the balloon envelope and are located so that adequate power is delivered to the system for any conceivable sun angle. All individual panels would have to be diode-isolated so that those which are greater than 1.57 radians (90 degrees) from the sun would not act as loads on the rest of the panels. Major attention needs to be paid to the current/voltage characteristics of the cells at various angles to the sun. These characteristics are temperature dependent, and under the configuration used here each panel would be operating at a different temperature because of radiation effects. The panels are connected either in series or parallel and are electrically integrated. Thus, they form an electrical energy source which will provide the required system power to operate the motor during the daylight hours and, at the same time, charge the batteries which are used for nighttime operation.

The use of advantageous wind fields was analyzed only in the sense that trade-offs between utilizing altitude control and not using altitude control were compared. Without the capability of changing altitude, the use of advantageous wind fields would not be feasible for this system. The most significant problem with this concept is determining where the winds are most favorable. To date, no acceptable wind sensing mechanisms are known to exist which could be applied to this type of system.

3.4 Electrical & Electronic Systems

Early in this study four different electrical systems were analyzed. The electronic requirements were virtually the same for all concepts. The term "electronics" as used herein includes navigation, command and control, stability control (autopilot), and telemetry.

The navigation unit provides the autopilot with the required error signals based on deviations from the desired station. The command and control assembly provides various switching and housekeeping functions when given commands from either on-board or radio command systems. The autopilot controls the direction of the airship to maintain stable flight. The telemetry system provides the down-link to the command station and provides system and flight evaluation and control data. Each of these systems will be discussed in further detail in Section 5.4.

A stand-by power source is provided and intended for use only if the main power source should experience a failure. The back-up battery powers vital control functions for 24 hours in case of a primary system failure. This would permit attempted restarts and trouble shooting with the option of terminating the flight at a time which best facilitates recovery.

All electrical systems use electric gimbal motors for directing the thrust vector of a propeller. The autopilot must have sufficient power, proper voltage, and correct dynamic characteristics to operate these motors.

The electrical systems were fit into four categories; pure battery, fuel cell, solar cell array, and combustion engine. All systems concepts except the combustion engine systems use an electric propulsion motor having conductors running from a control package, near the center of the balloon, to the motor at the stern. These wires carry the heaviest current in the system over the longest distance and must have very low impedance.

The simplest system, electrically, is a primary (nonrechargeable) battery for the basic power source. The computer inputs for this system were based on using lithium-organic batteries for the main power source and regulating only the electronics supply voltage. Figure 3.2 is a simplified block diagram for a primary battery system.

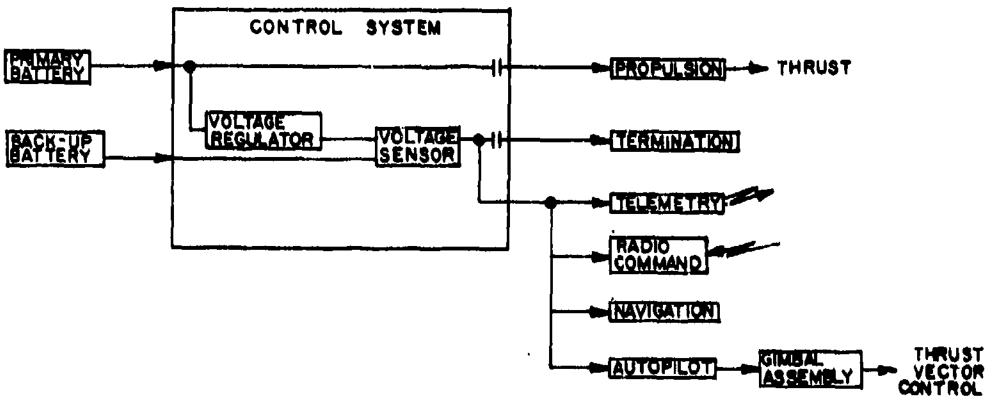

Figure 3.2 Battery system block diagram.

The power distribution for the combustion engine system is actually two systems, both supplied by the same alternator. An electrical system similar to that in an aircraft is used for ignition and starting. A second power system is used for electrical and electronic control systems. The mass of the secondary battery for this system is based on silver-zinc battery characteristics. Figure 3.3 is a simplified block diagram showing the increased complexity.

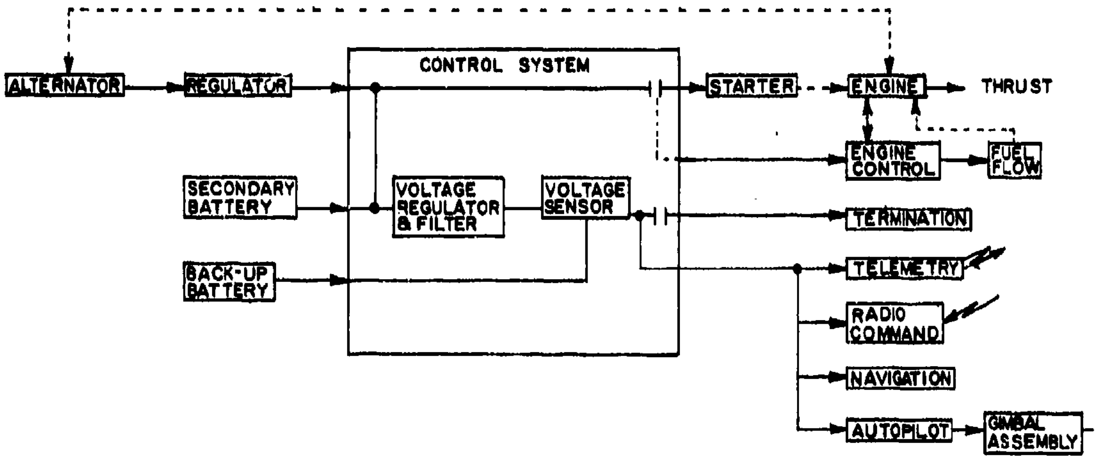

Figure 3.3 Combustion engine systems block diagram.

As explained in Section 4.3, the fuel cell system concept was chosen for this study effort. A simplified block diagram of the fuel cell electrical system is shown in Figure 3.4. The power losses in the control package of a fuel cell system are low since the propulsion power is adequately regulated by the fuel cell. The optimum voltage for this system was determined to be 30 volts.

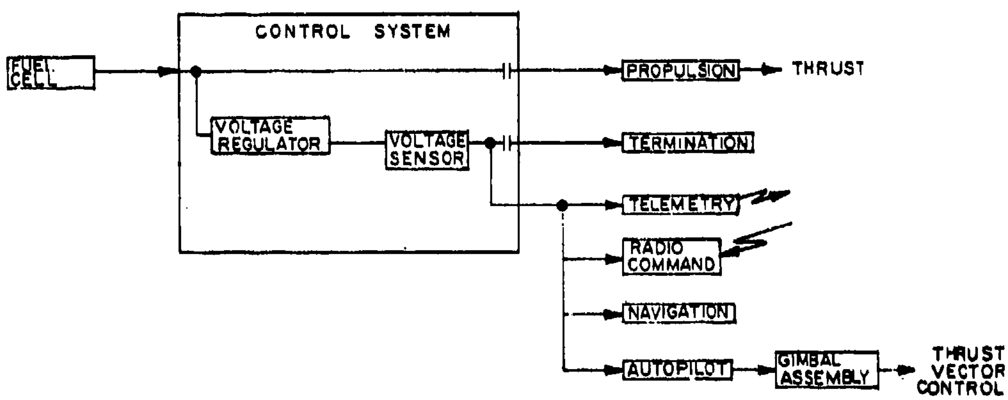

Figure 3.4 Fuel cell system block diagram

The solar cell array system is the most complicated system considered; however, it also has a greater endurance than the other systems. The primary mass contribution comes from the rechargeable battery which was assumed to be made up of silver-zinc cells. One fact learned during this study was that when short days are encountered sizing of the storage battery is determined from limits of charging current rates based upon energy storage efficiency. Silicon solar cell data were used to compute solar array mass. Due to the amount of power conditioning required in a solar cell array system, efficiency of the power distribution system is lower than the other concepts. A considerable number of electrical connections and wires are required in a solar powered system, making it more difficult to fabricate and launch. Figure 3.5 is a simplified block diagram of a solar cell system. The increased complexity over previous systems appears within the control system.

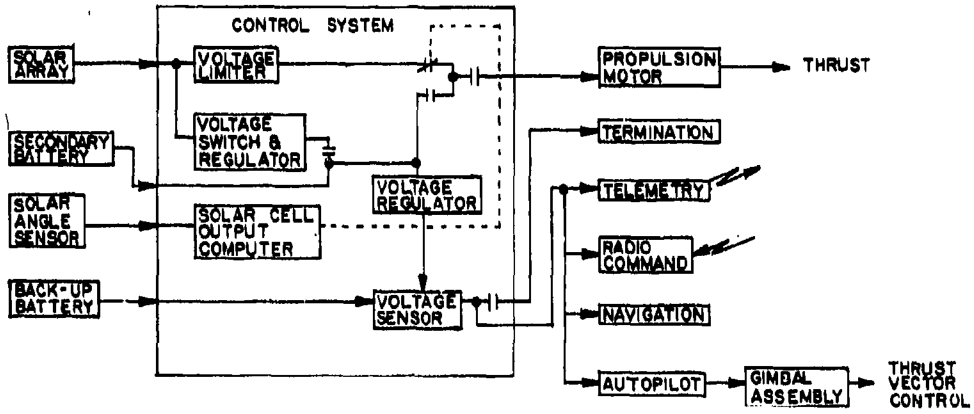

Figure 3.5 Solar array system block diagram.

4. SYSTEM CONCEPT CHOICE ANALYSIS

A significant portion of the effort under this contract was expended in studying system types and choosing one type for a complete design. This analysis was performed prior to the finalization of system performance requirements and is intended to be a tool for comparison purposes only. This section describes the methods of analysis and presents the results.

4.1 Computer Program

A detailed computer program, HASKV, was used to generate parametric information describing the system designs. A copy of the program and program output examples are included in Appendix A. The HASKV program was developed as an analytical aid in evaluating high altitude station keeping vehicles.[13] It is a versatile yet detailed program. The program can perform calculations involving the vollowing items:

1. Fifty-seven input parameters (constants for parametric equations).

2. Class C aerodynamic shape and natural shape balloons

3. Six different power sources:

   a. Gas turbine
   b. Wankel engine
   c. Diesel engine
   d. Fuel cell
   e. Solar cell array
   f. Battery

4. Altitudes from 16.5 km (54,000 ft) to 30.0 km (98,200 ft) in 1.5 km (5,000 ft) increments

5. Altitude control - 1.5 km (5,000 ft) or 3.0 km (10,000 ft) excusion

6. Wind speeds from 2.574 m/s (5 kn) to 15.44 m/s (30 kn) in 2.574 m/s (5 kn) increments

7. Mission time variation

8. Balloon diameters up to 200 m (660 ft)

Basically the program determines a system size which is capable of lifting the required mass. Required mass is a function of input conditions such as altitude, type of power source, wind speed, etc. It includes hull mass, payload mass, and all component masses required to power the system. For a given set of conditions, a plot of lifting capability versus system size, and a plot of required mass versus system size could be generated. These plots for a hypothetical set of conditions are shown below as a function of balloon radius:

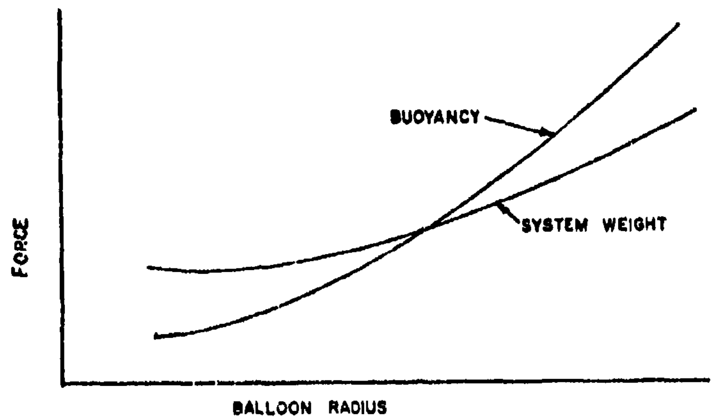

Figure 4.1 Hypothetical system weight and buoyancy versus balloon size.

A unique solution (R') is obtained if the two curves intersect. HASKV performs an iteration on balloon radius until the lifting mass equals the required mass. Output data generated by the program is then printed.

4.1.1. Flow Chart

A simplified flow chart of the HASKV computer program is shown in Figure 4.2. Literal phrases are substituted for mathematical expressions as an aid in discussing the program logic. Actual parametric equations are discussed separately.

4.1.1.1 Initialized Data. Variables that are a function of altitude are stored in the main program as arrays. Each element of the array corresponds to a fixed altitude and can be referenced by the main program. This decreases the amount of input required. Air density, helium lift, and pressure ratio are stored for all altitudes. In addition, standard

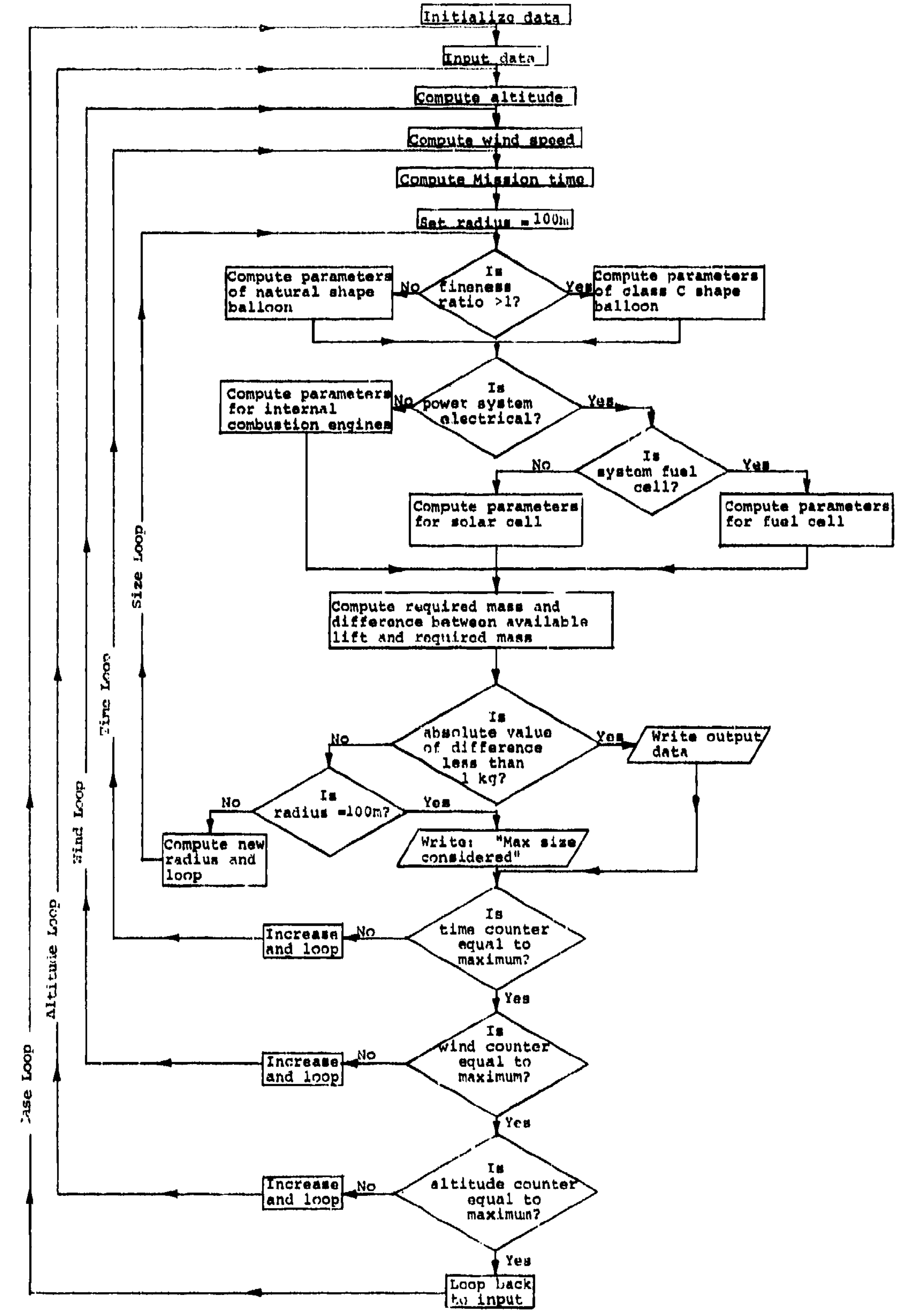

Figure 4.2 HASKV computer program flow chart.

sea level pressure and air density are stored.

4.1.1.2 Input Data. Necessary inputs include a heading, 57 input parameters and control cards. The heading may consist of a short phrase indicating the purpose of a run. If no more data are to be read, the program terminates.

The input parameters are used in the parametric equations as constants and are supplied as input variables so that effects of different choices can be analyzed. An example would be skin density per unit thickness. Since the skin density is an input variable, a system using a polyester envelope can be compared directly with one using a nylon envelope. All other parameters remain the same and the parametric equations are still valid. The large number of parameters which can be varied makes the program a powerful analytical tool.

Control cards supply information to the program regarding type of power source, altitude, wind speed, length of mission, and whether altitude control is or is not to be used. In the case of altitude, wind speed, and mission time, the card supplies initial value, maximum value, and the increment between each printing of output data. These control values are applied to the loop counters of the altitude loop, wind loop, and the time loop. Computer time is saved by analyzing specific ranges of interest without generating needless amounts of data.

Control cards may be stacked. After all loop counters have reached their maximum value specified by the present control card, a new control card is read. This enables different power sources, or altitude control versus no altitude control, to be run with the same input parameters. Each time a control card is read the heading, all input parameters with values, and the type of power source used are printed. If no more control cards are to be read, a new heading is read, new input parameters are read, and new control cards are read. When the input is exhausted, i.e., no new heading card, the program is terminated.

4.1.1.3 Altitude, Wind Speed, and Mission Time. These three variables are computed as a function of their respective loop counters. The general form is:

Variable = constant + second constant x counter.

All counters are whole numbers. Thus, altitude is computed as:

15,000 m + 1,500 m x altitude counter.

Initial value, maximum value, and the increment for each loop counter is specified by the control card. Each time the loop is executed, the loop counter is increased by the increment specified. The time loop is executed first, then the wind loop, and last, the altitude loop. Thus, each altitude increment lists data for each increment of wind and each wind increment list data for all time increments. Whenever these three values are calculated, they are printed.

4.1.1.4 Balloon Parameters. The program determines which balloon type is to be used by checking the fineness ratio. This ratio is included in the input parameter list. If the fineness ratio is greater than one, parameters for a Class C shape are calculated. Natural shape parameters can be calculated if the fineness ratio is less than or equal to one. No natural shape calculations were made for POBAL-S.

Such physical parameters as volume, surface area, skin thickness, and hull mass are computed by parametric equations. Data from the input parameter list and the current values of loop variables are utilized. This marks the beginning of the size loop or iteration loop. Consequently, the majority of the equations in this group are a function of balloon radius. At this point, net lift and power required for the balloon size being considered are computed.

4.1.1.5 Power Source Parameters. A decision must be made by the program as to which parametric equations are to be used. This is done by checking the value of K. It is the first parameter specified by the control card. K values and the corresponding power sources are:

Internal Combustion Systems:

1 Gas turbine
2 Wankel
3 Diesel

Electric Systems:

4 Fuel Cell
5 Solar cell array
6 Battery

All internal combustion engines use the same parametric equations. The variations are accounted for in the input parameter list. If K is less than or equal to 3, the internal combustion equations are used. For K greater than 3, the component masses common to the electrical systems are computed. These include the speed reducer and motor. A second check is then made on K. If K is less than 5, fuel cell parametric equations are used. If K is equal to 5, solar array parametric equations are used. For K greater than 5, parametric equations for a pure battery system are used.

The parametric equations of this group compute component masses for the power system. Included are equations for motor mass, fuel mass, battery mass, etc. These equations are functions of the power required computed earlier in the program.

4.1.1.6 Test for Solution. Required mass can now be computed by summing all the component masses for the power source, and payload. A difference is obtained by subtracting required mass from net lifting mass. If the absolute value of the difference is less than one kilogram, the present values are taken as solution values and printed. If this difference is greater than one kilogram, a check is made on the radius. If the radius is less than 100 m, a new radius is computed. The program loops back and computes new balloon and power parameters. Iteration continues within the size loop until a solution is found. If the solution has a radius equal to or greater than 100 m, "maximum size considered" is printed.

4.1.1.7 Time, Wind, and Altitude Loops. After output is printed, whether maximum size or solution data, the time loop counter is checked. If it is less than the maximum value specified by the control card, the counter is incremented as specified. The program loops back, calculates a new mission time, and begins a new iteration. After the time loop counter reaches the maximum value specified, a similar check is made on the wind loop counter. It is incremented and loops until it reaches the specified maximum value. The process is then repeated for the altitude loop counter. After all loops have been completed, the program loops back and reads new input. With each new input, the loops are executed in turn until they have been completed. Program termination occurs when all input data are exhausted.

4.1.2 Program Nomenclature

The following is a list of variable names used in the computer program. They are listed according to function in alphabetical order. Brief descriptions are included and appropriate units are indicated.

Initialized Data:

HLIFT Helium Lifting Mass Versus Altitude Array; kg/m^3

PRESR Pressure Ratio Versus Altitude Array

RHO Air Density Versus Altitude Array; kg/m^3

SPRES Standard Pressure at Sea Level; N/m^2

SRHO Standard Air Density at Sea Level; kg/m^3

Loop Counters:

IA Altitude Iteration

IAC Increment of Altitude Control

IT Time Iteration

K Integer for Power Source

KWD Wind Speed Iteration

Input Loop Variables: (Integers)

Altitude Iteration - Alt = 16,500 to 30,000 by 1,500, IA = 1 to 10; meters

IIA Initial Altitude

MIA Max Altitude

NIA Number of Altitude Increments Each Loop

Wind Iteration - VWind = 5 KN to 30 KN, KWD = 1 to 6

IWD Initial Wind Speed

MWD Max Wind Speed

NWD Number of Wind Increments Each Loop

Day or Hour Loop - Days = 1 to 10, IT = 1 to 10, HRN = 1 to 24, IT = 1 to 24

IIT Initial Time

MIT Max Time

NIT Number of Time Increments Each Loop

Input Parameters:

ADDM1 Additional Mass - Control Package, Diffuser, etc. Gas Turbine; kg

ADDM2 Additional Mass - Control Package, Regulator, etc., Fuel Cell; kg

ADDM3 Additional Mass - Control Package, Regulator, etc., Solar Array; kg

ADHE Bilaminate Adhesive Mass/Unit area; kg/m^2

AUTOM Autopilot Mass; kg

BASTM Ballast Mass for Natural Shape Balloon

BAT1 Battery Mass/Unit Energy (Out), Primary Battery; kg/kW-hr

BAT2 Secondary Battery Cell Mass/Cell Voltage - Corrected for Packaging; kg/V

BATCC Secondary Battery Capacity - Corrected for Cycle Life; kA

BATCY Secondary Battery Capacity - Corrected for Cycle Life; kA-hr

BCHEF Battery Charging Efficiency

BENGY Back Up Energy (kW-hr)

CD	Drag Coefficient
CELL1	First Order Constant for Fuel Cell Mass; kg/V
CELL2	Second Order Constant for Fuel Cell Mass; kg/V^2
CFCM	Constant Fuel Cell Mass; kg
CMM1	Constant Engine Mass - Gas Turbine; kg
CMM2	Constant Motor Mass - Electric Motor; kg
CSTRM	Constant Structure Mass; kg
DUTY	Ratio of Fuel Cell Operation Time to Mission Time
ECPB	Efficiency of Control Package - Battery
ECPPS	Efficiency of Control Package - Power Source
ECPSS	Efficiency of Control Package - Subsystem
ESPR	Speed Reducer Efficiency
EM	Motor Efficiency
EPROP	Propeller Efficiency
F	Free Lift/System Weight
FIN	Fineness Ratio
FINMR	Fin Mass Ratio of Envelope Mass
GEOF	Geometry Factor for Solar Array
GLC	Gore Length Constant
PAYM	Payload Mass; kg
PNBYPD	Ratio of Power Required at Night to That of Day
PROP	Propeller Mass/Unit Radius Length; kg/m
RAD	Radiator Mass/Unit Power (Out) - Fuel Cell; kg/kW
SA	Solar Array Mass/Unit Power (Out); kg/kW

SFC1 Specific Fuel Consumption - Gas Turbine; kg/kW-hr

SFC2 Specific Fuel Consumption - Fuel Cell; kg/kW-hr

SKIND Mass Density of Envelope Material; $kg/m^2/mm$ of Thickness

SKINR Ratio of Average Skin Thickness to Maximum Skin Thickness for an Envelope Constructed of Multiple Thicknesses

SMAT Stress Allowable for Envelope Material; N/m^2

SPR Speed Reducer Mass/Unit Power (Out); kg/kW

STRMR Structure Mass Ratio; kg

SUBPOW Independent Subsystem Power Required; kW

SUPERT Supertemperature/Absolute Temperature

TERMM Mass of Termination, Telemetry, and Navigation Packages

TMR1 Tank Mass Ratio - Gas Turbine; kg

TMR2 Tank Mass Ratio - Fuel Cell; kg

TURBOR Turbocharger Compression Ratio

UFLM Fuel Line Mass/Unit Length - Gas Turbine; kg/m

UMM1 Engine Mass/Unit Power Out - Gas Turbine; kg/kW

UMM2 Motor Mass/Unit Power Out - Electric Motor; kg/kW

VOLTFC System Voltage - Fuel Cell

VOLTSA System Voltage - Solar Array

WIRE1 Wire Mass/Unit Length - Turbine to Battery; kg/m

WIRE2 Wire Mass/Unit Length - Turbine, Autopilot to Gimbals; kg/m

WIRE3 Wire Mass/Unit Length - Kiloamp, Control Package to Motor; kg/kW/kA

WIRE4 Wire Mass/Unit Power - Interconnecting Wire - Solar Array; kg/kW

WIRE5 Wire Mass/Unit Length - Solar Array to Control Package; kg/m

Computed Variables:

ALENG Length of Balloon; m

ALIFT Available Lifting Mass; kg

ALPHA Helium Volume/Balloon Volume

ALT Altitude; m

BALNM Mass of Ballonet; kg

BALNR Ballonet Surface Area/Balloon Surface Area

BBATM Back Up Battery Mass; kg

BATM Secondary Battery Mass; kg

CELLM Cell Mass - Fuel Cell; kg

DAYS Number of Operating Days

DELTAP Differential Pressure; N/m^2

DIFF Difference Between Available Lifting Mass and Required Mass; kg

DRAG Aerodynamic Drag; N

ENVM Envelope Mass; kg

FINM Fin Mass; kg

FUELM Fuel Mass - Gas Turbine and Fuel Cell; kg

GL Gore Length; m

HRHO Air Density at Altitude; kg/m^3

HRN Hours of Night; Hours

HRS Hours of Sunlight; Hours

NG Number of Gores

PIM Power into Motor; kW

POP Power Out of Propeller; kW

PREQ Power Required; kW

PRESS Pressure at Altitude; N/m^2

PROPM Propeller Mass; kg

Q Dynamic Pressure; N/m^2

RADM Radiator Mass - Fuel Cell; kg

RENV Radius of Envelope; m

REQM Required Mass = Sum of Component Masses; kg

RP Radius of Prop; m

S Surface Area of Envelope; m^2

SPRM Speed Reducer Mass; kg

STRM Structure Mass; kg

SYSM System Mass; kg

TANKM Tank Mass - Gas Turbine and Fuel Cell; kg

TAPEM Tape Mass for Sealing Gores; kg

TBATM Total Battery Mass; kg

TFCM Total Fuel Cell Mass = Tank + Radiator + Cell; kg

THRUST Propeller Thrust = Drag; N

TMM Total Motor Mass; kg

TS Time on Station;- Hours

TSAM Total Solar Array Mass - Array Mass + Interconnecting Wire Mass; kg

TSKIN Thickness of Envelope; mm

TWIRM Total Wire Mass; kg

VOL Balloon Volume; m^3

VWIND Wind Velocity; m/s

4.1.3 Parametric Equations

The computer variables are also referenced and defined in the discussion of equations. To the left of each equation or discussion, a statement number is listed. This number corresponds to the left most number on the compiler listing in Appendix A. The equations are presented in their order of computation.

4.1.3.1 Altitude Control. (23-35)* A check is made for altitude control and the amount of control specified. When altitude control is specified, skin thickness and power required are computed at the lowest altitude (maximum differential pressure and maximum air density). The solution for floating equilibrium is determined at the maximum altitude (Minimum helium lift).

Variables for pressure, air density, and expansion ratio are determined for the altitude range being considered. For a natural shape balloon, no mass is computed for a ballonet.

(36) Ratio of ballonet surface area to balloon surface area, r_B (BALNR):

$$r_B = 1 - .27e^{1.19\alpha}$$

α = ALPHA = Helium volume/balloon volume

If altitude control is not specified, statements 24 and 25 set BALNR equal to zero, and ALPHA equal to one. Statement number 36 is skipped.

(37) Differential pressure, ΔP (DELTAP):

$$\Delta P = P \frac{(.862F\alpha + (1+F)\gamma)}{(1-.862\alpha)\quad(F+1)}$$

*See explanation of number, paragraph 4.1.3.

$F = F$ = Free lift/(system weight)

α = ALPHA + Helium volume/balloon volume

P + PRESS + Ambient pressure at altitude

4.1.3.2 Balloon Equations. All balloon parameters are computed in the SHAPE subroutine. Statement numbers listed here correspond to the compiler printout of the SHAPE subroutine included in Appendix A.

4.1.3.2.1 Natural Shape. Natural shape parameters are based on the following assumptions:

1. Ballast requirement of 10% of gross mass/day
2. $\Sigma^* = .1$
3. $W_b/W_p^* = .32$
4. $C_D = .33$ Based on $(\text{volume})^{2/3}$

It should be noted that the HASKV program is not completely accurate for a natural shape balloon. Equations for structure mass, propeller radius, and wire lengths are based on a Class C shape. Since the natural shape balloon uses a gondola, structure mass would be larger and wire mass smaller. Also, the propeller radius was sized to operate in the wake of an aerodynamic shape balloon.

(5) Volume, $\forall$(VOL):

$\forall = 3.45\ R^3$

R = RENV = Radius of Envelope

(6) Gross lift, G(GROSS):

$G = \forall(b)$

b = HLIFT = Helium lift at altitude

*SBSC Nomenclature

(7) Ballast mass, M_b (BASTM):

$M_b = G(1.-.9^N)$

N = DAYS + Mission time in days

(8) Envelope mass, M_e (ENVM):

$M_e = .243G$

4.1.3.2.2 Class C Shape.

(12) Volume, V(VOL):

$V = 4.0584\ fR^3$

f = FIN = Fineness ratio

R = RENV = Radius of envelope

(13) Surface Area, S(S):

The basic equation is: $S=KL^2$

L = ALENG = Inflated length

K = Constant = Function of f

$L = 2Rf$ and $S = 4KR^2f^2$

K as function of f was determined graphically to be:

$K = 2.641f^{-1.0432}$

Substituting, the computer equation becomes:

$S = (4)2.641R^2f^{(2-1.0432)}$

$= 10.564R^2f^{.9568}$

(14) Skin thickness, t(TSKIN):

$t = 1000(\Delta P)R/\sigma$

σ = SMAT = Material stress allowable

ΔP = DELTAP = Differential pressure

(15-23) Envelope mass, M_e (ENVM):

$$M_e = (\sigma_a + \rho_e (t) t_{ave}/t) S$$

σ_a = ADHE = Adhesive mass/m²

ρ_e = SKIND = Density of envelope material kg/m² (mm)

t_{ave}/t = SKINR = Factor applied to envelope thickness for thickness variation

(18) Tape mass, M_T (TAPEM):

$$M_T = N(GL) T_w (T_t) \rho_t$$

Assume: Tape width, T_w = 1.25 inches = .0318 m

Tape thickness, T_t = tape + tape adhesive = 4t

Tape density, $\rho_t = \rho_e$

$$M_T = .0318(N)\ (GL)\ (4t)\rho_e$$

$$= .127N(GL)\ (t)\rho_e$$

N = NG = Number of gores

GL = GL = Gore length

(19) Add tape mass to envelope mass:

$$M_e = M_e + M_T$$

(20) Fin mass, M_F (FINM):

$$M_F = r_f M_e$$

r_f = FINMR = Ratio of fin mass to envelope mass

(21) Ballonet mass, M_B (BALNM):

$$M_B = r_B S(\alpha_a + \rho_e t/2)$$

(23) Total envelope mass, M_e (ENVM):

$$M_e = M_e + M_B + M_F$$

Return to Main Program.

(58) Net lift, L_s (ALIFT):

$$L_s = \mathcal{V} b_h - M_e$$

b_h = HLIFT(IA) = Helium lift at altitude

(59) Aerodynamic drag, D(DRAG):

$$D = qC_D \mathcal{V}^{.667}$$

q = Q = Dynamic pressure

C_D = CD = Drag coefficient

(60) Power required, P_{req} (PREQ):

$$P_{req} = .001DV \text{ (kW)}$$

V = VWIND = Velocity

This is propulsion power required out of the propeller. The program repeatedly used PREQ for computing component masses. Its value, however, depends upon the component being considered. For example, if PREQ is divided by propeller effiency, it becomes the power required out of the speed reducer. Its value is changed but the variable name is not. In specific instances where the power in or out of a component is a parameter to be used later, a new variable is defined and stored.

(63) Propeller radius, R_p(RP):

$$R_p = .45R$$

The ratio of .45 of envelope radius is based on an approximation of the balloon wake which optimized propeller performance.

4.1.3.3 Power Source Equations. All component masses of the power source are computed within the power subroutine. Statement numbers listed here correspond to the compiler printout of the POWER subroutine included in Appendix A.

4.1.3.3.1 Combustion Engine Equations.

(5) Back up battery mass = total battery mass, M_{BB}(TBATM):

$$M_{BB} = B_p E_{BU}$$

B_p = BAT1 = Mass coefficient of primary storage battery

E_{BU} = BENGY = Back up energy

(7) Engine mass, M_E(TMM):

$$M_E = M_e P_{req} \rho_o / (\rho CR) + M_{E_O}$$

M_e = UMM1 = Engine mass/unit power out

ρ_o = SRHO = Standard sea level air density

ρ = RHO = Air density at altitude

CR = TURBOR = Turbocharger compression ratio

M_{E_O} = CMM1 = Engine mass at zero power (Y intercept)

(8) Fuel mass, M_f(FUELM):

$$M_f = sfc(P_{req}) t_{os}$$

sfc = SFC1 = Specific fuel consumption for internal combustion engine

t_{os} = TS = Time on station

(9) Fuel tank mass, M_{ft} (TANKM):

$$M_{ft} = R_{t/f} M_f + M_{fl}(.6L)$$

$R_{t/f}$ = TMR1 = Ratio of tank mass to fuel mass - I.C. engines

M_{fl} = UFLM = Fuel line mass/unit length

(10) Tail structure mass, M_{str} (STRM):

$$M_{str} = R_{str}(M_E + M_p + .9M_a) + M_{so}$$

R_{str} = STRMR = Ratio of structure mass to supported mass

M_p = PROPM = Propeller and hub mass

M_a = ADDM1 = Additional mass required for engine operation

M_{so} = CMM1 = Structure mass when supported mass = zero (Y intercept)

(11) Wire mass, M_w (TWIRM):

$$M_w = .6L(N_1 w_1 + N_2 w_2)$$

N_1 = 2 = Number of wires

w_1 = WIRE1 = Mass coefficient of alternator to control package wire

N_2 = 3 = Number of wires

w_2 = WIRE2 = Mass coefficient of command unit to engine wire

4.1.3.3.2 Electric Power Source Equations.

(14) Speed reducer mass, M_{sr} (SPRM):

M_{sr} = SPR = Speed reducer mass/unit power out

$P_{sr(out)}$ = PREQ = Power out of speed reducer

(16) Motor mass, M_m(TMM):

$M_m = m_m P_{m(out)} + C_m$

m_m = UMM2 = Motor mass/unit power out

$P_{m(out)}$ = PREQ = Power required out of the motor

C_m = CMM2 = Motor mass at zero power (Y intercept)

(17) Power into motor, P_{im}(PIM):

$P_{im} = P_{m(out)}/E_m$

E_m = EM = Efficiency of motor

(18) Required power out of power source, P_{req}(PREQ):

$P_{req} = P_{im}/E_{ps} + P_{ss}/E_{ss}$

E_{ps} = ECPPS = Efficiency of control package for power source

P_{ss} = SUBPOW = Subsystem power required

E_{ss} = ECPSS = Efficiency of control package for subsystem power

4.1.3.3.2.1 Fuel Cell.

(20) Cell mass, M_C(CELLM):

$M_C = C_o + C_1 V + C_2 V_2$

V = VOLTFC = System voltage for fuel cell

C_o = CFCM = Fuel cell mass at zero volts (Y intercept)

C_1 = CELL1 = Coefficient for fuel cell mass/volt

C_2 = CELL2 = Coefficient for fuel cell mass/volt^2

(21) Fuel mass, M_f(FUELM):

$M_f = sfc\ P_{fc(out)}\ t_{os} D$

sfc = SFC2 = Specific fuel consumption of fuel cell

$P_{fc(out)}$ = PREQ = Power required out of fuel cell

D = DUTY = Duty cycle or ratio of operating time to mission time

Fuel mass is considered independent of the fuel cell and is printed separate of fuel cell mass.

(22) Fuel tank mass, M_{ft} (TANKM):

$M_{ft} = R_{t/f} M_f$

$R_{t/f}$ = TMR2 - Ratio of tank mass to fuel mass

(23) Radiator Mass, M_r (RADM):

$M_r = m_r P_{fc(out)}$

M_r = RAD = Radiator mass/unit power out of fuel cell

(24) Fuel cell mass, M_{fc} (TFCM):

$M_{fc} = M_c + M_{ft} + M_r$

4.1.3.3.2.2 Solar Array.

(31) Power required from battery, P_{OB} (POB):

$P_{OB} = P_{im}(P_N/P_D) + P_{ss}/E_{ss}$

$P_{N/D}$ = PNBYPD = Ratio of power required at night to that of day

(32-35) Secondary battery mass, M_B (BATM):

A battery mass is first computed based on the capacity (amp - hr) of the battery. The charging current required to reach full charge during daylight hours is then computed. If it exceeds the maximum allowable charge current for the battery, the number of parallel strings is increased. The amount of increase is equal to calculated charge current divided by allowable charge current. Battery mass is now sized by charging current and not capacity.

(32) M_B (BATM):

$M_B = P_{OB}(B_S)T_N/B_{cy}$

B_s = BAT2 = Ratio of cell mass to cell voltage - corrected for packaging losses.

T_N = HRN = Hours of night

B_{cy} = BATCY = Battery capacity corrected for number of charge - discharge cycles.

(33) Charging current, I_c (XIC):

$I_c = B_{cy}/(T_s E_B)$

T_s = HRS = Hours of sunlight

E_B = BCHEF = Battery charging efficiency = electrical to chemical conversion

(35) Battery mass sized by charging current, M_B (BATM):

$M_B = M_B(I_c/B_{cc})$

B_{cc} = BATCC = Maximum allowable charge current for battery

(39) If P_N/P_D is less than one, motor mass is increased for second motor, M_m(TMM):

$$M_m = M_m + P_{im}(E_m)\ (P_N/P_D)m_m + C_m$$

All variables as defined previously.

(40) Power required out of solar array, P_{osa}(PREQ):

$$P_{osa} = P_{req} + 1.22\ P_{OB}E_B/ECP_B$$

1.22 = Ratio of charging voltage to discharging voltage.

ECP_B = ECPB = Efficiency of control package for battery

(41) Solar array mass, M_{sa}(TSAM):

$$M_{sa} = P_{osa}F_g(m_{sa}+w_4)$$

F_g = GEOF = Geometry factor

M_{sa} = SA = Solar array mass/unit power out

w_4 = WIRE4 = Interconnecting wire for solar array

4.1.3.3.2.3 Battery.

(46) Primary battery mass, M_{PB}(TBATM):

$$M_{PB} = B_p(P_{req}T_s+E_{BU})$$

All variables previously defined.

4.2 Analysis of Parametric Data

A series of graphs have been developed which summarize the computer output of the parametric study. These graphs, along with other pertinent information, were the basis for the selection of an optimum vehicle choice to meet the mission requirements. The basic power sources considered in this study; namely, solar cell array, fuel cell, battery, gas turbine, Diesel engine, and Wankel engine have been plotted. For reasons explained below and in Section 4.3, the most thorough comparison was made between solar cell array and fuel cell powered systems. By analyzing these graphs, comparisons can be made between these power sources to determine the most optimum system for a given set of conditions. In addition to the power source comparisons, these graphs show the parameters to which a particular system is most sensitive; such as, balloon material type and stress limit, free lift, coefficient of drag, and mission requirements (duration, altitude, speed, payload mass, and payload power). The system sensitivity to certain parameters is discussed in more detail in Section 4.2.2. Essentially then, this analysis has explored mission, feasibility, and construction parameters; and this analysis has helped to define the final mission requirements.

4.2.1 Discussion of Graphs

The following graphs, Figures 4.3 - 4.9 were derived using a standard value for the basic design parameters. Generally one of these parameters was varied while the remainder were set at the standard values. The standard parameter values are:

Material type - biaxially oriented Nylon 6

Material stress limit - 8300 N/cm^2

Altitude - 21 km

Free lift - 20%

Coefficient of drag - .05

Duration - 7 days

Payload mass - 90 kg

Payload power - 0 W

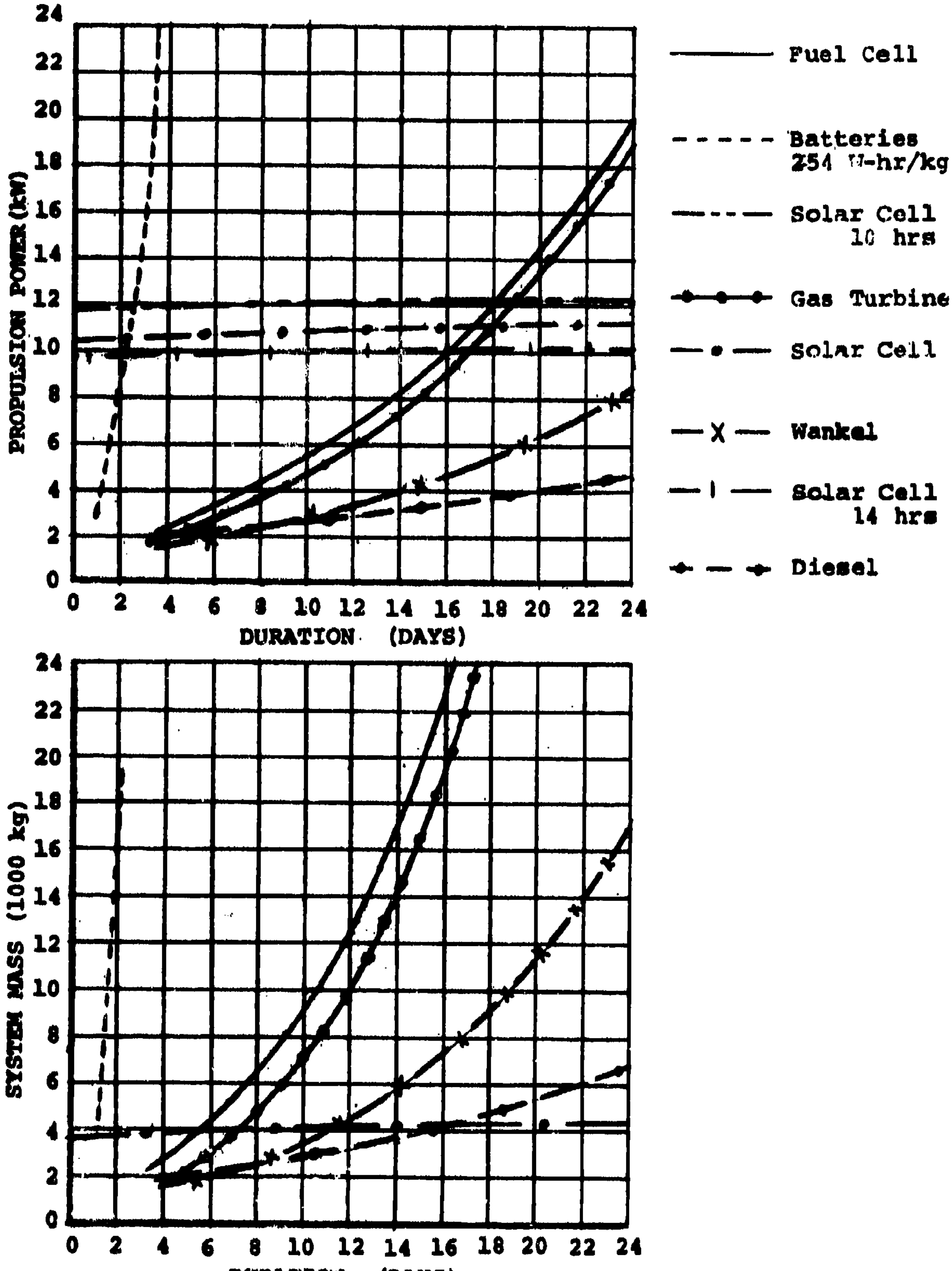

Figure 4.3 Effects of duration on propulsion power and system mass for all concepts.

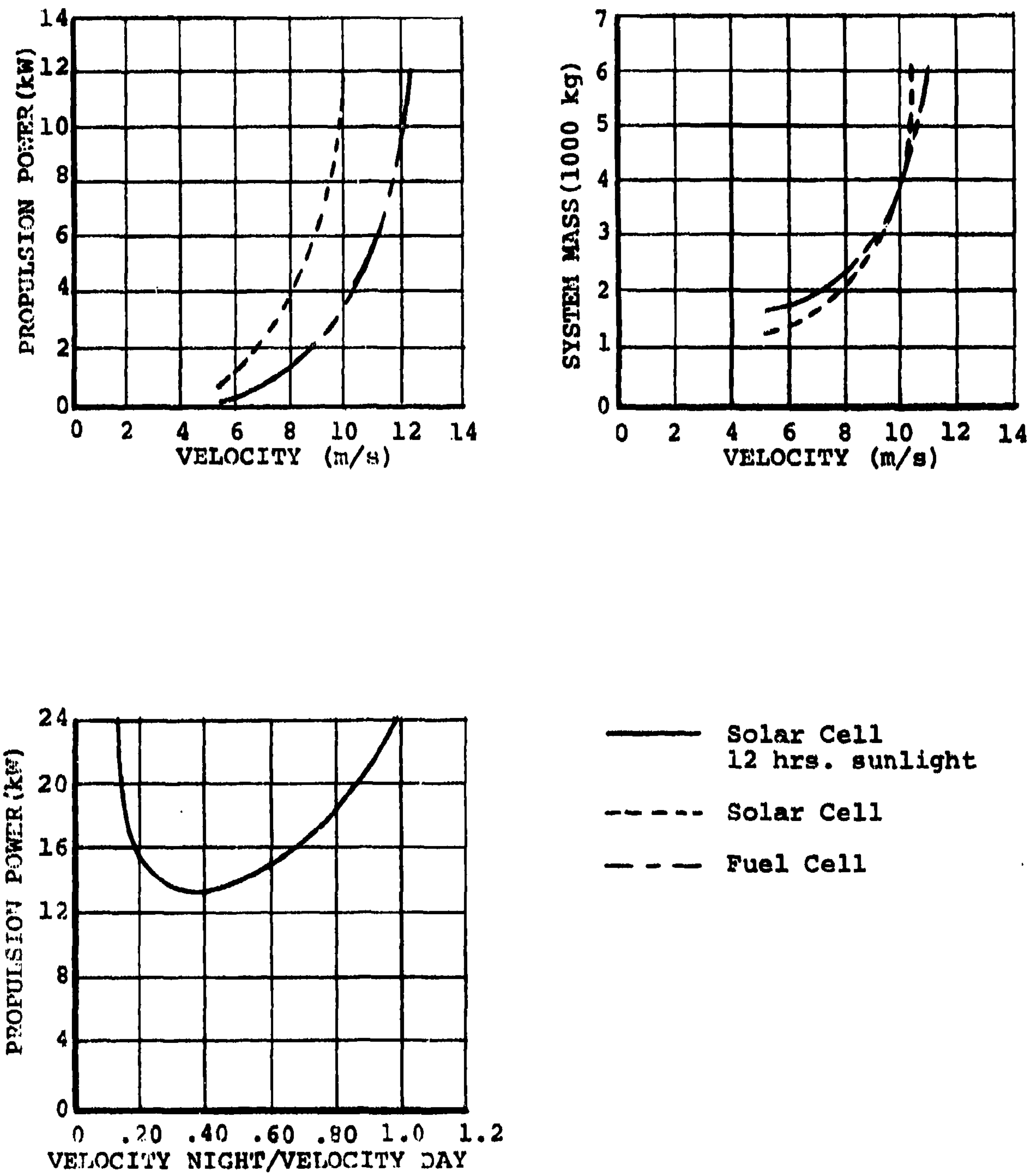

Figure 4.4 Effects of velocity on propulsion power and system mass.

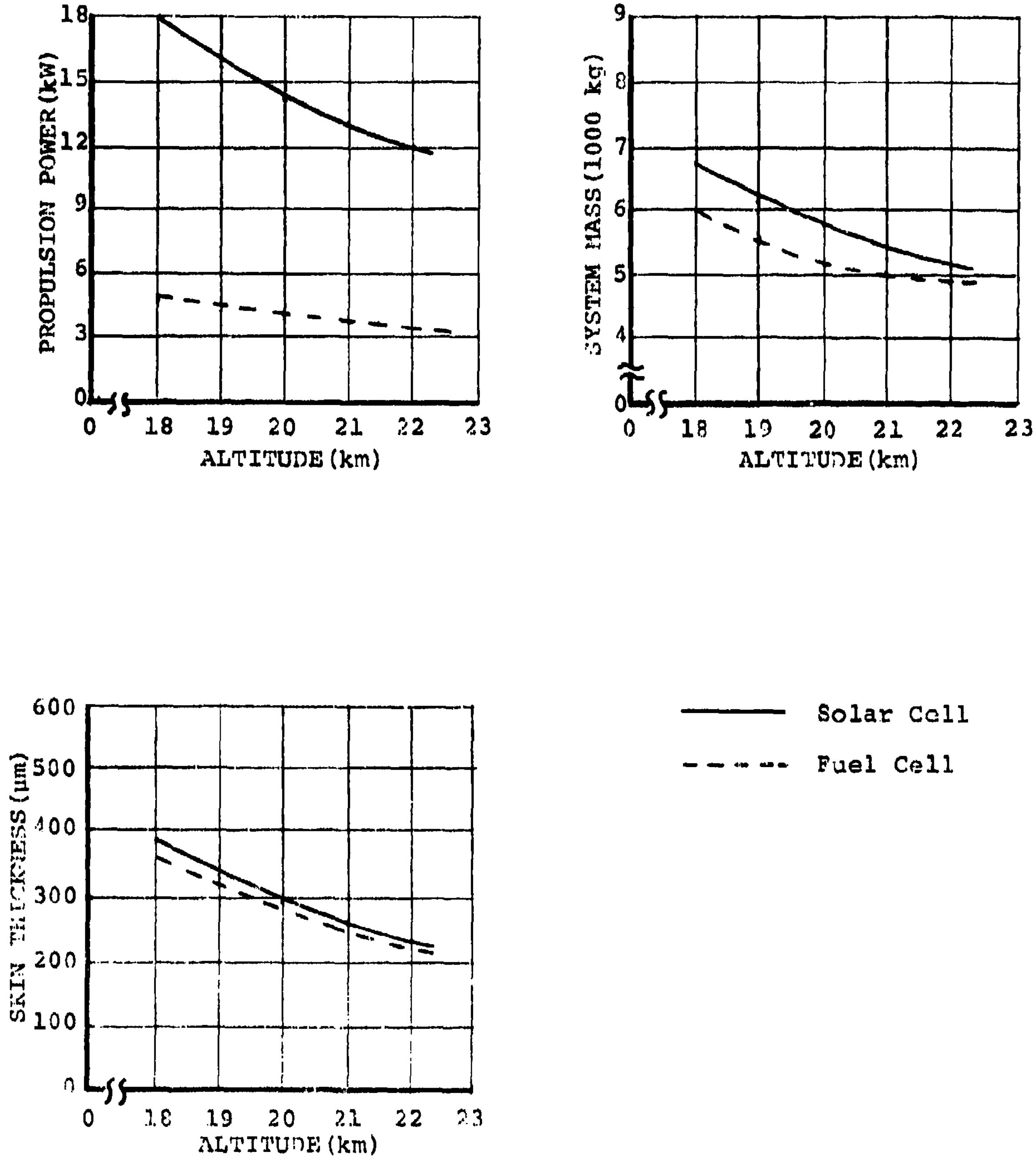

Figure 4.5 Effects of altitude on system design.

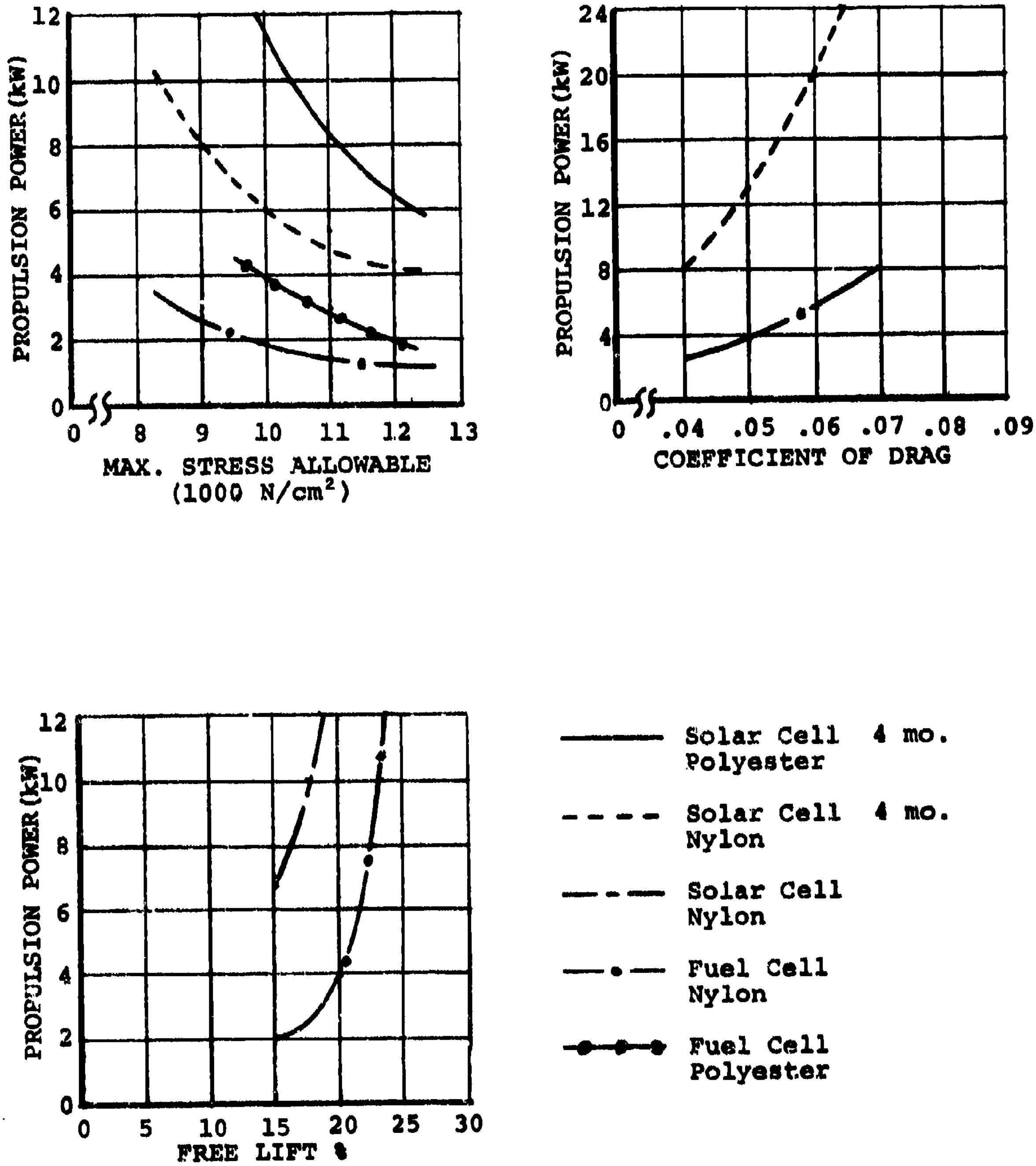

Figure 4.6 Effects of material stress, coefficient of drag, and free lift on propulsion power.

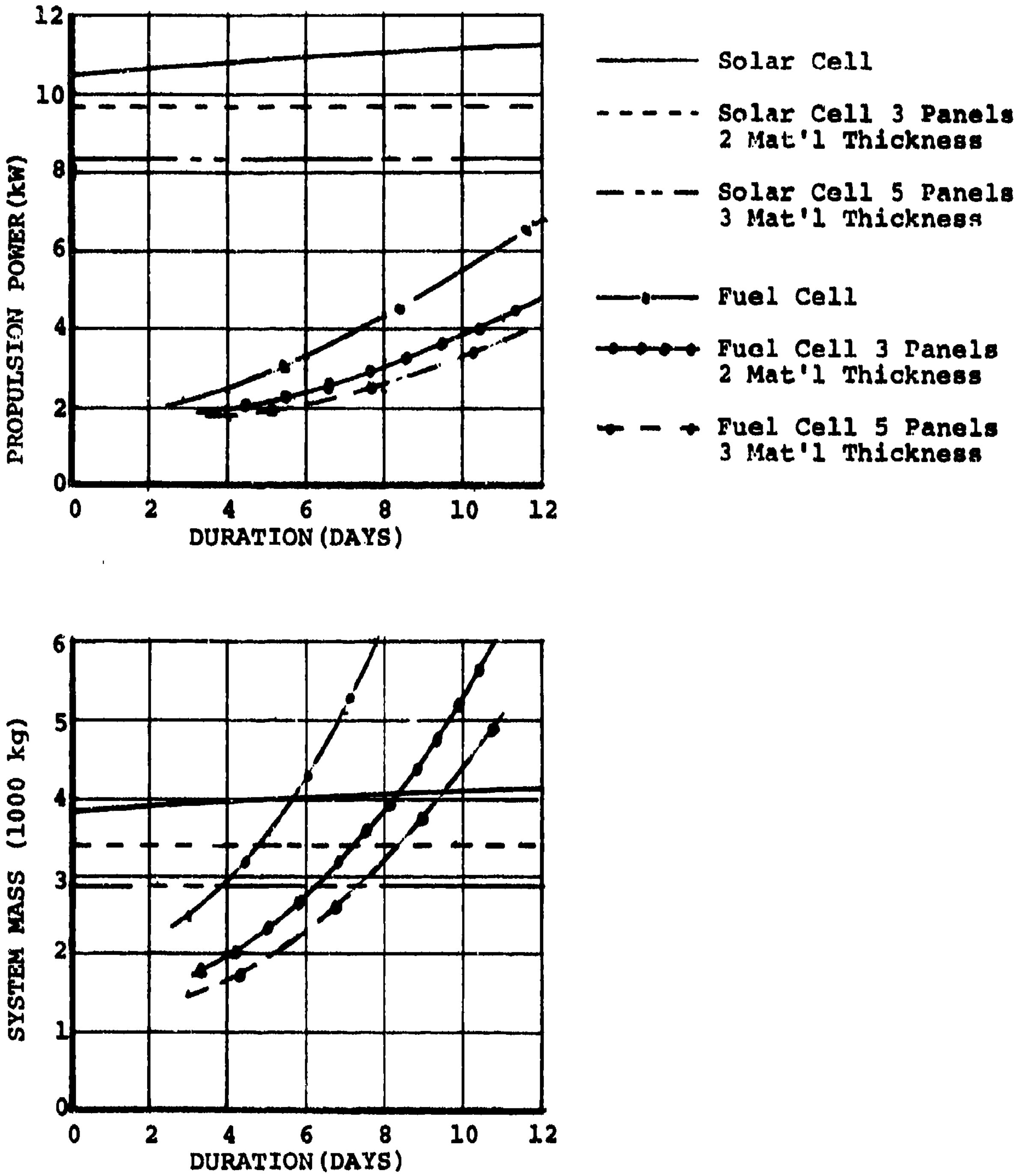

Figure 4.7 Effects of using more than one material thickness on propulsion power and system mass.

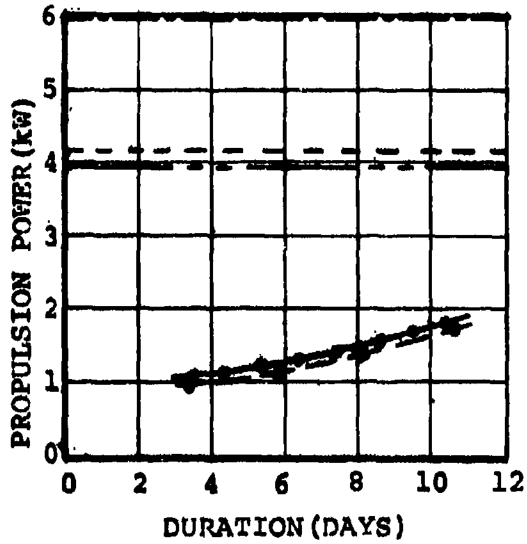

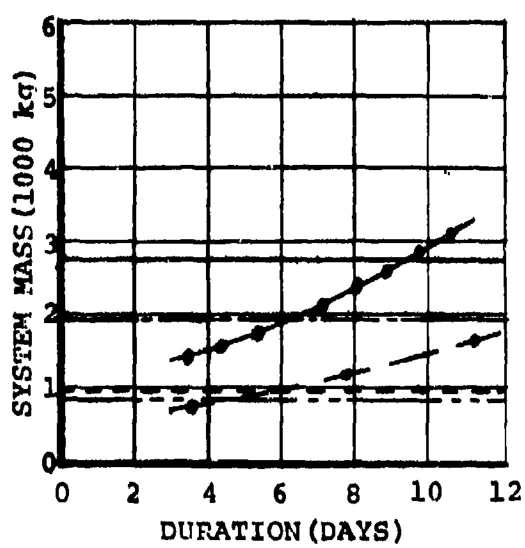

Solar Cell A/C*18-21 km
Vn/Vd = .5

Solar Cell A/C 18-21 km
V//Vd = .2

Solar Cell 21 km

Solar Cell A/C 18-21 km

Fuel Cell A/C 18-21 km

Fuel Cell 21 km

*A/C = Altitude Control with an average velocity of 7.7 m/s.

Note: All curves generated for nylon film with a stress of 12,400 N/cm^2

Figure 4.8 Effects of using altitude control on propulsion power and system mass.

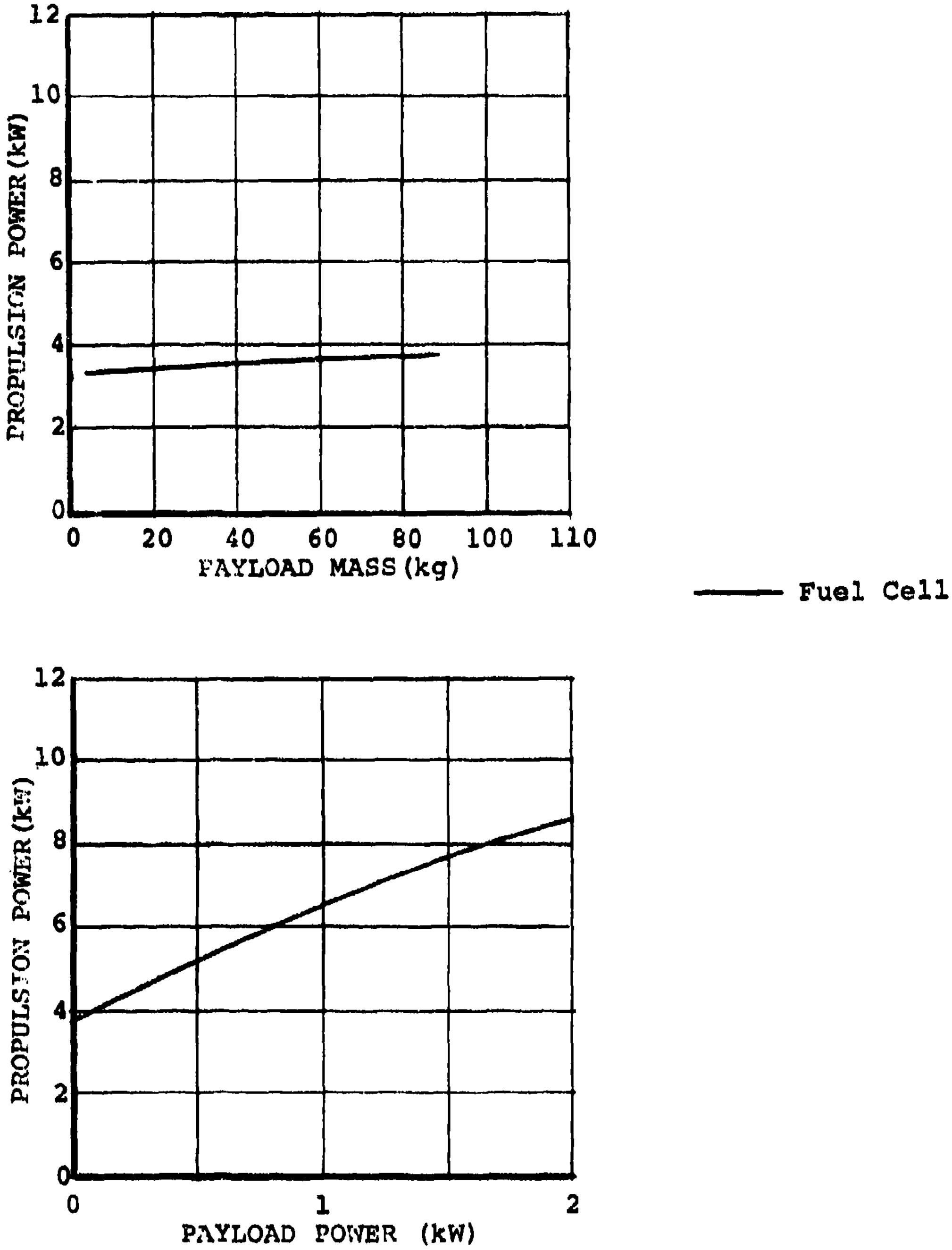

Figure 4.9 Effects of payload mass and power requirements on propulsion power.

Velocity ratio - .333 (Solar cell array only)

Tank mass ratio - .5 (Fuel cell only)

Sunlight - 12 hr/day (Solar cell array only)

4.2.1.1 Discussion of Figure 4.3. The graphs presented in Figure 4.3 compare the propulsion power and system mass of all the basic concepts considered in this study contract. The power values shown represent the net power required out of the propeller to propel the airship forward; i.e., thrust multiplied times velocity. The mass versus duration and power versus duration curves appear similar because mass is proportional to the square root of the propulsion power cubed.

Since system power and mass are excessively large for a solar cell array system operating at 10.3 m/s (20 kn) airspeed, it was decided to fly 5.1 m/s (10 kn) at night and 15.4 m/s (30 kn) during the day to give a 10.3 m/s (20 kn) average for 24 hours. Thus, the solar cell array curves are shown with a V_N/V_D ratio of 10:30 (V_N/V_D = .333, see Figure 4.4). By flying at 5.1 m/s (10 kn) airspeed at night the battery mass required to operate the system while the solar cells are inoperable is reduced by a factor of 46. This reduces the system mass considerably as noted on the mass versus duration curve. Here the crossover with the fuel cell system is between 5 and 6 days, whereas on the power versus duration curve the crossover is at 18 days. This results because the power value furnished by the solar cell array must be sufficient for 15.4 m/s (30 kn) operation whereas the other concepts operate continuously at 10.3 m/s (20 kn).

On these base data curves the charge-discharge cycles for the batteries have been considered; and consequently, the solar cell array power and mass requirements increase slightly as the number of charge-discharge cycles for the batteries increase. On the power versus duration curve, three solar cell array curves are plotted for 10, 12, and 14 hours of sunlight to allow for operation of the solar powered airship at different latitudes and times of year. With 2 hours less sunlight the propulsion power required increases approximately 11% whereas with 2 additional hours of sunlight the propulsion power decreases approximately 8%.

The power required and the system mass are excessively high, as shown, for the battery case. The best available batteries 254 W-hr/kg (115 W-hr/lb) are presented. Batteries will not be considered in any of the other graphs since system size becomes too large beyond a one day mission.

The base data curves, as well as all remaining curves, show a fuel cell system utilizing a TMR value of .5; i.e., the tank mass is .5 times the fuel mass. The relative advantage of using a lightweight tank can be shown by using a TMR value of .85. For a 7 day mission, the power required drops by approximately .5 kW and system mass by approximately 20% for the TMR value of .5 as compared to .85.

The gas turbine, Wankel and Diesel engine curves are all hypothetically superior power sources in terms of propulsion power required and system mass. However, none of these power sources have been tested for high altitude operation. A development program would need to be performed in order to instill confidence in any of these systems, whereas the fuel cell and the solar cell array have been used for space flights with high reliability. Also, fuel cells and solar cells are available. The Wankel and Diesel curves are much lower than the gas turbine curve due to a lower specific fuel consumption, i.e., .024 kg/kW-hr (.4 lb/hp-hr) versus .73 kg/kW-hr (1.2 lb/hp-hr). All three of the internal combustion power sources would require either a ballonet or pump and valving scheme to maintain altitude as fuel is consumed. This would require additional power and system mass which has not been included in these curves. These curves consequently would be shifted higher on the graph to compensate for the additional power and mass. Since these power sources are not considered reliable or tested sources, this effort was not pursued.

4.2.1.2 Discussion of Figure 4.4. Wind velocity is one of the most sensitive parameters for any of the given systems. It has been decided that the most favorable winds exist at the 21 km (70,000 ft) altitude level. The first two graphs of Figure 4.4 show the effect of velocity on propulsion power and system mass. The velocity scale of the graphs is average velocity so that a comparison can be made between the two systems although the solar cell system has been designed to fly at higher velocities during daylight hours. For the solar powered system, power increases from approximately .5 kW at 5.1 m/s (10 kn) to approximately 3 kW at 7.7 m/s (15 kn), and from 7.7 to 10.3 m/s (15 to 20 kn) power increases from 3 kW to 13 kW. If the system size were constant, propulsion power would increase as the cube of the velocity; however, since the system necessarily grows larger to accommodate the increased propulsion system weight the power increases even more than the cube of the velocity.

The system mass for the solar cell nearly doubles between 5.1 and 7.7 m/s (10 and 15 kn) and triples between 7.7 and 10.3 m/s (15 and 20 kn). Beyond an average velocity of 10.3 m/s (20 kn) the system mass grows even faster.

The third graph of Figure 4.4 was plotted to determine the optimum flight velocity for day and night operation for a solar cell powered vehicle to obtain a 10.3 m/s (20 kn) average airspeed for a 24 hour period. By flying 15.4 m/s (30 kn) during the day, while the solar cells are powering the vehicle, and 5.1 m/s (10 kn) during the night, on battery power, system power and mass are minimized. However, this curve is relatively flat near the optimum velocity ratio and slight deviations from a V_N/V_D value of .333 would be acceptable.

4.2.1.3 Discussion of Figure 4.5. The three graphs of Figure 4.5 show the effect of altitude on propulsion power, mass, and skin thickness. As altitude is increased, less power is required due to lower density air. This, along with a lower superpressure which results because of the decreased absolute pressure, reduces the thickness of the envelope. As the envelope thickness decreases, the system mass consequently becomes lighter. By going from 18 to 21 km (60,000 to 70,000 ft) the propulsion power for a solar cell system decreases by approximately 25% (6,850 kg to 5,150 kg). But even more important is the decrease in skin thickness. The envelope skin thickness for a solar cell system drops from 390 μm (15.4 mil) to 220 μm (8.7 mil). The 220 μm (8.7 mil) material could possibly be manufactured by laminating two layers of nylon whereas the 15.4 mil material would require a quad-laminate. This would increase system mass slightly since two additional layers of adhesive would be required for the quad-laminate. The computer program assumed a bi-laminate material with one thickness of adhesive. By going to multi-laminate material the system mass would be even larger than the graph shows.

4.1.1.4 Discussion of Figure 4.6 The first graph of Figure 4.6 shows power versus maximum stress allowable for a solar cell array and a fuel cell system employing polyester and nylon films. As shown, either system is very sensitive to the type of and maximum allowable stress of the material. Both nylon and polyester have been plotted for stress levels from 8,300 to 12,400 N/cm^2 (12,000 to 18,000 lb/in^2). This graph does indicate the need for a materials study; for example: if a nylon material with an allowable stress of 12,400 N/cm^2 (18,000 lb/in^2) could be used an approximate savings of 65% could be realized in propulsion power for a solar cell system as well as a substantial decrease in system mass.

The second graph of Figure 4.6 shows the sensitivity of the systems to the coefficient of drag, the parameter for which very little reliable data have been generated. All of the graphs in this series utilize a coefficient of drag of .05 which is based on analysis and past experience with a high altitude airship.[10,14] For a solar cell system, the graph shows propulsion power increasing 2.5 times as C_D increases from .04 to .06.

Free lift is another parameter to which the system is very sensitive as shown in the third graph of Figure 4.6. The minimum free lift required is dependent on the negative supertemperature. It was determined that the minimum free list should be 20% to maintain pressurization at the 21,000 m (70,000 ft) altitude level. Beyond 20%, as shown by the graph, system power requirements, as well as mass, grow very rapidly for either the solar cell or fuel cell vehicles.

4.2.1.5 Discussion of Figure 4.7. The graphs presented in Figure 4.7 compare the power and mass of the basic systems with the power and mass of systems which utilized more than one material thickness for the balloon construction. The graphs show the tradeoff for both a solar cell array and a fuel cell system using either two or three material thicknesses. This requires a junction between the different thicknesses of material. Since stresses are highest near the largest diameter of the balloon and diminish near the ends, lighter gauge materials can be used at the nose and tail ends. This reduces the balloon mass and minimizes the system size. The two material thickness case would incorporate the thinner material at the nose, the heavier material through the midsection, and the thinner material again at the tail end. The same technique is used in the three material thickness case with two additional locations added to change material thickness. For a solar cell array powered system using two material thicknesses, a savings of 27% can be realized in system power and 37% in system mass. By going to three material thicknesses, a savings of 35% can be realized in system power and 48% in system mass. Thus, by varying the material thickness at discrete locations in the envelope a substantial savings in power and mass can be accomplished.

4.2.1.6 Discussion of Figure 4.8. The comparison with and without altitude control is shown in Figure 4.8 by the curves labeled A/C for altitude control. The altitude control curves are plotted using a velocity of 7.7 m/s (15 kn) since the reason for using altitude control is to seek out a minimum wind field, whereas the curves without altitude control are plotted with a velocity of 10.3 m/s (20 kn). The solar cell array altitude control curves are plotted with V_N/V_D values of 5/25 and 10/20 to determine the most favorable combination of day-night velocities to obtain a 24 hour average of 7.7 m/s (15 kn). By flying 10.3 m/s (20 kn) during the day and 5.1 m/s (10 kn) at night the solar cell power and system mass are minimized. The propulsion power as well as mass for both solar cell array and fuel cell is substantially larger by incorporating altitude control. These curves were generated with a nylon material skin stress of 12,400 N/cm^2 (18,000 lb/in^2) in order to obtain a solution. Also, altitude control complicates the system design and construction of the system.

4.2.1.7 Discussion of Figure 4.9. Payload requirements in the range from 0 to 90 kg (0 to 200 lbm) and from 0 to 2 kW affect the fuel cell system propulsion power as shown in Figure 4.9. It should be recalled that the power values shown are in addition to the payload power, inefficiency losses, gimbal operation, and electronic system requirements. The payload mass has little effect as would be expected, since the 90 kg (200 lbm) payload mass is such a small part of the total system mass. The payload power variation does, however, make significant changes in the system propulsion power requirements.

4.2.2 Sensitivity Analysis

An analysis was performed to determine the sensitivity of the system design to small changes in numerical values of all design parameters. The HASKV computer program was used to generate data for a one per cent variation of each parameter. Each parameter was varied independently, and all variations were taken as positive. Thus, parameter X became $X + \Delta X = (1.01)$. Except for X, all the other parameters were the same. A complete solution was required for each parameter that was varied. The system mass change, ΔM, and absolute percentage change, $|\Delta M/M|$, were calculated. The following table gives the results of the analysis in order of decreasing sensitivity.

The most sensitive design parameter is the allowable material stress, SMAT, where a 1% increase reduces the system mass by over 4%. The next most sensitive design parameter is the envelope material density, SKIND, where a 1% increase will increase system mass by 3.7%. Material thickness factor, SKINR, significantly affects the system design. By constructing the envelope from different material thicknesses, as discussed in Section 4.2.1.5, a considerable savings in system mass can be realized. Parameters such as free lift, F, and supertemperature, SUPERT, greatly influence the system design as noted by the mass changes. Prediction of these parameters is very critical because of their influence on system mass. It is obvious that discretion must be used in all assumptions if a feasible system is to be designed.

Parameter Increased By 1%	Mass Change ΔM	Absolute Mass Change ΔM/M
SMAT*	-66.86 kg	4.01 %
SKIND	61.81	3.70
SKINR	55.83	3.35
F	43.55	2.61
SUPERT	27.30	1.64
SFC2	10.74	.644
CD	10.53	.631
PAYM	9.77	.585
SUBPOW	9.44	.566
TMR2	4.87	.292
CFCM	4.74	.284
FINMR	4.73	.283
CELL1	4.72	.283
VOLTFC	4.71	.282
ADHE	4.68	.280
PROP	4.65	.279
RAD	4.62	.277
UMM2	4.55	.273
STRMR	4.50	.269
FIN	4.08	.245
EPROP	- 1.65	.099
ESPR	- 1.65	.099
EM	- 1.53	.092
ECPPS	- 1.47	.088
ECPSS	- .58	.035
CMM2	.05	.0029
WIRE3	.05	.0029
BENG4	.03	.0018
CELL2	.02	.0012
CSTRM	.01	.00059

*See Section 4.1.2 for definition of nomenclature.

TABLE 4.1 SENSITIVITY OF SYSTEM MASS TO VARIOUS DESIGN PARAMETERS

4.3 System Concept Choice

The parametric study investigated concepts applicable to the system requirements. Other than the engineering analysis of the graphs there are several other factors which influence the choice of the system concept to be designed for the mission. The primary factors are cost, availability, reliability, vulnerability, and logistics. There is little specific information available at this time on any of these factors since this is a specialized design utilizing state-of-the-art components almost exclusively. However, general comments regarding the effect of each of these factors are discussed below. In addition tc this discussion a System Concepts Comparison table, Table 4.2, has been compiled summarizing the primary factors and should be referred to.

Reliability of various system components and complexity of the entire system which determines feasibility is the most important choice factor. Solar cell arrays and fuel cells are proven and reliable power sources. Fuel cell operational designs encompassing environments ranging from undersea to outerspace and including underground use have been accomplished. Solar cells as well have a proven record for outerspace flights and have been used on a short duration powered balloon flight.[10]

Batteries are a very reliable power source; however, as discussed in Section 4.2.1.1, a battery powered vehicle becomes excessively heavy for flights beyond a one day mission.

Reliability of internal combustion engines and gas turbines has not been proved for altitudes above 12 km (40,000 ft). Above this altitude ignition cannot be assured and a turbocharger is required to maintain a high compression ratio. A heater may also be required for the fuel. These additional components would necessarily complicate the design of these power sources and decrease reliability. The internal combustion engine and gas turbine engine could someday prove to be the most favorable power sources for short duration (one week), but without a development effort they must be considered unreliable.

Cost is considered to be an important choice factor. However, there are other serious considerations. Since only parts of this system will be recoverable (see Section 5.5) it is necessary to compare the cost effectiveness of various system concepts under normal operational use. Of the various types of power sources considered it is highly likely that

SYSTEM CONCEPT (POWER SOURCE)	ADVANTAGES	DISADVANTAGES	MANUFACTURING COSTS	AVAILABILITY	RELIABILITY
Solar Array	Extended duration for future development	Array likely not recoverable Cost Complexity - Electronics System size large for 7 day duration	High	6 mo.-1 year	Good - Excellent
Fuel Cell	Proven reliability	Development necessary Fuel & Tanks - "Exotic"	Moderate	1 year	Good - Excellent
Gas Turbine	System size minimized Cost	High light-off speed Unproven for high altitude Development necessary Requires altitude stabilization Gimbaling of engine	Low to Moderate	1 year	Fair - Good
Wankel	System size minimized Cost	Heating may be required Unproven for high altitude Development necessary Requires altitude stabilization Gimbaling of engine	Low	6 mo.	Fair - Good
Diesel	System size minimized Cost	Heating may be required Unproven for high altitude Development necessary Requires altitude stabilization Gimbaling of engine	Low	6 mo.	Fair - Good
Batteries	Simplicity	Excessively large system Cost Structure design	High	4 mo.	Excellent

TABLE 4.2 SYSTEM CONCEPTS COMPARISON

the solar array would be most difficult, if not impossible, to retrieve. Since the solar cells are adhered to the balloon surface and cover a large area they cannot be detached in flight and the balloon itself is not considered retrievable. For long duration missions the economic problem is not as serious since the solar cell cost can be amortized over a longer period of time.

The fuel cell is considered recoverable; however, for safety reasons the tanks may be separated before being released from the balloon and parachuted separately. There is also a possibility that the fuel cell and tanks may be damaged upon impact. To keep from damaging the fuel cell a midair snatch recovery may be desirable.

All components of the internal combustion and gas turbine power sources are considered recoverable, but here again a snatch recovery may be required to eliminate impact damage.

Except for variations in power source costs all other components of the various systems, such as motors, reducers, telemetry, structures, propeller, etc., will incur similar expenses providing they are of the same size. It is generally conceded, however, that the smaller the system the lower the cost.

Availability of power sources and components is of prime consideration. Development of components must also be taken into account in the lead time necessary for procurement since the majority of the components are unique to the system design; and consequently, they are not off-the-shelf items. There are no major problems anticipated in procurement and no definite advantages of one type over another; however, actual procurement time necessary for the various power sources and components can only be estimated at this time.

Vulnerability is not considered to be a very important factor for variations in system concept. Because of the fragile nature of the balloon itself, necessary design measures such as wear patches and protective coverings are required of any of the power source systems and components. Since the mission requirement is for a station keeping vehicle the system is not vulnerable to impact shocks associated with launches and landings.

The logistics involved will naturally affect the operational costs of the system. However, except for the fuel cell LO_2 and LH_2 logistics costs would not vary significantly between system concepts; and, as with vulnerability, logistics is not a very important factor in making a tradeoff between the systems.

In review of the System Concepts Comparison table and the graphical analysis, if it is assumed that all concepts are feasible, then reliability and cost are considered to be the most important factors. Since all of the low cost systems have unproved power sources these systems are being ruled out without an R & D program to develop a gas turbine, rotary piston, or Diesel engine.

As mentioned previously, the battery choice can be ruled out since it is not operationally feasible because of system size. The two remaining power sources, fuel cell and solar cell array, are considered the only feasible sources for a system.

The fuel cell concept appears attractive for missions up to one week in duration. Beyond one week the fuel cell system becomes increasingly large due to the additional fuel required to propel the system. As mentioned, the fuel cell is a very reliable, proven source with little development effort necessary. With operational restrictions and increased cost, the solar array powered vehicle is not considered as being competitive with the fuel cell powered system for short duration. It should be noted that for extremely long duration missions the solar array concept would be the only feasible choice.

The final choice then for this 7 day mission was the fuel cell powered vehicle. Even though the biaxially oriented nylon film has not been fully investigated it was decided to assume its use in the design because of the relative advantages of using this film as compared to polyester film. The parametric analysis reveals that employing altitude control is not justified and would compromise the reliability of the system. When altitude cannot be controlled a nominal altitude of 21.0 km (70,000 ft) is desirable for minimum winds. Also, skin thickness, power and mass requirements decrease as altitude increases so that 21.0 km (70,000 ft) is advantageous in optimizing the system as compared to 18.0 m (60,000 ft).

5. SYSTEM DESIGN

The system design for the POBAL-S powered airship is based on the use of an aerodynamic shaped superpressure balloon meeting the following performance requirements*.

Duration	7 day under continuous operation
Airspeed	Constant at 8.18 m/s (15.9 kn)
Altitude	Constant at 21 km (70,000 ft)
Payload Weight	890 N (200 lb)
Payload Power	Continuous 500 W

The airship is propeller driven with the power being supplied by a fuel cell through an electric motor. The overall airship is shown in Figure 5.1.

5.1 Vehicle

The POBAL-S vehicle consists of the balloon, which is the basic floating platform, along with the stern structure and gondola which provide mechanical support interfacing between the balloon and the components contained within these structures.

5.1.1 Balloon

The balloon is the inflatable member of the system. From a manufacturing and technology standpoint, the balloon is considered to include not only the basic envelope, or hull, but also the fins. These components are discussed below.

5.1.1.1 Hull. The POBAL-S hull is a Class C shape with a fineness ratio of 5.0. The inflated length is 113 m (371 ft) and the volume is 29,270 m^3 (1,034,000 ft^3). The primary envelope material is a biaxially oriented Nylon 6 film lamination.** The airship hull is shown in Figure 5.2.

The envelope load distribution for a pressurized aerodynamic shape hull is approximately that of a cylinder; longitudinal skin loading being about half the circumferential loading. In addition, the loading is proportional to the distance from the axis to the envelope, measured perpendicular to the envelope. Thus, the loads are maximum at the maximum

*See footnote on page 7.

**Tests were performed on this material and are reported on in Appendix B.

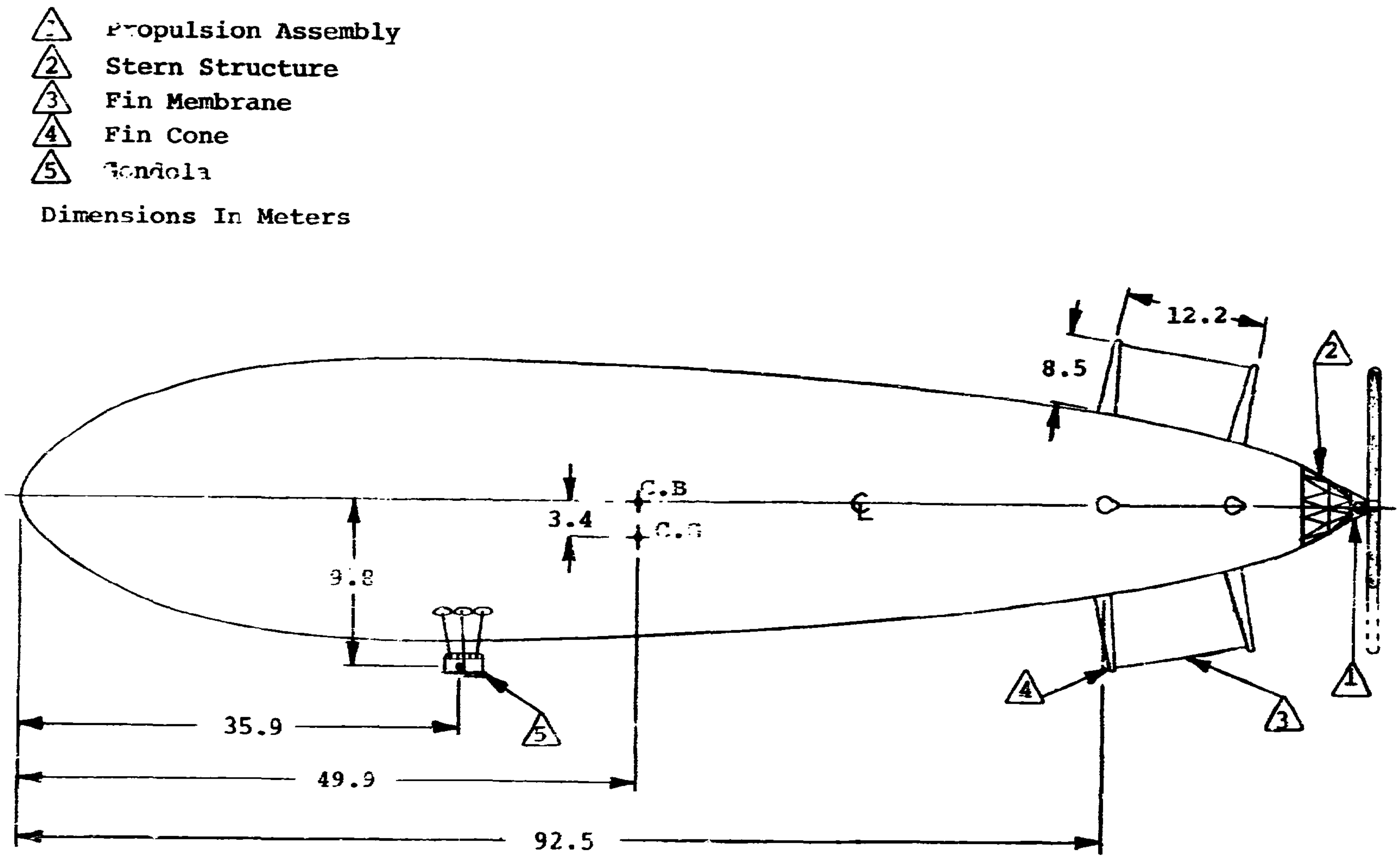

Figure 5.1 POBAL-S airship.

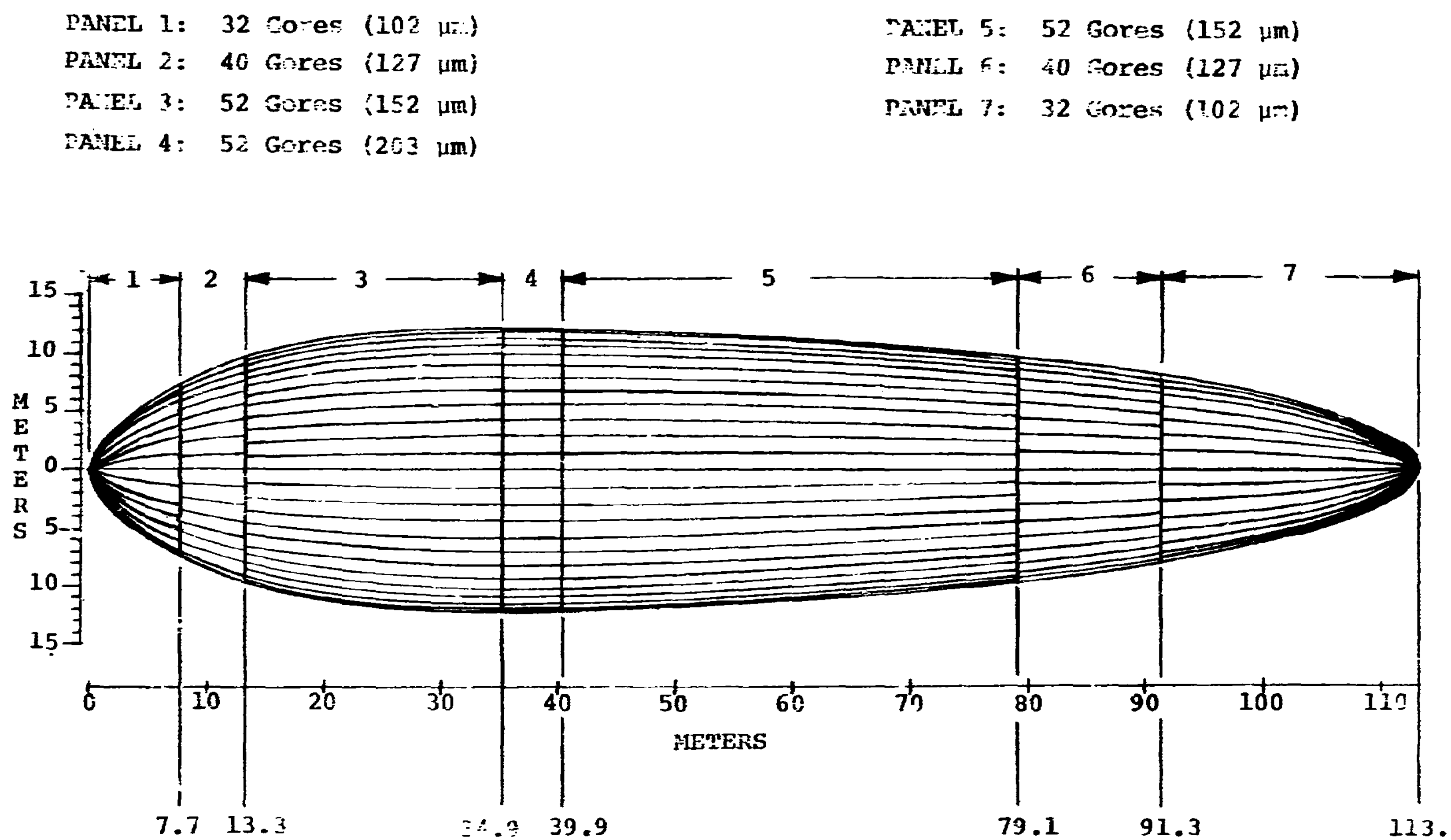

Figure 5.2 Envelope gore configuration.

diameter and minimum at the fore and aft ends. Minimum hull mass requires a material whose thickness can be varied to maintain a nearly constant stress over the length of the balloon.* Skin thickness variation for the POBAL-S hull is accomplished by constructing the hull in seven sections using four different thicknesses. The four thicknesses required are obtained by using multiple laminations of 25.4 μm (1 mil) material. Presently, 25 μm (1 mil) is the maximum thickness available for biaxially oriented Nylon 6 in the 1500 mm (59 in) width. For the design stress of 9,825 N/cm² (14,250 lb/in²), the four laminates are 102 μm (4 mil), 127 μm (5 mil), 152 μm (6 mil), 203 μm (8 mil).

The gore seals should be constructed as a butt seal with an outside tape 5.1 cm (2 inches) wide and inside tape 3.8 cm (1.5 inches) wide. Outside tape thickness will be 25 μm (1 mil) greater than the inside tape thickness. A seal construction requirement is that the total tape thickness, excluding adhesive, be 25 μm (1 mil) greater than the maximum laminate thickness being sealed. The fore and aft sections use a total tape thickness of 127 μm (5 mil), the 127 μm (5 mil) sections use a tape thickness of 152 μm (6 mil), the 152 μm (6 mil) sections use a tape thickness of 178 μm (7 mil), and the center section uses a tape thickness of 229 μm (9 mil).

The balloon should be assembled as described below. First, all sections are sealed leaving the bottom longitudinal seal open. Then the sections are sealed together still leaving the bottom seal open. A final trim is made to remove stress concentration points at junctions, and then the final longitudinal seal is made along the length of the balloon. End caps are finally installed. All external and internal attachments should be installed on individual gores prior to sealing of the gore. In instances where this is not feasible, attachments should be made as early in the assembly sequence as possible.

All loads on the balloon are carried by the balloon acting as a pressurized beam. The critical bending moment which causes the beam to buckle is[7]:

$$M_c = \Delta P \pi r$$

*Hull mass would increase by 11% for the same hull constructed with longitudinal gores of a single 152 μm (6 mil) laminate.

where ΔP is the differential pressure and r is the radius of the cross section.

The force, F, required to buckle the balloon at any given section is:

$$F = M_c/L$$

where L is the axial length from the section to the point where the force is acting. Substituting for M_c the equation becomes:

$$F = \Delta P \pi r^3/L$$

Upon examination of the equation, it should be noted that ΔP is constant for any section of the balloon. Also, since the radius is cubed, its influence on the maximim supportable load F is much greater than the lever arm L. Thus, it is reasonable to expect the critical buckling section to be located at the tail where r is small. This will occur at the tail since the radius approaches zero but must still carry the bending moment due to the stern structure and propulsion components.

The buckling force is calculated with the assumption that it acts at the gimbal axis, one meter aft of the balloon. A differential pressure of 238.5 N/m² (0.346 lb/in²) is used. This assumes an operating altitude of 21 km (70,000 ft), 20% free lift, and -10% supertemperature. This is anticipated to be the minimum pressure condition. Station 111.13 corresponds to the location, where the tail reinforcing battens terminate. At this location r has a value of 2.266 m (7.435 ft) and L has a value of 2.870 m (9.416 ft). Using these values, the critical buckling load is determined to be 3,038 N (683 lb). Since the actual applied load at the gimbal is only 801 N (180 lb), the margin of safety is 2.8. This is more than adequate to account for transient loading conditions.

If F is set equal 801 N (180 lb) the equation can be solved for the critical buckling pressure. Using a safety load factor of 1.5:

$$\Delta P_{crit} = (1.5)\ (801\ N)\ (L)/(\pi r^3)$$

$$= 62.9\ N/m^2$$

For the POBAL-S balloon at 21 km (70,000 ft) with 20%

free lift, 94.3 N/m^2 (0.37 lb/in^2) corresponds to a supertemperature of -12.6%. The margin of safety for -10% supertemperature is high, but because of the uncertainty in predicting minimum supertemperature, a pressure sensor should be used to shut the propulsion system down before critical buckling pressure is reached. A manual remote override should be provided in case the automatic switch malfunctions.

5.1.1.2 Fins. Fin sizing and location, as shown in Figure 5.1, is based on a scale model airship similar to POBAL-S.[15] Total surface area for the cross configured fins is 284.8 m^2 (3,066 ft^2). The mean aerodynamic center is 48.88 m (150.5 ft) aft of the center of buoyancy.

The fins are constructed of biaxially oriented Nylon 6 material and consist of a 25 μm (1 mil) membrane supported by two air inflated cones. The support cone material is 51 μm (2 mil) thick. Physical dimensions of a fin are approximately 5.8 m (19 ft) by 12.2 m (40 ft). The base diameter of a cone is 1.32 m (4.33 ft), and the tip diameter is 0.20 m (0.66 ft).

The cones are separate of the balloon envelope and are pressurized by an air pump, Gast model 0330. Relief valves would be installed on individual fins or within the pressurizing system. The air pump can operate continuously, can pressurize to 68% of ambient pressure, and can develop a flow rate of 9.4 x 10^{-4} m^3/ sec (2 ft^3/min) at no back pressure. Because constant pressure can be maintained, the problem of structural failure due to leakage is avoided.

Since the cones are air inflated separate of the balloon, the critical buckling section will be at the hull/fin interface, providing the cone pressure is always greater than the hull pressure. The maximum allowable differential pressure for an inflated cone is a function of the hoop stress. The hoop stress is [16]:

$$S = pR/(t \cos \Theta)$$

where p is the differential pressure, R is the radius of cir-

[15] McLemore, Clyde H., Wind-Tunnel Tests of a 1/10-Scale Airship Model with Stern Propellers, NASA TN D-1026, Langley Research Center, National Aeronautics and Space Administration. January 1962.

[16] Roark, Raymond J., Formulas for Stress and Strain, McGraw-Hill. 1965.

cumference, t is the material thickness and Θ is the half cone angle.

The maximum allowable differential pressure is reached when the hoop stress equals the allowable material tensile stress, F_t. By rearranging the equation, the maximum inflation pressure is determined by:

$$p' = (F_t \ t \cos \Theta)/R'$$

where the prime designates maximum values.

If the material is stressed to 8,274 N/cm² (12,000 lb/in²), the present conical configuration can withstand a differential pressure of 6,305 N/m² (0.914 lb/in²). This is more than 1.3 times the ambient pressure at 21 km (70,000 ft). Maintaining a cone pressure greater than the balloon pressure is dependent upon the air pump and not limited by the material stress. Based on a supertemperature of 10%, the maximum balloon differential pressure will be 1,330 N/m² (0.193 lb/in²) or less than 0.3 times the ambient pressure.

Since the air pump performance is adequate to maintain a cone pressure greater than the hull pressure, the following analysis takes the hull/fin interface as the critical buckling section.

Air loads are assumed to be distributed as follows:

1. Fin aerodynamic loads are applied evenly along the quarter cord.

2. All loads are reacted at the base of the cones.

3. Deflection of the cone is computed for an evenly distributed load.

4. Skin friction drag of the membrane is neglected.

Since the lift force acts at the quarter cord, the forward cone reacts three-fourths of the load and the aft cone one-fourth. It is only necessary to show the integrity of the forward cone. Critical buckling force is dependent upon the balloon's minimum differential, and is given by:

$$F_b = M_c/.5L$$

where F_b is the buckling force, M_c is the critical bending moment, and L is the inflated length of cone (.5L is used since the load is assumed to be evenly distributed.

The critical bending moment, M, is:

$$M_c = \Delta P \pi R^3$$

where ΔP is the cone differential and R is the cone base cross section radius. Substituting for M_c the equation for critical buckling forces becomes:

$$F_b = 2\pi R^3 \Delta P/L$$

For the present configuration:

$\Delta P = 2.38.5\ N/m^2\ (0.0346\ lb/in^2)$

$R = .66$ m (2.2 ft)

$L = 5.8$ m (19 ft)

The critical buckling load is 73.8 N (16.6 lb). It is a vector sum of three-fourths of the fin lift and all of the aerodynamic drag acting on the cone. An approximate drag force is determined by assuming the cone to be a cylinder with a splitter plate having a C_D value of 0.59[17]. Based on frontal area and 8.158 m/s (15.86 kt) airspeed, the drag force is 9.5 N (2.1 lb). The critical lift force reacted by the cone is:

$$F_{LC} = (73.8^2 - 9.5^2)^{1/2}$$

$$= 73.2\ N\ (16.5\ lb)$$

Since the cone reacts to three-fourths of the aerodynamic lift of the fin, the total lift generated by the fin, L_f is 97.7 N (21.9 lb). This load is the critical buckling lift for the fin.

A maximum allowable angle of attach for the fin can be calulated from:

$$L_f = q a_t \alpha S_t$$

where q is the dynamic pressure, a_t is the fin lift curve

[17]Hoerner, Sighard F., Fluid-Dynamic Drag. 1958.

slope, α is the fin angle of attack, and S_t is the fin area.

The fins are expected to operate with a lift curve slope in the range of 1.7 to 2.9 rad^{-1} (0.03 to 0.05 deg^{-1}). This analysis assumes a value of 2.3 rad^{-1} (0.04 deg^{-1}) for a_t. In addition a 1.5 factor, n, is applied to the critical fin load as a transient condition.

For a velocity of 8.158 m/s (15.86 kn), the angle of attack must be less than 0.16 rad (9.1 deg) to prevent buckling. Since the fins are located on the balloon axis, the angle of attack limitation can be applied directly to the balloon. The additional control provided by the gimbaled thrust vector, should enable the autopilot to maintain an angle of ±.052 rad (±3 deg). The fin design has a margin of safety near 2.0.

The deflection of the beam by the "Method of Dummy-Unit Loads" is evaluated as:[18]

$$Y = \int_0^L \frac{Mm}{EI}\, dx$$

where M is the bending moment in terms of x, m is the bending moment in terms of x due to a unit load acting at the section where y is to be avaluated, E is the modulus of elasticity, and I is the section moment of inertia.

For an evenly distributed load of "w" per unit length:

$$M = wx^2/2$$

and for a unit load at the end point:

$$m = x.$$

Section moment of inertia for a thin film beam is:

$$I = \pi r^3 t$$

where:

$r = .1 + .56\ x/L$ (x_o is opposite cantilevered end)

[18] Bruhn, E.F., Analysis and Design of Flight Vehicle Structures, Tri-State Offset Co., Cincinnati. 1965.

The integral becomes:

$$Y = \frac{L^3 w}{2E\pi t(.56)^3} \int_0^L \frac{x^3\,dx}{(x + .1786L)^3}$$

For the design parameters, the integral yields a deflection of 0.043 m (0.14 ft). Based on test results from pressurized cylinder beams a deflection of 0.15 m (0.49 ft) to 0.23 m (0.75 ft) is predicted.[7] However, the loading condition was an end load versus an assumed distributed load. Classical beam analysis shows the end deflection due to a distributed load to be 37.5% of the deflection due to an end load condition. When this factor is applied to the values predicted by the tests, the deflection range is 0.056 m (0.18 ft) to 0.086 m (0.28 ft). This indicates that buckling will occur before any significant deflection takes place due to cone bending.

5.1.2 Stern Structure

The stern structure houses the power train and the gimbal mechanism which controls the airship flight stability and direction. It is composed of three sections as shown in Figures 5.3 and 5.4. They are designed to react bending, torque, and thrust loads into the envelope. All of the framework is constructed from 6061-T6 aluminum tubing with 1.25 mm (0.049 in) wall. This alloy combines excellent weld properties with good machinability. The design is based upon an engineering stress analysis to show integrity of the structure. The analysis was modeled after a similar effort on a tail mounted gimbaled propeller system using a unit load solution in combination with expected loading conditions[19]. It is expected that the maximum load condition will result from gyroscopic moments and yaw forces on the propeller.

The stern assembly is attached by lacing the battens to the hull. This is a proven design but requires additional rigging time during launch. No attachment should be made to the termination ring since it is not a structural member but is included only to protect the envelope and maintain batten rigidity during launch.

---

[19] Soudry, J. G., Structural Analysis Report, Silent Joe II Program, GER 14356, Goodyear Aerospace Corporation, Advanced Research Projects Agency, Order No. 1255. 29 April 1969.

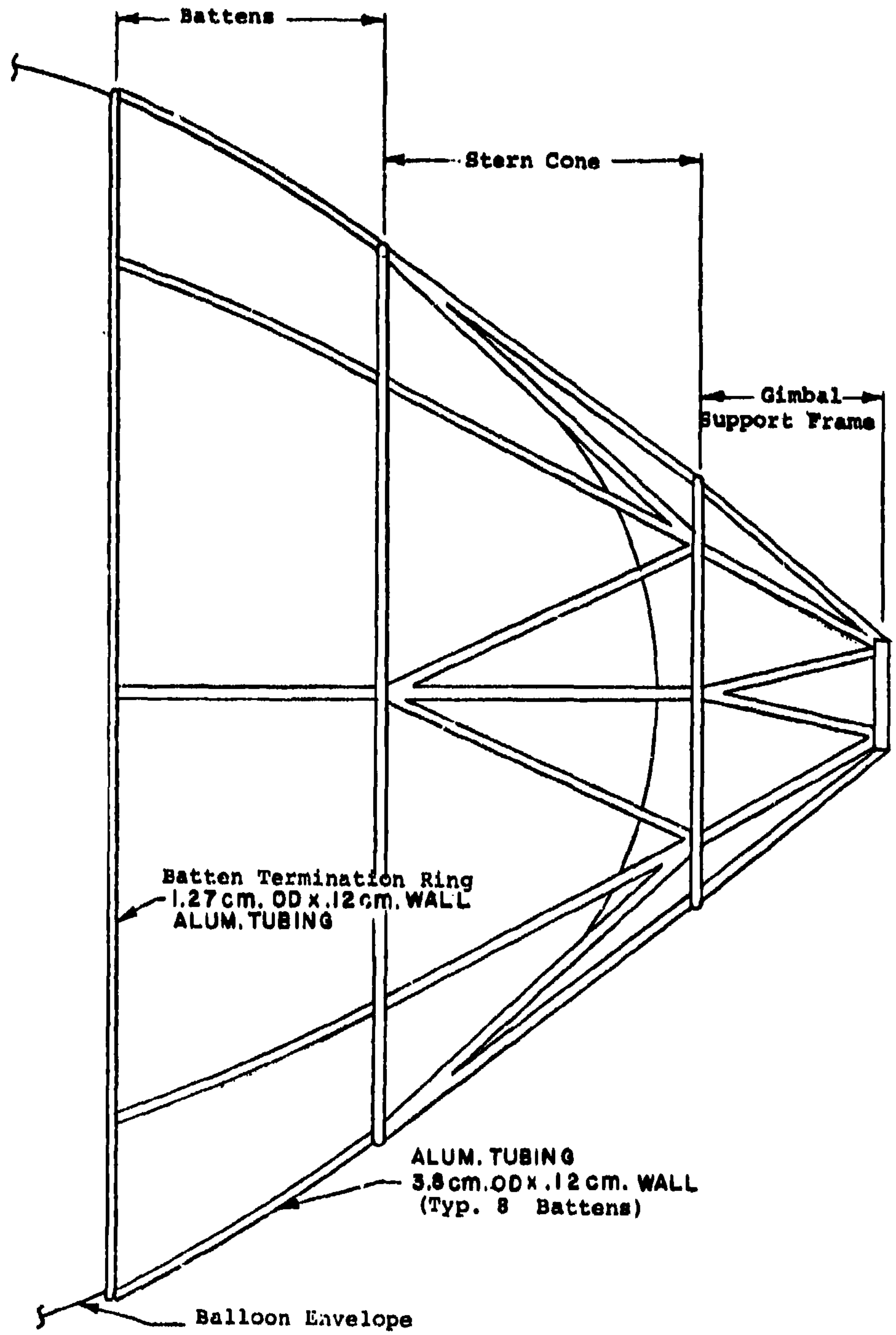

Figure 5.3 Stern structure, side view.

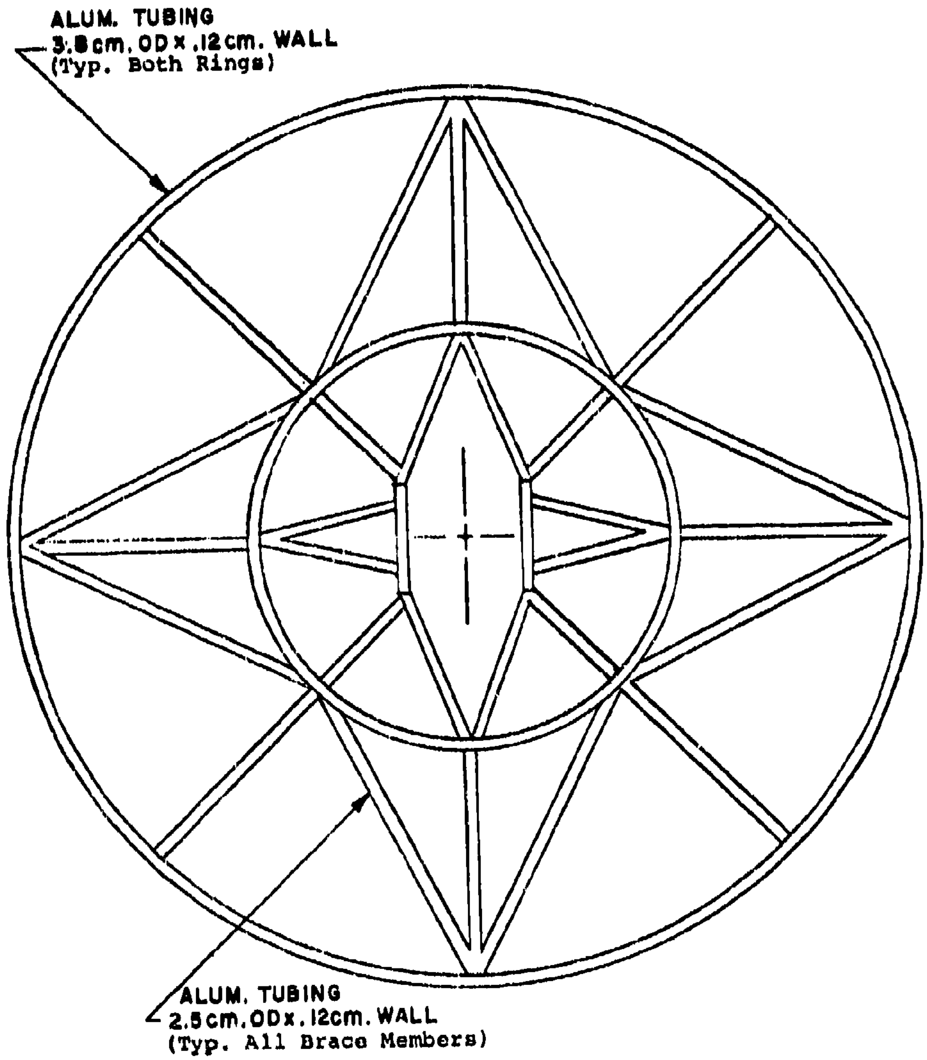

Figure 5.4 Stern structure, end view

5.1.3 Gondola

The gondola houses the fuel cell with associated hardware and fuel tanks, the payload, the command telemetry system, control unit, and the autopilot. Pratt & Whitney derived the original design of the framework under a subsequent contract with the sponsor; and except for some changes in the framework, the design shown in Figure 5.5 is essentially identical to the original design[20]. One of the primary purposes of the expendable membrane support is to protect the fuel cell, associated hardware, and payload upon termination of the mission as discussed in Section 5.5. When the flight is terminated the entire gondola will be parachuted back to earth. Since high winds may be encountered upon descent, the impact vector may be as much as .79 rad (45 deg) causing the gondola to roll after impact. Thus, the parachute will be cut loose upon impact, preventing the gondola from being dragged. The landing shock of the gondola will be attenuated by the aluminum radiator panel, the crushable aluminum honeycomb base, the external frame, and the elastomeric shear mounts.

The water storage bag will be fabricated from 1.7 N/m^2 (5 oz/yd^2) urethane coated nylon fabric. This bag will store approximately .205 m^3 (45 gallons) of water which is to be discharged by the fuel cell.

The total weight is 5,007 N (1,126 lb) when the expendable membrane support, housekeeping electronics, and parachute are all accounted (See Section 5.1.4). The center of gravity of the gondola is located 35.9 m (118 ft) from the nose of the balloon as shown in Figure 5.1. The C.G. is maintained in the same position horizontally but shifts approximately 0.18 m (7.1 in) down as the fuel is consumed.

The gondola is suspended beneath the balloon by a distance equal to the height of the gondola in order to minimize drag and reduce the tension on the load lines. This results in the suspension lines pulling at an angle of .93 rad (53.5 deg) from the vertical as seen in Figure 5.6. The total load in the suspension lines is 8675 N (1950 lb) and one-half of this load is transmitted into each side of the

[20] Handley, L. M., Study of Fuel Cell System for Powered Balloon, PWA-4792, Pratt & Whitney Aircraft. Air Force Cambridge Research Laboratories, AFCRL-TR-73-0447. September 1973.

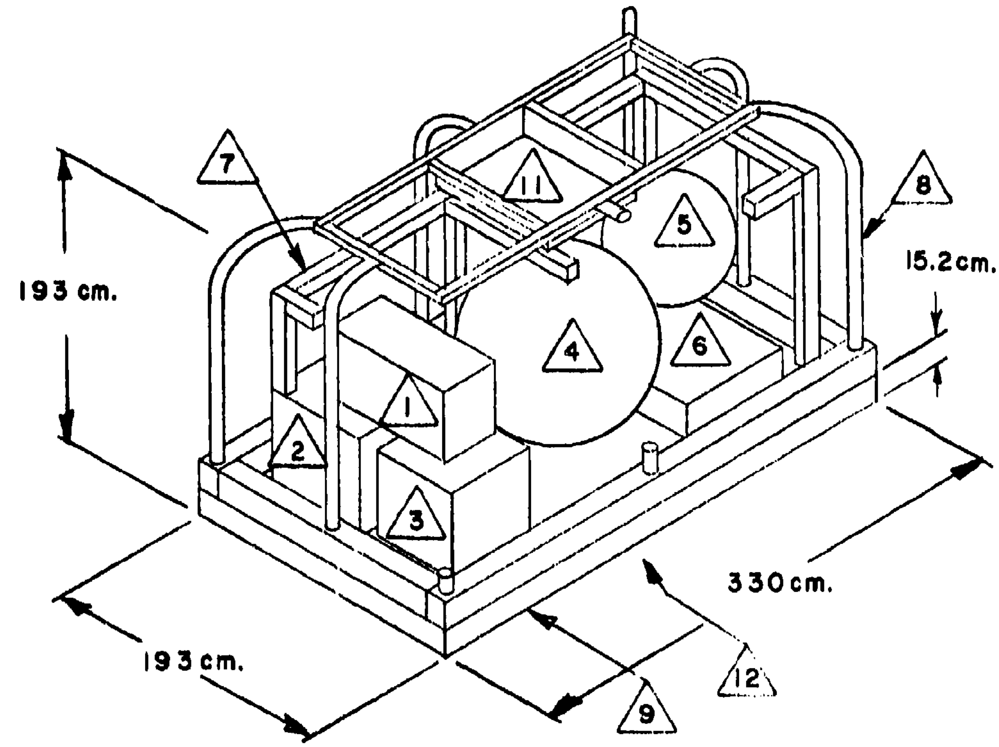

1 Fuel Tank
2 Payload
3 Housekeeping
4 H_2 Tank
5 O_2 Tank
6 H_2O Bag
7 Support Frame
2.5 cm. Alum. Sq. Tubing
8 Roll Cage
1.58 cm. O. D. Alum. Tubing
9 Honeycomb Base
10 Honeycomb Bumper
11 Parachute Box
12 Radiator (Below Base)

Figure 5.5 Gondola.

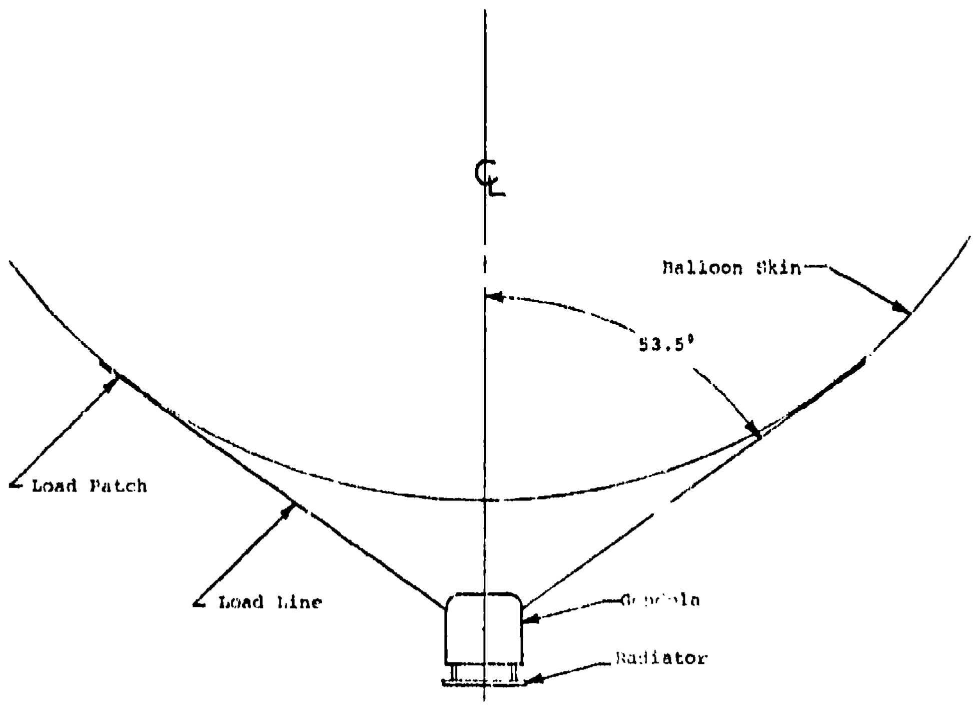

Figure 5.6 Gondola suspension, end view.

balloon. To prevent overstressing of the envelope under pressurized conditions the hull in this area is designed with 203 μm (8 mil) instead of 152 μm (6 mil) material (See Figure 5.3).

Three load patches on either side of the gondola, as shown in Figures 5.1, 5.6 and 5.7, are used to hold the gondola. The load patches would be constructed from a high strength nylon fabric and would be adhered to the balloon skin using a liquid adhesive.* The patch would be of a catenary type construction with nylon webbing sewn along the parabola to distribute the load uniformly throughout the patch. Load lines, which would be lightweight steel cables, would lead from a "V" ring on the patch to an eyebolt on the edge of the platform.

Seven additional patches, two on each side and three directly over the gondola, will be used during the launch sequence. These are shown in Figure 5.6 and are discussed further in Section 5.5.

5.1.4 Weight Summary and Distribution

Table 5.1 summarizes the system weights; i.e., a breakdown of the weights of major vehicle components along with weights of components contained within the structure. The horizontal position of the center of gravity is also presented. The center of gravity distances are measured from the nose of the airship. The airship center of buoyancy is located at 49.9 m (164 ft) from the nose. Vertical alignment of the airship center of gravity to the center of buoyancy determines the gondola location.

5.2 Propulsion Drive Train

The propulsion drive train consists of the motor, speed reducer, and propeller with the electrical energy being supplied by the fuel cell which is discussed in Section 5.5.1. The framework which houses the drive train was discussed in Section 5.1.2. The following is a summary of the drive train power allocations:

---

*Tests were performed to determine structural integrity of the patches. These tests are reported on in Appendix B.

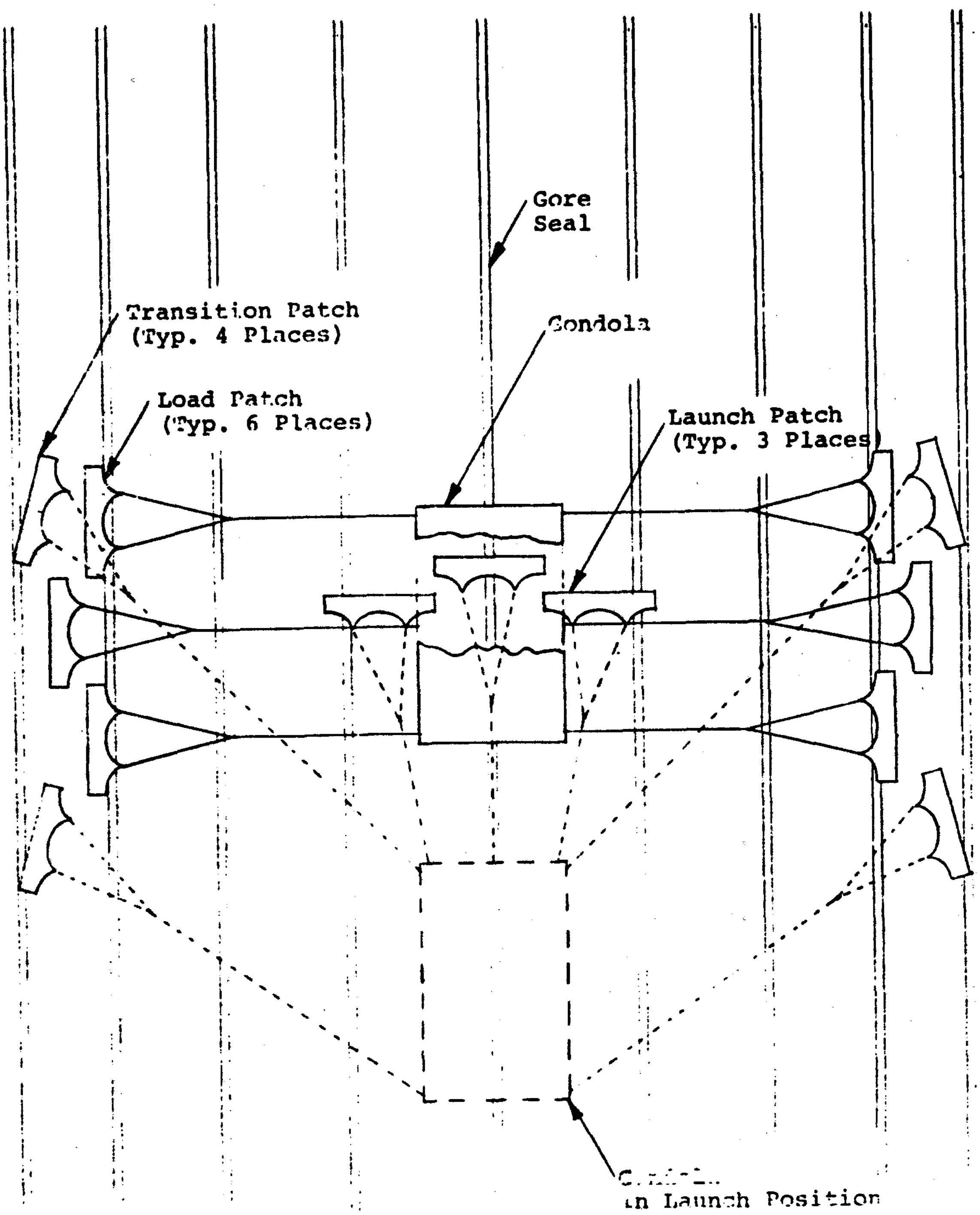

Figure 5.7 Patches for gondola suspension.

Item	Weight* (N)	C.G. (m)
Balloon		
Fins	168.7	98.20
Hull	12,039.8	50.92
Total Balloon	12,208.5	51.57
	(2,744.7 lb)	(169.20 ft)
Stern Structure		
Motor	34.3	
Converter	222.7	
Gimbal Motors	3.9	
Speed Reducer	68.7	
Structure	192.3	
Prop	196.2	
	718.1	113.84
	(161.4 lb)	(373.51 ft)
Gondola		
Payload	889.8	
Housekeeping Electronics	290.4	
Fuel Cell	636.1	
H_2 Tank (Full)	685.0	
O_2 Tank (Full)	1,650.2	
Water Bag (empty)	22.2	
Radiator	97.9	
Piping and Wiring	66.7	
Frame Structure	348.1	
Parachute Assembly	311.0	
Total Gondola	5,007.4	35.9
	(1,125.8 lb)	(117.8 ft)
Wire, Gondola to Motor	216.8	74.0
	(48.7 lb)	(242.8 ft)
Total System Weight	18,150.8	49.9
	(4,080.7 lb)	(163.6 ft)

*All weight calculations assume the acceleration due to gravity to be 9.81 m/s^2. This estimates the gravitational forces to be 0.7% greater than actually experienced at float altitude.

TABLE 5.1 SYSTEM WEIGHT SUMMARY

	Input Power	Efficiency	Output Power
Motor	1.80 kW	75%	1.35 kW
Speed Reducer	1.35 kW	96%	1.30 kW
Propeller	1.30 kW	78%	1.01 kW

5.2.1 Propulsion Motor

The propulsion motor preliminary design was furnished by Lear Motors Corporation. Several motor vendors had been contacted, and this particular design appeared to be most advantageous. The prime factors in the selection of the propulsion motor, in addition to the normal considerations of power, speed, etc., were efficiency, weight, and high altitude capability. It was felt that the high altitude capability could best be provided by a brushless DC motor. Most brushless motors consist of an electronic unit and a rotating machine. It is beneficial to have the mass of the rotating machine very small in order to provide flexibility in the design of the gimbaled structure. The brushless concept fits this need nicely by having an electronic converter unit which may be located remotely from the rotating machine if desired. Also, the motor is very light weight and small in size. A specific advantage of the Lear Reno motor is the ability to start and stop the motor with a 0-5 VDC, TTL (transistor-transistor logic) compatible logic signal. This eliminates the heavy contactors required to start and stop other types of propulsion motors. It should be noted that this feature is available due to the use of transistors as switches in the electronic converter. A more powerful motor would necessitate the use of SCR's (silicon controlled rectifiers), which are difficult to turn off, and thereby, require external circuity involving power losses and weight penalties.

The Lear design is not the DC to AC inverter driving an AC motor scheme used by many brushless motor manufacturers. Instead, a patented means of electronic commutation is employed. The efficiency of the Lear motor and electronics was the highest of all motors. The proposed design develops 1.35 kW (1.81 hp) at a speed of 1050 rad/s (10,000 rpm). The current drain is 60 A steady state at 30 VDC and 72A while starting.* The start-up time of the motor under full

*The design received from Lear Motors Corporation was based on 24 VDC operation. The value for current has been adjusted for 30 VDC operation.

load is estimated to be three minutes maximum. Size 00 copper wire is proposed to carry current from the fuel cell to the motor. This wire has a weight of 5.9 N/m (0.404 lb/ft), and two wires are required. The efficiency of the motor, including its electronic converter, is 75%. The size of the motor is 12 cm dia x 12 cm (4.7 in dia x 4.7 in) and the converter is 32 x 32 x 16 cm (13 x 13 x 6.3 in). The total weight is 247 N (58 lb) and the heat sink requirements are 216 W at 50°C for the converter plus 245 W at 90°C for the motor. Figures 5.8 and 5.9 show physical characteristics of the motor and converter respectively. Performance characteristics are shown in Figure 5.10.

5.2.2 Speed Reducer

A speed reducer with a reduction ratio of 133:1 is required to interface the 10,000 rpm motor with the 75 rpm propeller. Figures 5.11 and 5.12 illustrate the proposed belt type reducer. The Gates Rubber company was contacted for design information concerning sheave diameters, size of belts, belts per stage, and number of stages for optimum efficiency. The three stage reducer will have an operating life of 4000 hours at 96% efficiency. Maximum allowable temperature for continuous operation is 82°C. Physical size is estimated to be 36 x 34 x 18 cm (14 x 13 x 7.1 in) and the weight is estimated at 68.7 N (15.4 lb).

5.2.3

Sensenich Corporation provided the aerodynamic design of the propeller to be used on POBAL-S. The design was based upon requirements furnished by Raven plus the flow distribution into the propeller disc area based upon tests performed on a tail powered airship model.[15]

The basic design details are as follows:

Number of blades	3
Diameter	10.36 m (34.0 ft)
Rotation speed	75 RPM
Thrust	119 N (26.8 lb)
Efficiency	78%
Volume of each blade	0.3613 m^3 (12.76 ft^3)
Surface area of each blade	7.273 m^2 (78.29 ft^2)

Figure 5.13 shows the propeller outline with sections. The graphs of Figure 5.14 show the distribution of surface

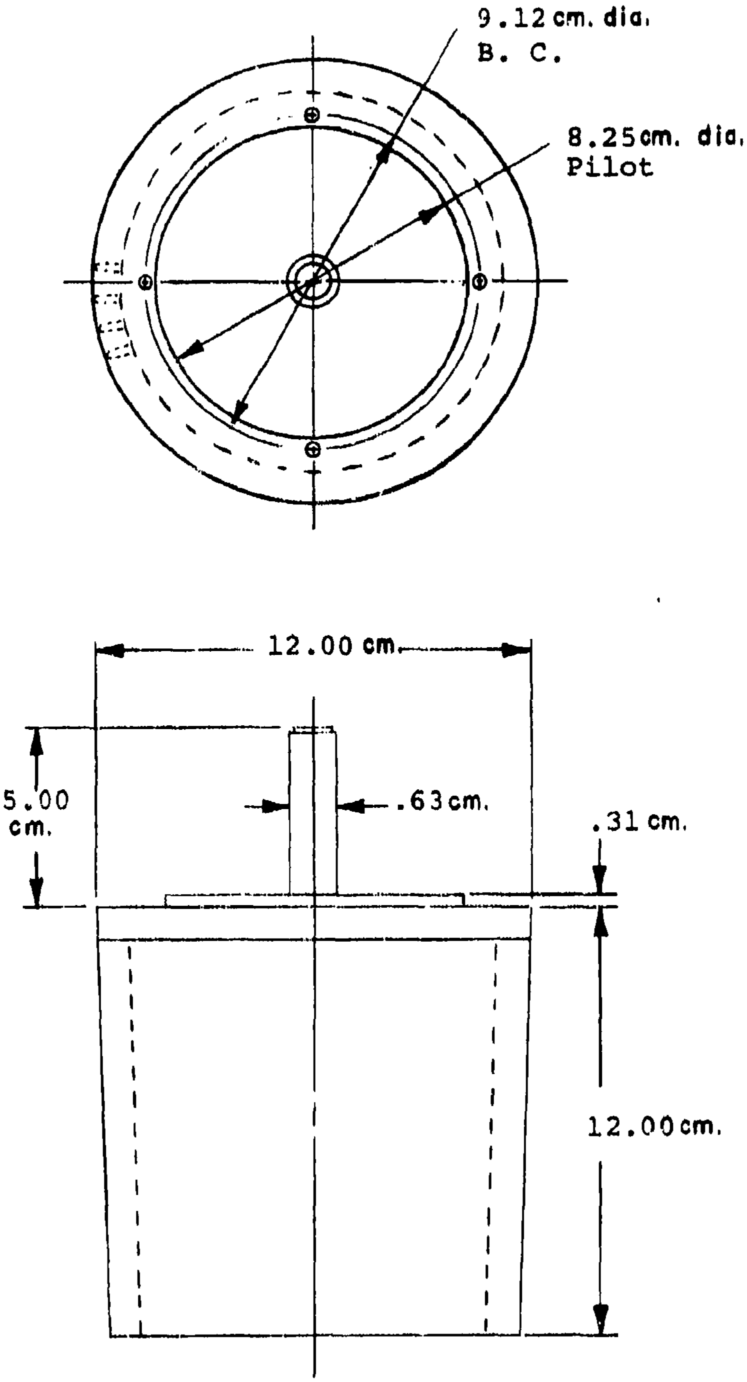

Figure 5.8 Motor configuration.

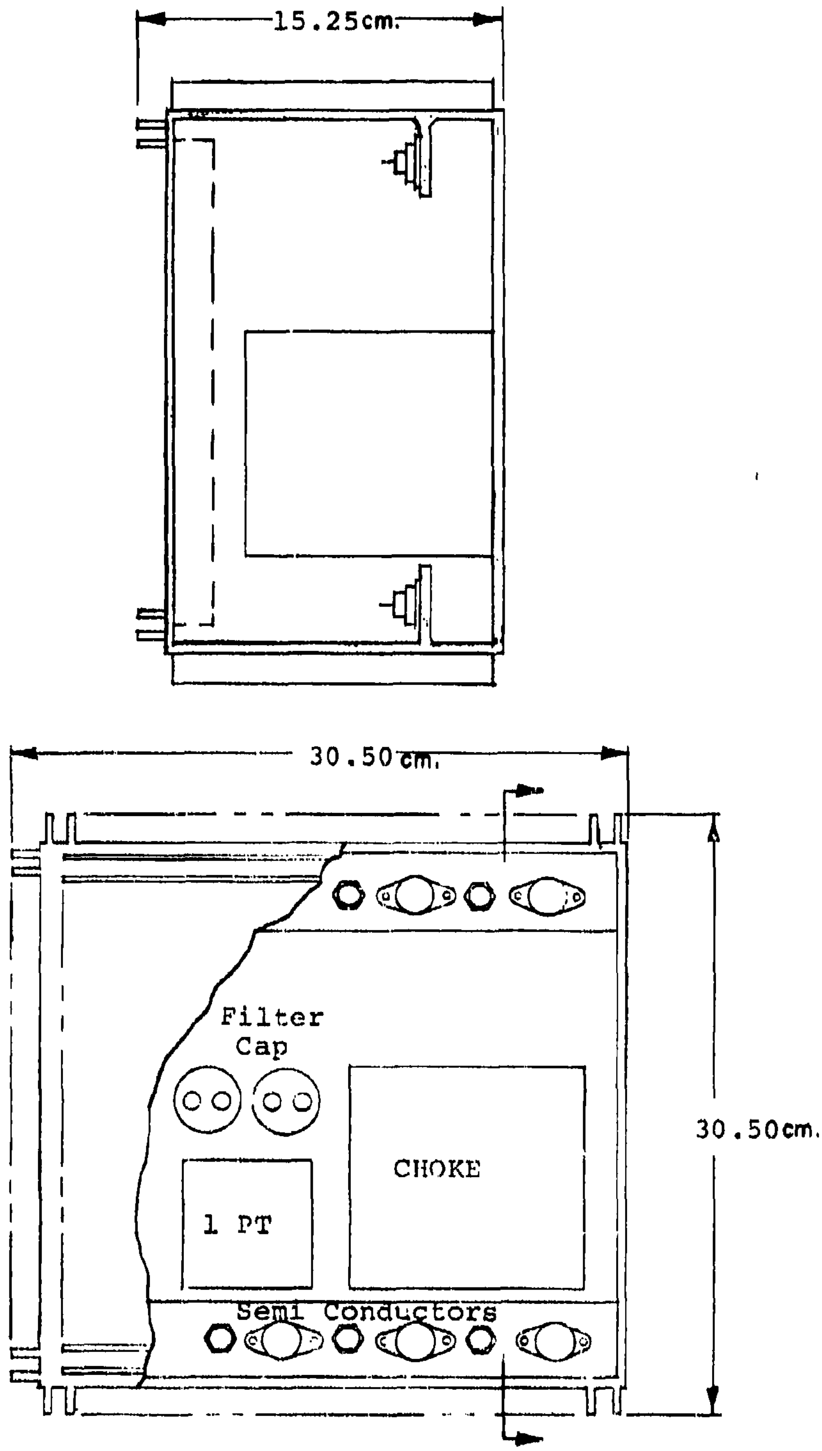

Figure 5.9 Converter configuration.

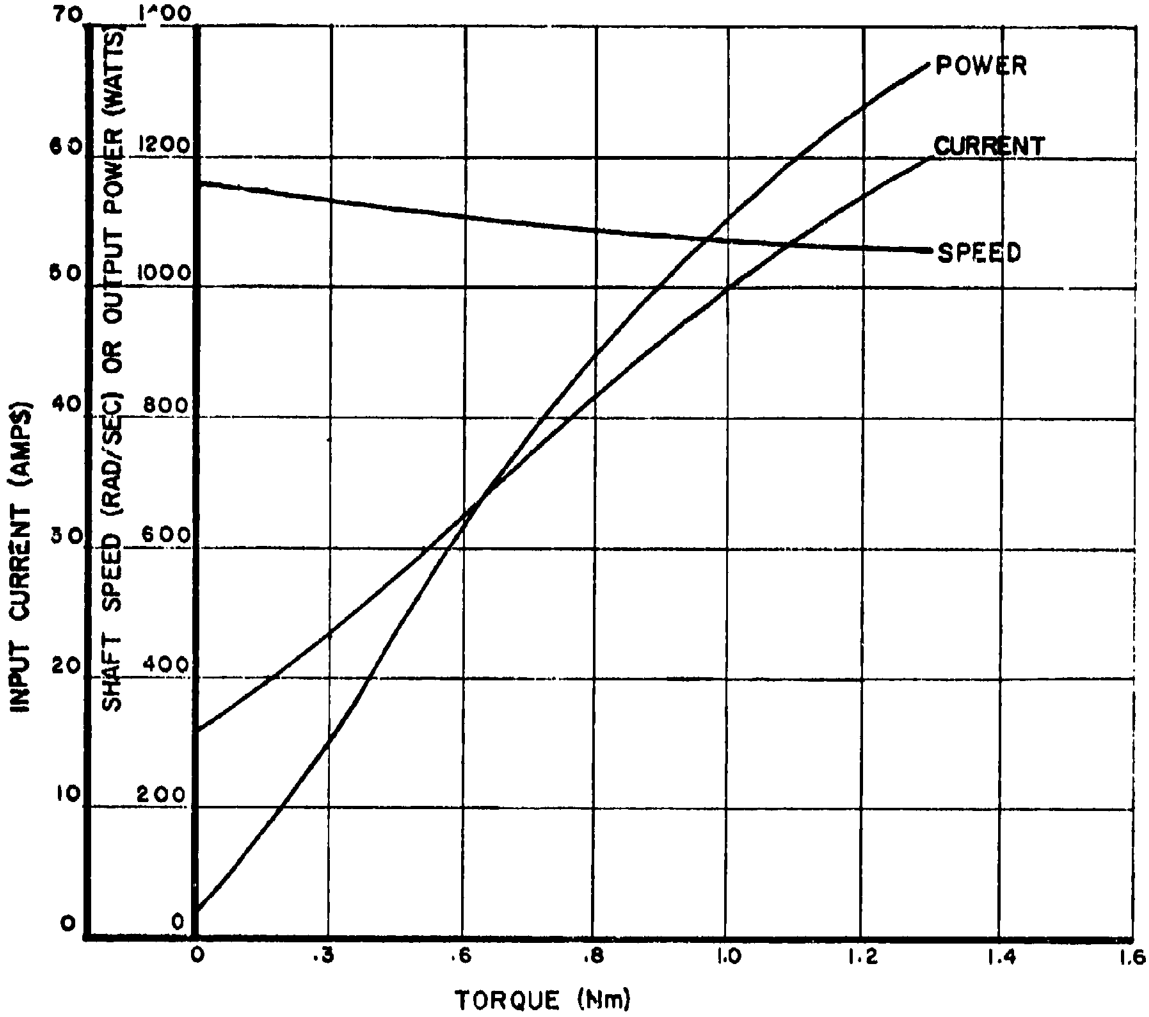

Figure 5.10 Motor performance characteristics.

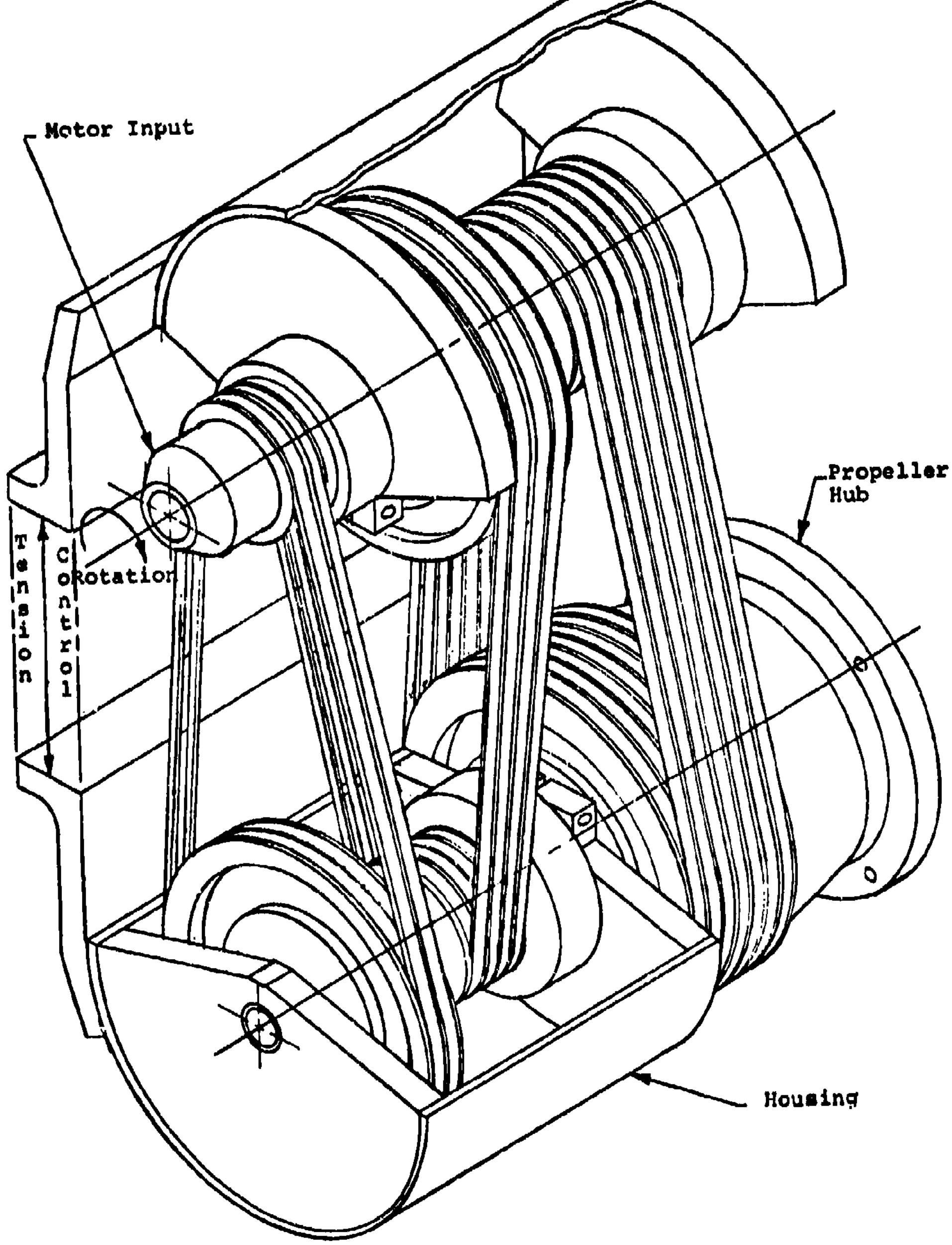

Figure 5.11 Speed reducer.

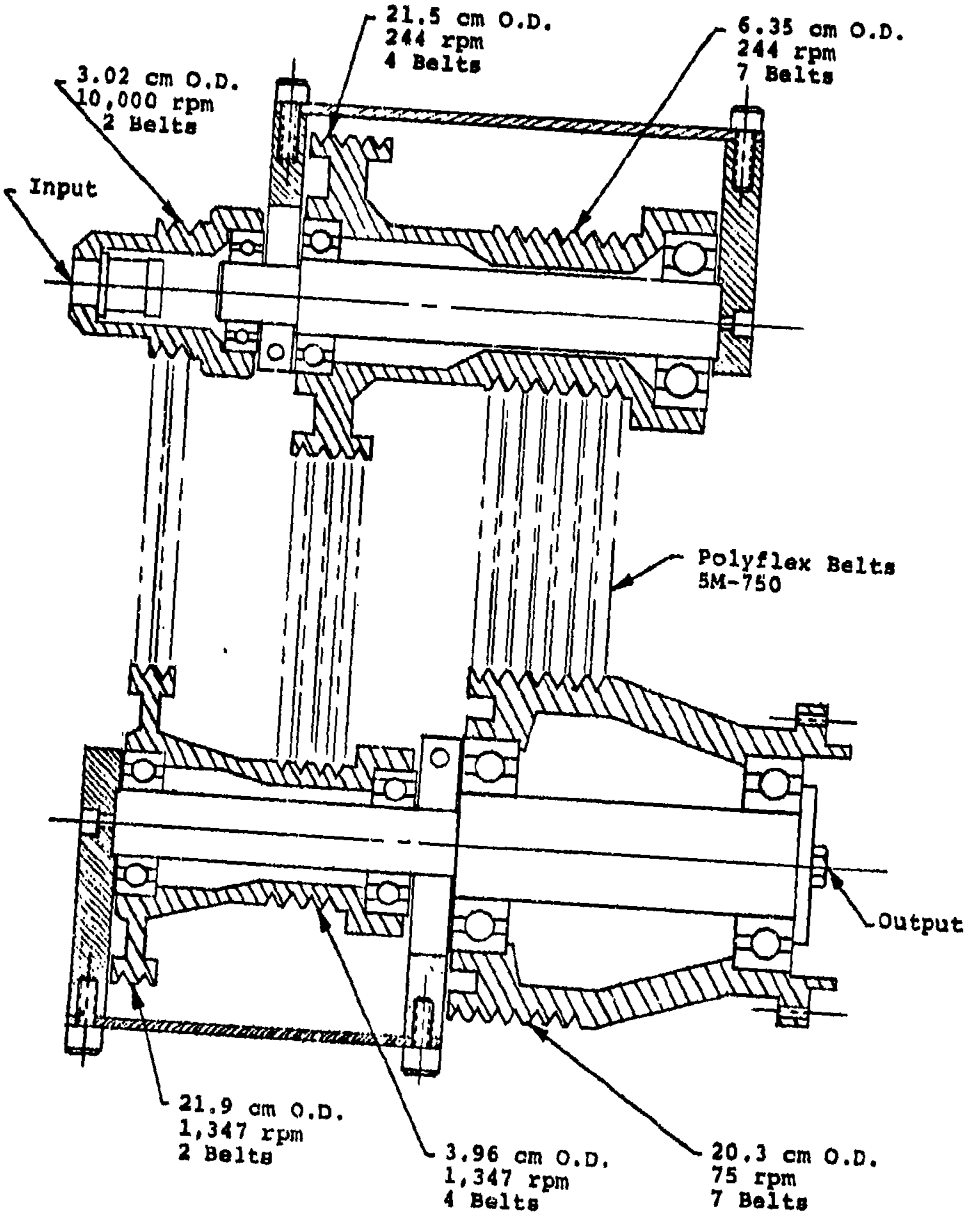

Figure 5.12 Speed reducer, section view

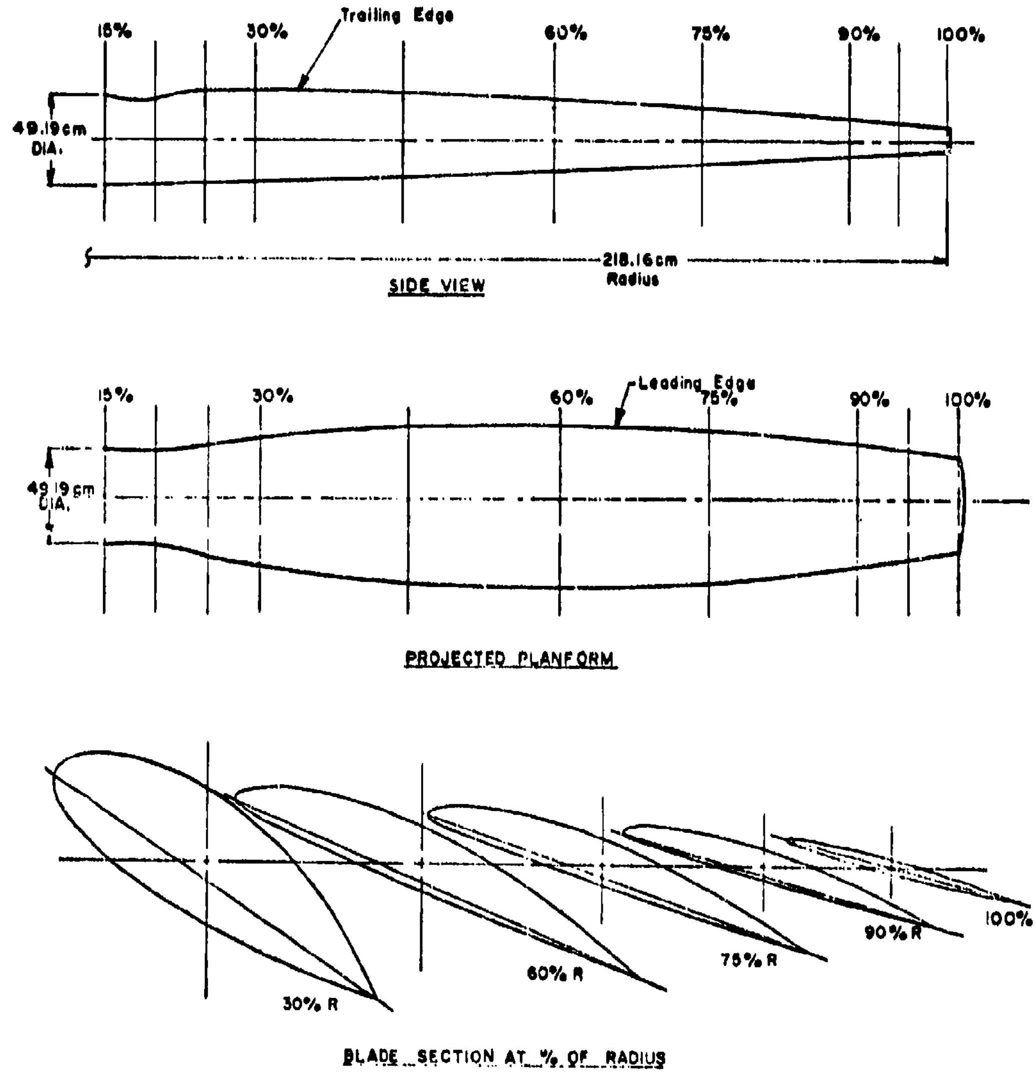

Figure 5.13 Propeller blade shape.

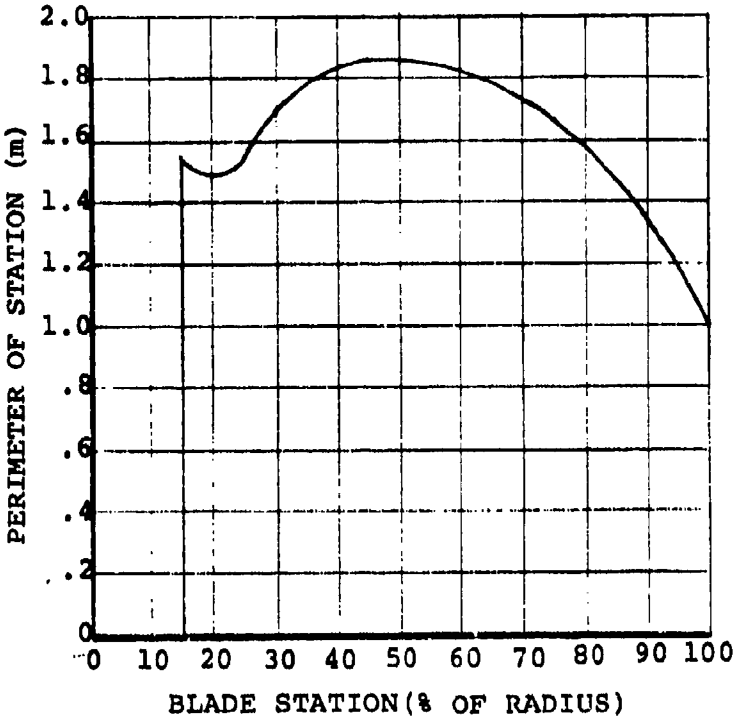

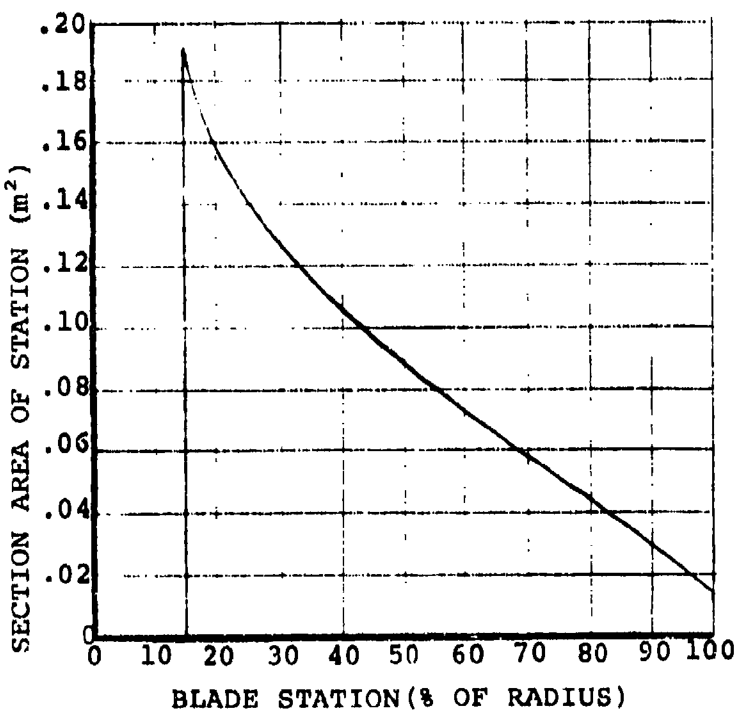

Figure 5.14 Propeller blade perimeter and section area for determination of blade surface area and volume.

area and volume elements of each propeller blade.

The fabrication design was derived at Raven Industries and is based upon past experience using two and three bladed light weight propellers. Because of the size of the propeller required to efficiently propel the airship at these altitudes it is essential that extreme weight saving techniques be used. Consequently, the propeller will be constructed utilizing 6.4 mm thick x 6.4 mm cell (.24 in thick x .25 in cell) Hexcell honeycomb of .018 mm (.0007 in) aluminum with face sheets of .051 mm (.002 in) Mylar and .127 mm (.005 in) aluminum as shown in Figure 5.15. Honeycomb design and construction is more detailed than other types of structure, however, it represents the best choice when a high stiffness to weight ratio is required. Until the fabrication technique is actually tested, the weight of the propeller cannot be accurately estimated, but based upon the recommended construction the estimated weight is 196 N (44 lb).

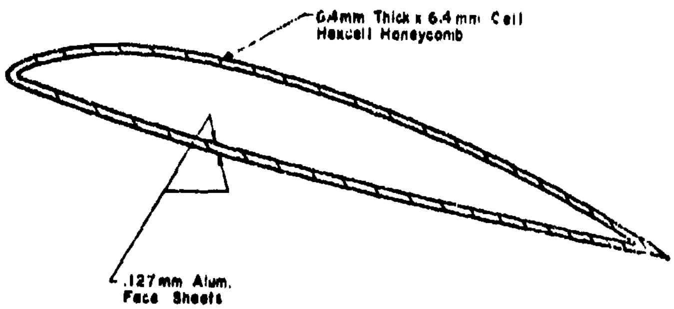

Figure 5.15 Propeller blade construction.

5.2.4 Thermal Analysis

A simplified thermal analysis has been performed to determine if special precautions will be necessary in controlling the operating temperature of the motor or speed reducer. The analysis accounted for heat dissipation only through radiation. Consequently, the temperature estimates are higher than would actually be experienced since convective and conduction heat losses are ignored.

The motor, electronic converter, and speed reducer were considered as a single unit mounted on a common heat sink. The maximum allowable operating temperatures are 90°C for the motor, 50°C for the converter, and 82°C for the speed reducer. The radiating surface areas were estimated as 452 cm^2 (70 in^2), 3072 cm^2 (476 in^2), and 3165 cm^2 (491 in^2) respectively for a total of 6689 cm^2 (1037 in^2).

The radiation impinging the unit is considered to be 1390 W/m^2 (129 W/ft^2) solar, 119 W/m^2 (11 W/ft^2) albedo, and 250 W/m^2 (23 W/ft^2) terrestial. The absorption factor is estimated to be that of a white body, 0.22 for solar or albedo and 0.98 for terrestial.[21] The absorption area is considered to be one half of the total radiating area for solar and albedo radiation which results in heat inputs of 102 W solar and 9 W albedo. The absorption area for terrestial radiation is estimated to be 1510 cm^2 (234 in^2) which results in 37 W terrestial input. The internal heat generated by the motor (with converter), and speed reducer is estimated to be 500 W. Thus, the total heat input is 648 W. Using an emittance of 0.92 for a white body at 50°C in the Stefan-Boltzman equation, the total radiating surface area required is estimated to be 11,410 cm^2 (1769 in^2) which is almost twice the radiating area available.[21]

It appears that special precautions may need to be taken to avoid overheating any of the power train components. Several solutions can be considered, such as, separating the converter from the motor and speed reducer, shading the unit from solar radiation, using various coatings for thermal control, increasing the radiation area, or any combination of the above alternatives. However, a more exact analysis should be performed prior to incorporating any of these alternatives.

5.3 Flight Control System

The purpose of the flight control system is two-fold; it keeps the airship stable, and it permits remote control of the flight course. Although lighter than air vehicles move slowly, they require some form of control to achieve stable flight. The flight control system consists of a two-axis gimbal mechanism which is driven by an autopilot and associated sensors. The propulsion motor is mounted on a platform which is gimbaled to provide pitch and yaw devia-

[21] Van Vliet, Robert M., Passive Temperature Control in the Space Environment, MacMillan & Co., 1965.

tions. This structure is discussed in Section 5.4. Reversible electric gimbal motors drive rotary-to-translational actuators which are essentially independent of each other. A block diagram of the control system is shown in Figure 5.16. Each channel is a servo-system which reacts to an error signal that represents the difference between a desired attitude and the actual attitude. Also, rate damping is provided to prevent oscillations.

The estimated gimbal design characteristics are as follows:

Gimbal position range = ±0.785 rad (±45 deg)

Maximum gimbal rate = 0.0524 rad/s (3 deg/s)

Maximum acceleration = 0.00873 rad/s^2 (0.5 deg/s^2)

Gimbal lever arm = 17.8 cm (7.01 in)

Gimbal friction torque = 2 Nm (1.47 ft-lb) @ 0.0524 rad/s

Gimbal static moment of inertia = 167 Nms^2 (123 ft/lb/s^2)

Propeller gyroscopic torque on gimbal = 81.6 Nm (60.2 ft-lb)

Gimbal position deadzone = 0.008 rad (0.458 deg)

Using these estimates, the preliminary design of the control system was completed. In the final design and stability analysis these values would be expected to change slightly. In the following sections each servo loop is examined in greater detail.

5.3.1 Gimbal Mechanism

The gimbal mechanism of the control system contains the mechanical components represented in Figures 5.16 and 5.17. Mechanical parts include the gimbal motor, actuator, and position transducer. The yaw axis is formed by gimballing the propulsion assembly within the gimbal frame. A ballscrew operating between the frame and speed reducer housing provides yaw control. The pitch axis is made independent by gimballing the frame within the support structure. Pitch control is provided by a ballscrew operating between the support structure and a lever attached to the pitch shaft. The key factors in this mechanism are reliability and mini-

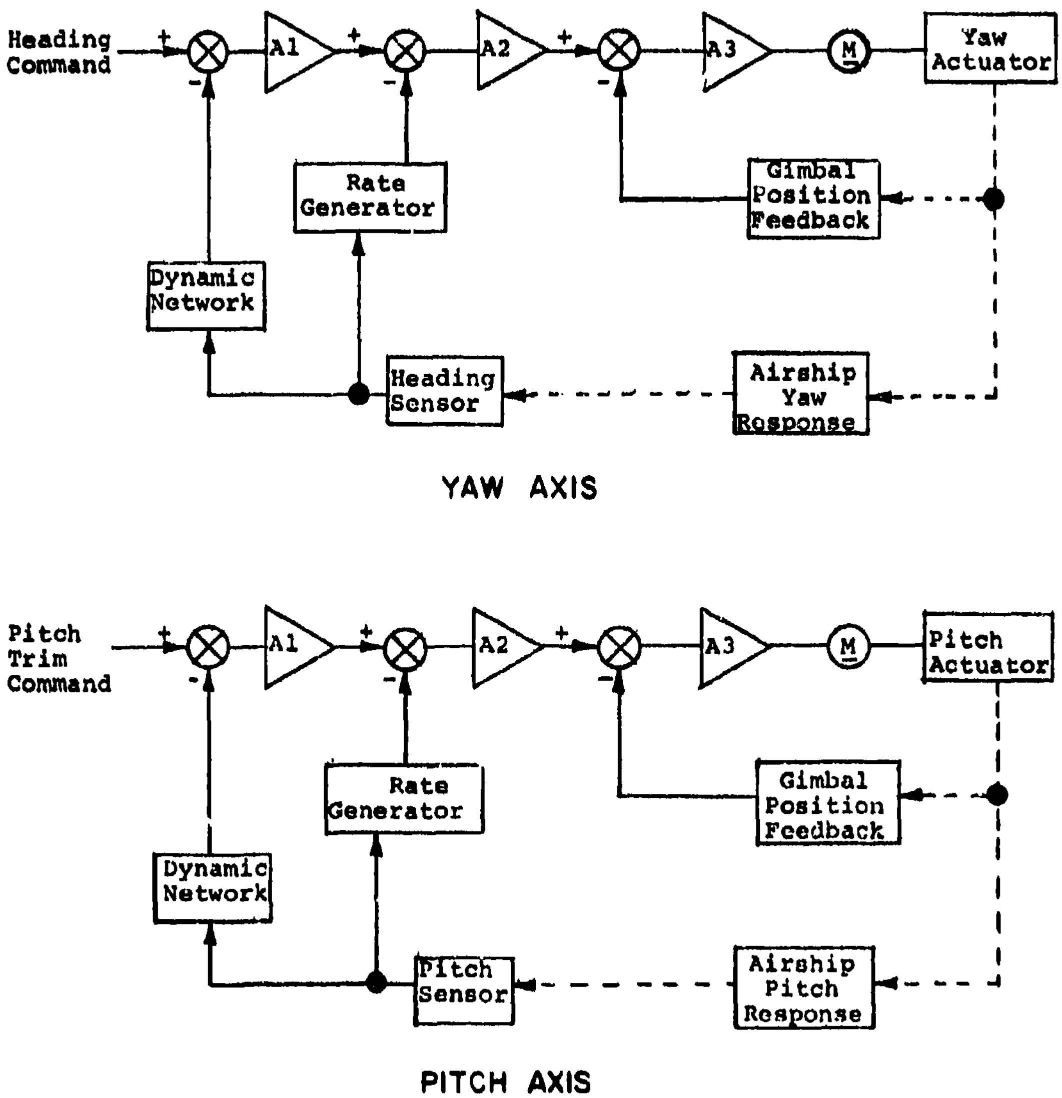

Figure 5.16 Flight control system block diagram.

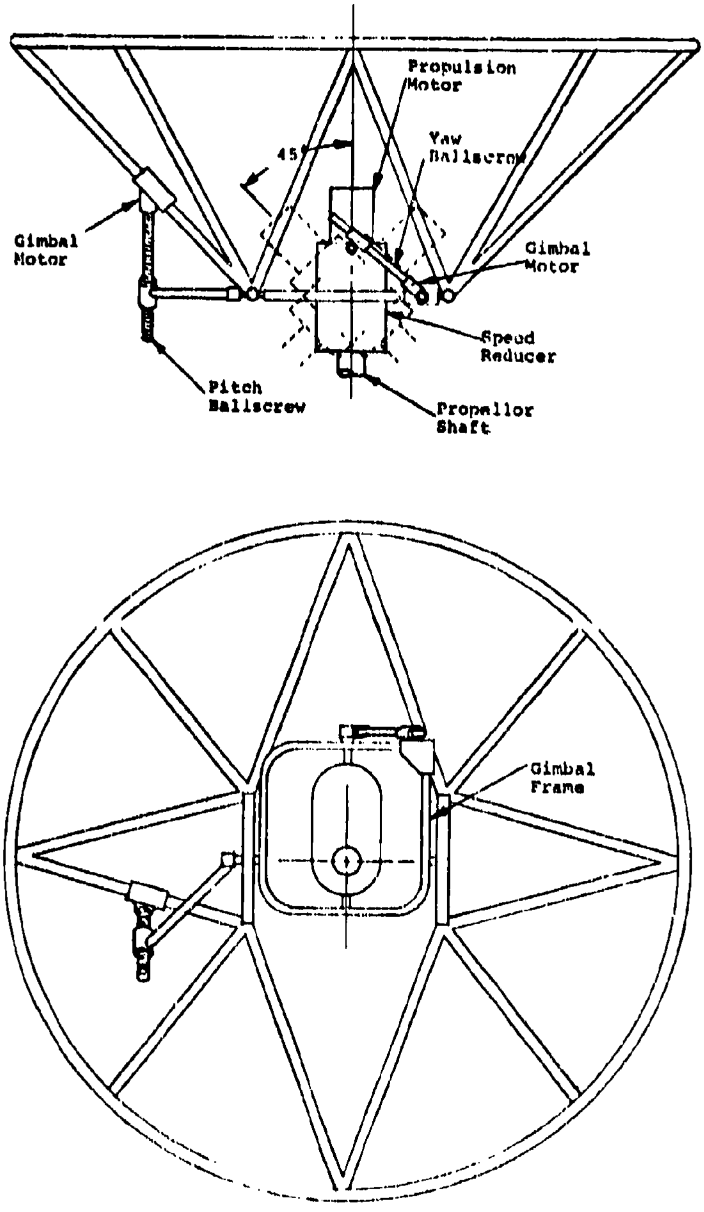

Figure 5.17 Gimbal mechanism.

mum weight.

The gimbal motor chosen is a DC, permanent magnet, high speed motor with a reducing gearhead attached. The high speed motor with gearhead has a low starging threshold. good position accuracy, and moderate starting torque. Figure 5.18 is a representation of the gimbal position loop including the servo amplifier. The transfer function for the mechanical portion of this loop was developed as:[22]

$$\frac{\Theta_G(S)}{\Theta_m(S)} = \frac{K}{T^2S^2+2\zeta TS+1}$$

where:

$$K = \frac{L}{K_gK_L}$$

$$T = \sqrt{\frac{J_GL^2}{2\pi\eta K_L^2K_s}} = \frac{L}{2.51K_L}\sqrt{\frac{J_G}{\eta K_s}}$$

$$2\zeta T = \frac{K_DL}{K_sK_L}$$

$$\zeta = \frac{K_DL}{K_sK_L2T}$$

Θ = angular displacement

η = efficiency of the ballscrew

G = subscript denoting gimbal

J = moment of inertia

K_D = damping coefficient due to kinetic friction

K_g = step down ratio of gearhead

---

[22] Beemer, Jack D., et al., POBAL-S R & D Design Evaluation Report, Part II, Report No. 0673006, Raven Industries, Inc. Air Force Cambridge Research Laboratories, Contract No. F-19628-73-C-0076. 6 July 1973.

K_L = length of lever arm

K_S = twist of shaft

S = the Laplacian operator

L = lead of the ballscrew (linear motion per revolution)

m = subscript denoting motor

The total starting moment of inertia of the gimbal is:

$$J_G = J_I + J_P$$

where J_I is the moment of inertia required to overcome the inertia of the gimbaled mass and J_p is the moment of inertia required to balance the gyroscopic torque forces caused by the gimbaling of the spinning propeller. Friction is assumed to be negligible at this point. The J_I term is estimated to be 167 Nms^2 (123 $ft/lb/s^2$), and J_p is calculated to be 9347 Nms^2 (6895 $ft\text{-}lb\text{-}s^2$) which yields a value of 9514 Nms^2 (7018 $ft\text{-}lb\text{-}s^2$) for J_G.

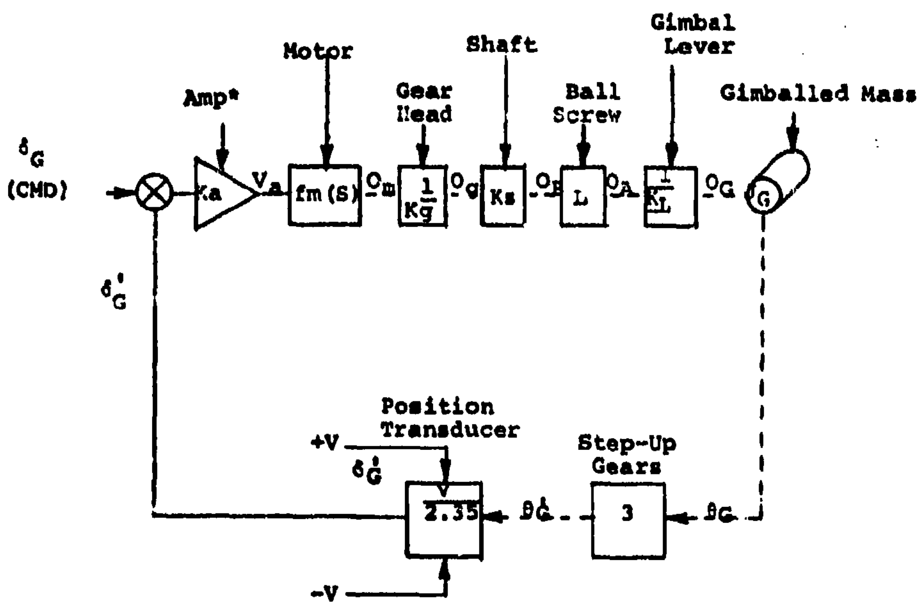

Figure 5.18 Gimbal position loop.

The K_s factor represents a torsional displacement in the gearhead shaft and was computed to be 3.90 x 10^{-4} Nm/rad (251 ft-lb/deg). The K_D parameter is a gimbal damping constant which is very difficult to predict. It is primarily dynamic friction of the gimbal bearings and will be highly dependent on lubricant and temperature. By estimating the required gimbal torque, T, to be 2 Nm (1.5 ft-lb) at an angular velocity, ω, of 0.0524 rad/s (3.0 deg/s) K_D is:

$$K_D = \frac{T}{\omega} = 38.2 \text{ Nms } (28.2 \text{ ft-lb-s})$$

The ballscrew selected is Saginaw Steering Gear type 0500-0125-SGT. It has a lead of 3.18 mm/rev (0.124 in/rev), a 1.3 cm (0.5 in) diameter shaft, and must be at least 28 cm (11.0 in) long. At that length the ballscrew can withstand 4450 N (1000 lb) compression load and travel at 25.4 cm/s (10 in/s). The gimbal lever arm required is 17.8 cm (7.01 in) long, which means the travel rate would be approximately 0.93 cm/s (0.37 in/s) to achieve 0.0524 rad/s (3.0 deg/s). This is well within the rated capabilities of the ballscrew. The SGT series is a standard ground thread model which has a backlash assumed to be tolerable. If deadzone is a problem in the final design, there are other ballscrew models available with preloading to further reduce backlash.

The motor-gearhead combination selected is a Globe Motors Part No. 54539-10 which has the following characteristics:

Input Voltage: 24 VDC

No Load Motor Speed: 942 rad/s (8,996 rpm)

Armature Inertia: 3.7 x 10^{-7} Nms^2 (2.7x10^{-7}ft lb 5^2)

Input Current: 0.45 A

Output Shaft Size: 0.794 cm (0.313 in) dia. x 1.27 cm (0.50 in) long

Size: 3.175 cm (1.24 in) dia. x 7.34 cm (2.89 in) long

Breakaway Voltage: 3.6 VDC

Mass: 0.2 kg

Torque Ratio: 17

Speed Ratio: 27.94

Efficiency: 40%

Motor Torque: 0.00706 Nm (1 oz-in)

The motor speed at rated load is approximately 640 rad/s (6400 rpm). The actual gimbal rate produced with this design is 0.0681 rad/s (3.9 deg/s) which is greater than the minimum requirement 0.0524 rad/s (3.0 deg/s). The motor transfer function was calculated to be:[22]

$$\frac{\Theta(S)}{V(S)} = \frac{24.8}{S(1 + 0.445\ S)} \quad \frac{rad/s}{V}$$

The most common feedback transducer used in servo loops is a potentiometer. These are normally high quality linear devices which are available from many manufacturers. The step-up gears are used to drive the position feedback potentiometer in order to economically get maximum resolution. Typically, single turn units have 4.71 rad (270 deg) of rotation, and the gimbal swing is 0.785 rad (45 deg) or a total of 1.57 rad (90 deg). Therefore, a step-up of 1:3 may be used. Referring to Figure 5.16 the feedback transducer output is to represent 0.785 rad (45 deg) of gimbal movement. The maximum output is ± 15 VDC. The analog of gimbal linear displacement, δ_G, is:

$$\delta_G^1 = \frac{15V}{.785rad} \Theta_G$$

where Θ_G is the gimbal angular displacement.

The servo amp gain must be sufficient to drive the motor when the maximum permissible gimbal error occurs. Since the maximum permissible position deadzone ($\Delta\Theta_G$) is assumed to be 0.008 rad (0.46 deg), and the breakaway voltage of the motor is 3.6 V, the approximate gain of the servo amplified (K_a) must be:

$$K_a = \frac{3.6V}{(\delta_G^1)\ (\Delta\Theta_G)}$$

$$= 23.6$$

This gain is within the current "state-of-the-art" for existing servo amplifiers.

The open loop transfer function for this preliminary design can be summarized as:[22]

$$\frac{\delta'_G(S)}{\varepsilon(S)} = \frac{K_a K_m\ L\ (3)V}{K_g\ (2.35)K_L} \left[\frac{1}{\frac{J_G L^2}{2\pi K_L^2 \eta K_s} S^2 + \frac{K_D L}{K_s K_L} S+1}\right]\left[\frac{1}{S(1+0.445S)}\right]$$

where: $K_a = 23.6$

$K_m = 24.8\ \frac{rad/s}{V}\quad (1420\ \frac{deg/s}{V})$

$K_s = 3.90 \times 10^4$ Nm/rad (502 ft-lb/deg)

$L = 5.05 \times 10^{-4}$ m/rad (2.89×10^{-5} ft/deg)

$V = 15$ V

$K_g = 27.94$

$K_L = 0.178$ m (0.584 ft)

$J_G = 9514$ Nms^2 (7018 ft-lb-s^2)

$\eta = 0.9$

$K_D = 38.2$ Nms (28.2 ft-lb-s)

Several factors must be considered in the final design of the inner control loops in addition to any stability enhancement features:

1. A means must be provided to limit electrical power to the gimbal motor before the gimbal assembly reaches its mechanical limit.

2. Mechanical couplings must be designed to minimize deadzone and tests must be performed to determine the minimum gimbal displacement necessary to start the motor.

3. Circuits must be designed such that ground loops, oscillations, and hot spots are precluded.

5.3.2 Autopilot & Sensors

The autopilot contains the circuitry that provides the gains, filtering and dampening necessary to insure stable flight. The autopilot for this vehicle consists of a pitch and yaw channel, both completely independent of each other.

A block diagram of the autopilot is shown in Figure 5.19. The time constants and gains are determined by a stability analysis of the complete control system (see Section 5.3.3). The block diagram indicates that both pitch and yaw channels have similar computations. A sensor detects actual airship attitude which is subtracted from a desired attitude to form an error signal, $\Delta\psi$. The error signal is used as a direct input and as a derived rate signal by passing it through a high pass filter. The derived rate signal, ψ, becomes a rate damping factor when it is subtracted from the attitude error signal. The resultant is a gimbal command signal proportional to the attitude error and damped in proportion to the rate of change of the attitude error. A limiter is added to prevent the gimbal mechanism from trying to move beyond its mechanical, or electrical limits, and beyond the safety limits of the airship.

During developmental testing the autopilot should have gain changing circuitry incorporated for varying autopilot parameters in-flight. It is anticipated that all forward circuit gains, feedback gains, and lead/lag constants should be adjustable in 3 increments. Also, as shown in Figure 5.19, the airship may be flown manually by using radio command to apply the proper voltage directly to the gimbal motor. This manual control is intended only as a back-up function in case of autopilot malfunction. Mechanical relays are shown in the diagram for simplicity, but solid state devices would most likely be used.

The autopilot unit may be mounted anywhere in the gondola but the pitch sensor and heading sensor should be located with some discretion. The pitch sensor should be mounted directly under, and as close as possible to, the longitudinal axis of the airship. This would minimize pitch errors due to possible rolling motions of the airship. Likewise, the magnetometer (heading reference) should be located directly under the longitudinal axis and as high as practical in the gondola to minimize roll effects. Some testing will be required to determine the effects of the gondola structure on the magnetometer accuracy.

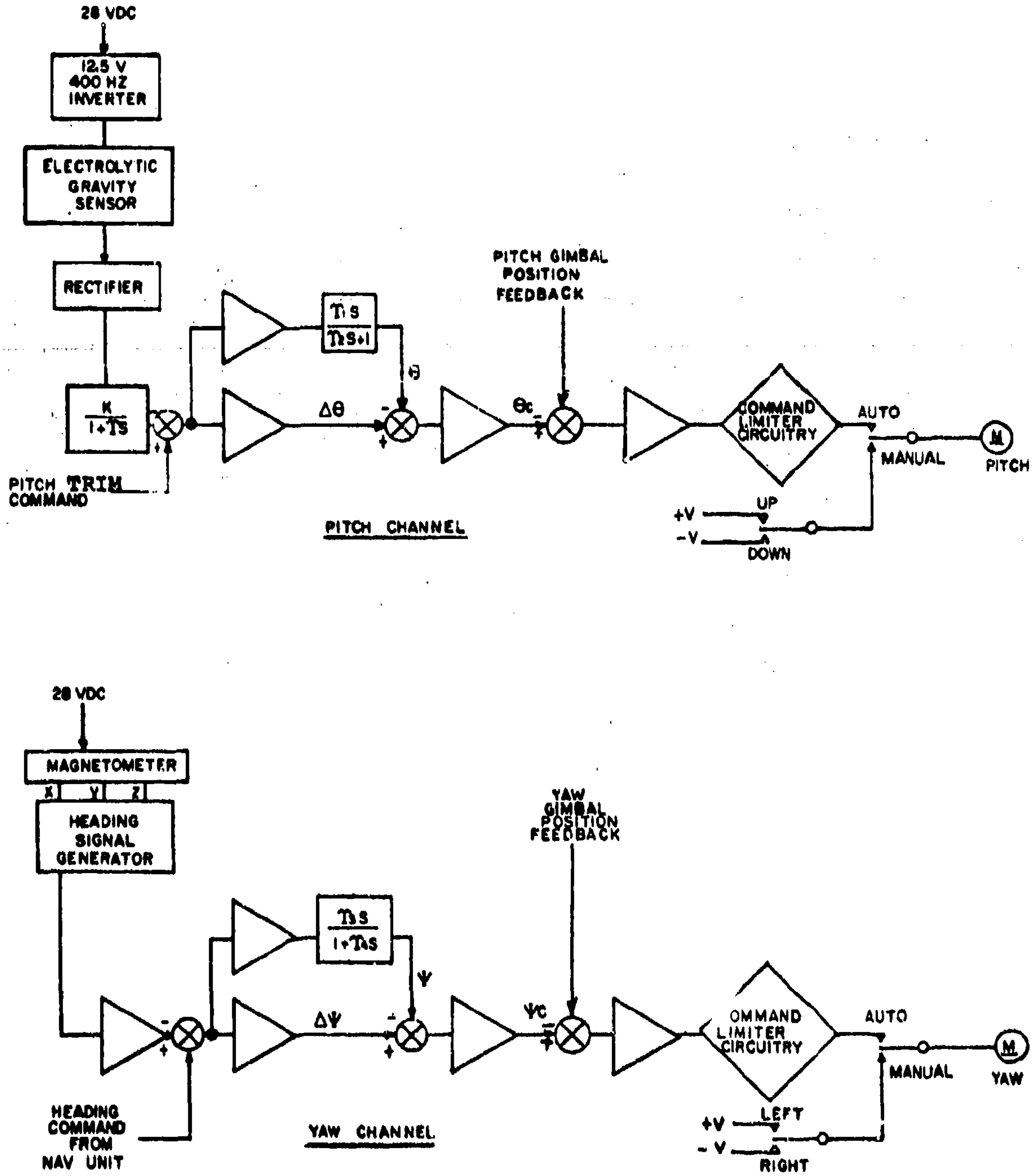

Figure 5.19 Autopilot block diagram.

5.3.2.1 Pitch Control. The pitch control serves to keep the airship flying level as altitude is determined by the balloon buoyancy. If desired, the airship can be flown with a fixed pitch angle by applying a DC voltage offset to the pitch error input. The pitch sensor is chosen to be a gravity sensing electrolytic transducer such as the type EP10-750 by Hamlin, Inc. It has a range of ±0.21 rad (12 deg) and an analog of 20.1 VAC/rad (0.340 VAC/deg) for small angles, when excited with 12.5 VRMS at 400 Hz. The response time constant of this device is approximately 0.8 seconds; therefore, the transfer function of the pitch sensor is:

$$\frac{V_{AC}}{\Delta\Theta} = \frac{20.1}{1 + 0.8S} \quad \frac{\text{VRMS}}{\text{rad}}$$

The output must be rectified and filtered to interface with the autopilot. A 12 ms low-pass filter will limit the peak-to-peak ripple to less than 10% of the peak AC voltage. The average of DC output voltage would be 0.95 times the peak AC voltage or 1.34 times the RMS input voltage. This assumes an infinite load on the filter, which is not practical. However, amplifiers are available with very high input impedances; therefore, a loss factor of 0.9 is assumed. The low pass transfer function then becomes:

$$\frac{V_{DC}}{V_{AC}} = \frac{1.21}{1 + 0.012S}$$

5.3.2.2 Yaw Control. The yaw control loop is similar to the pitch except for the sensor and the heading command inputs. The heading sensor is assumed to be a magnetometer such as Schonstedt Instrument Company's UAM-53C-1. It has an output analog of 0.0210 Vm/A (1.67 V/oersted) and weighs 2.9 N (0.66 lb). Its operating temperature range is +4.4 to +60°C; and it may require a heater and thermostat unless it can be located near a heat source. Since field intensity and flux density are equal in a nonmagnetic medium, the output analog of the magnetometer is 1.67×10^4 V/T (1.67 V/gauss). The earths magnetic flux density decreases as the inverse cube of the distance from the center of the earth. The earth radius is 6378 km (3963 mi) so an additional 21 km (13 mi) would cause a reduction in flux density of approximately one per cent.

The magnetometer is sensitive to the horizontal component of magnetic flux which varies from 5×10^{-6} to 4×10^{-5} T (0.05 to 0.4 gauss) over the surface of the earth.[23] This indicates that the gain of the heading sensor signal will have to be selectable over a range of from one to eight in order to fly anywhere in the world. A hypothetical example: the horizontal component of flux density at Sioux Falls, South Dakota is about 2×10^{-5} T (0.2 gauss). The output voltage would range from zero to a maximum of 0.334 V. If the magnetometer is mounted with the X-axis aligned with the longitudinal axis of the balloon, the voltage would be:

$$V_y = 0.334 \sin \psi$$

where ψ is the magnetic heading. The frequency response is 130 Hz at 0.5 gauss. The transfer function of the magnetometer is:

$$\frac{V_y}{\Delta\psi} = \frac{0.334\psi}{(S^2 + \psi^2)\ (1 + 0.00122S)}$$

Since a sinusoid gives a decreasing voltage as ψ increases beyond 1.57 rad (90 degrees), the magnetometer output must be linearized by a heading signal generator circuit which is shown following the magnetometer (Figure 5.19). In the final design, the heading signal generator circuit would combine the signals from all three axes into a linearized signal. The transfer function of this source would likely be more complicated than the one above, but would be similar in form. This function would be combined with the remaining loop functions and used in the final stability analysis.

5.3.3 System Stability

If the airship is to perform properly in flight it must follow a stable flight path. This requires that the autopilot function so as to command the gimbal mechanism in a proper fashion. Because of the interface and mechanical components involved it is not only essential to check out the airship stability on the assumption that the autopilot is reacting as anticipated; but it is also essential to determine that the basic electronics are stable when under operation. Thus, system stability encompasses both airship performance and electronics operation.

[23] Handbook of Geophysics and Space Environments, Shea L. Valley, ed., Air Force Cambridge Research Laboratories. 1965.

5.3.3.1 Autopilot Stability. The method normally used to determine if the electronics circuitry of the autopilot is stable is to analyze the servo system with innermost loop and progress to the outer loop after the inner loops have been stabilized. The inner and outer loops are shown for the yaw channel in Figure 5.20. The innermost loop is actually a gimbal position loop and will be analyzed first.

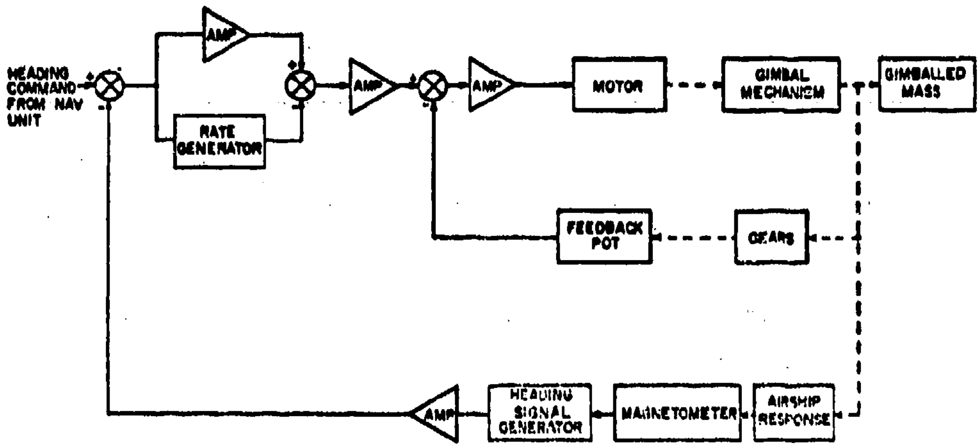

Figure 5.20 Heading control, yaw channel.

5.3.3.1.1 Gimbal Position Loop. This feedback loop is necessary to permit the gimbal motor to accurately hold the gimbaled mass in the desired position and to move it in a stable manner.

Inserting values of the preliminary design into the transfer function shown in Section 5.3.1 one obtains:

$$\frac{\delta'_G}{\varepsilon} = \frac{(23.6)\ (24.8)\ (1.02 \times 10^{-4}\ (6.38)\ (3)}{S\left[(0.000589)^2\ S^2 + (2)(0.00236)(0.000589)S+1\right]\ (1+0.445S)}$$

This loop is shown in Figure 5.21. The stability of the loop can be determined by applying the frequency analysis method to the open loop transfer function.

The above transfer function was analyzed by the computer program STABAN which is listed in Appendix C. A Bode plot of computer solution is shown in Figure 5.22. As shown, the inner loop is stable with a gain margin of about 106 db and a phase margin of approximately + 66 deg; therefore, equalization is unnecessary. It should be noted that normal stability analysis methods ignore the 180 degree phase shift through the amplifier. This means 180 degrees on the Bode plot really represents an in-phase signal (360 degrees) and is the critical point to examine.

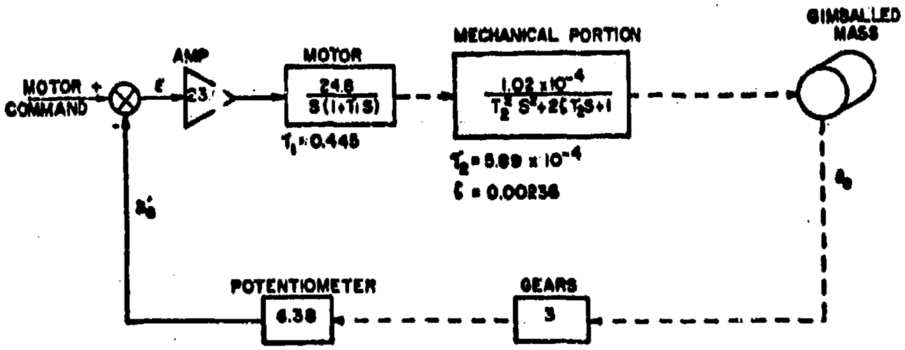

Figure 5.21 Gimbal position loop.

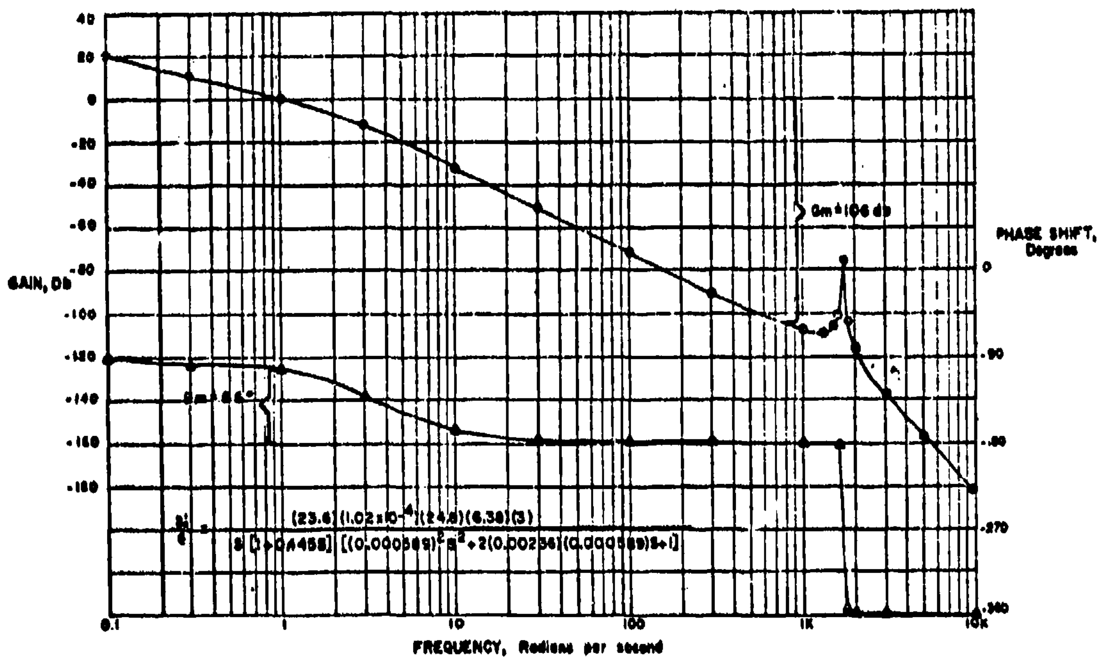

Figure 5.22 Bode plot, gimbal position loop.

The inner loop can be reduced to a single path by using the relationship:

$$F = \frac{G}{1 + GH}$$

In this case, G is the motor and gimbal mechanism, while H is the feedback potentiometer and associated gears. (See Figure 5.16). The forward loop transfer then becomes:

$$F = \frac{0.0524}{(\tau_1^2 S^2 + 2\zeta_1 \tau_1 S+1)\ (\tau_2^2 S^2 + 2\zeta_2 \tau_2\ S + 1)}$$

where: $\tau_1 = 0.625$

$\zeta_1 = 0.703$

$\tau_2 = 5.88 \times 10^{-4}$

$\zeta_2 = 0.00237$

The gimbal motor position loop may be represented by a single block containing this transfer function. This block may be used in further analysis of both the pitch and yaw channels.

5.3.3.1.2 Pitch & Yaw Control Loops. Combining the inner loop transfer function from the previous section and sensor details from Section 5.3.2., gives the diagrams shown in Figure 5.23. The undefined gains and time constants should be calculated when the airship transfer function is known. The theoretical derivation of the airship transfer function, must be performed to fully complete this analysis but is impractical without some empirical data from a scale model. The necessary values can then be calculated and the stability tested with the STABAN program. If the computer program indicated marginal stability, lead and/or lag filters should be added along with gain adjustments, and stability retested. This process should be repeated until the phase margin and gain margin are acceptable.

The yaw loop is the same as pitch except for the heading command signal input. The time constants required will undoubtedly be different than pitch due to differences in response to the airship. Only the y-axis transfer function is shown for the magnetometer but the x and z axes have similar functions. All three signals will be utilized by the heading signal generator to convert V_y into a linear signal.

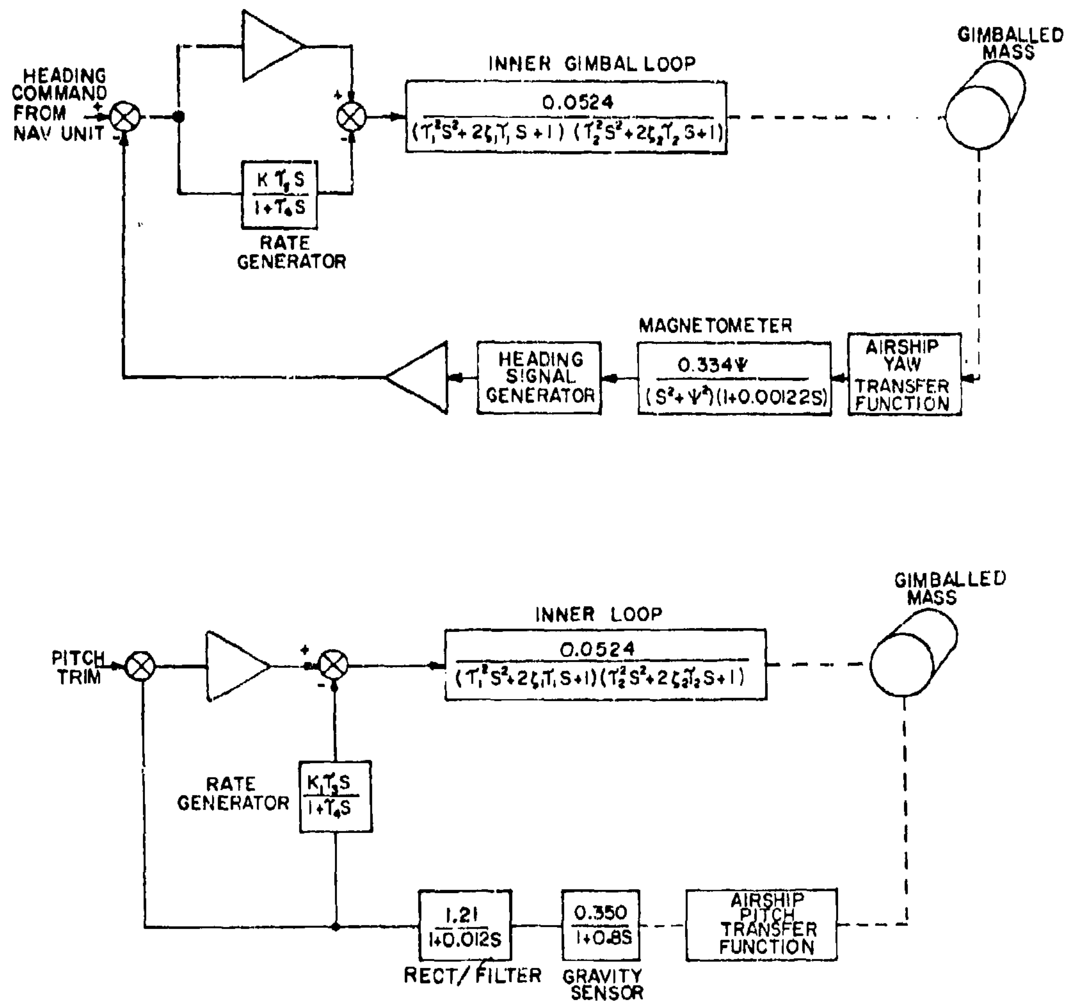

Figure 5.23 Pitch (bottom) and yaw (top) control loops.

5.3.3.2 Airship Flight Stability. The aerodynamic characteristics of the airship with respect to stability in flight, are an important consideration since airships are naturally unstable. The gimbaling of the thrust vector is used to hold the airship on course and create "stable flight" characteristics. The autopilot governs the motions of the gimbal mechanism by a predefined gimbal position based upon heading and pitch error and error rate feedback signals. The most meaningful way to check the airship flight stability is to model the system with a computer and study its synthesized reactions to various hypothetical situations. Such a technique empolying a digital computer was used successfully for High Platform II.[10] The discussion here will be limited to the basic equations which were used and the results obtained.

The geometry used in the equation is shown in Figure 5.24. The basic equations which are used are of the form:

Sum of Forces = (mass)(acceleration)

$$\Sigma F_X = m_X a_X$$

$$\Sigma F_Y = m_Y a_Y$$

$$\Sigma F_Z = m_Z a_Z$$

Sum of Moment = (moment of inertia)(angular acceleration)

$$\Sigma M_{YY} = I_{YY} \ddot{\Theta}$$

$$\Sigma M_{ZZ} = I_{ZZ} \ddot{\psi}$$

Sum of forces in x direction equal mass times acceleration in x direction:

$$T \cos(\tau-\beta)\cos(\tau+\alpha) - D_a - D_H - D_V - (W-b)\sin\gamma = M_X \nu$$

Sum of forces in y direction equals mass time acceleration in y direction:

$$- S_a - L_V + T \cos\delta \sin(\tau-\beta) = m_Y \nu \ (\dot{\Phi})$$

Sum of forces in z direction equal mass time acceleration in z direction:

$$- L_a - L_H - T \cos\tau \sin(\delta+\alpha) + (W-B) \cos\gamma = -m_Z \nu \dot{\gamma}$$

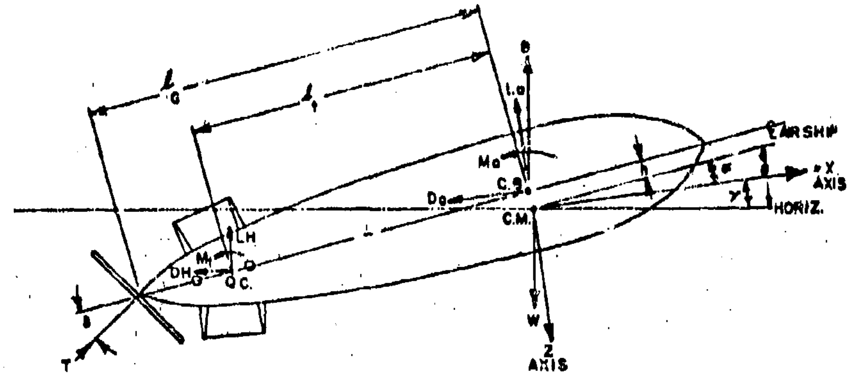

CURVILINEAR FLIGHT IN VERTICAL, $\overline{XZ}$, PLANE

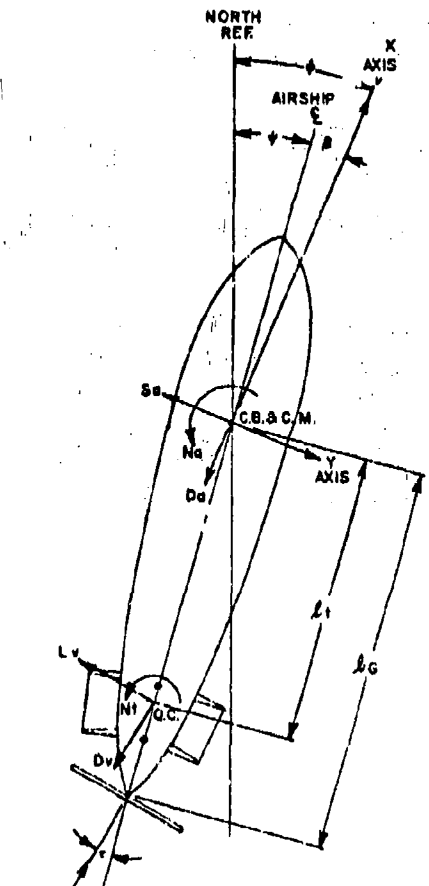

T = Thrust
W = Weight Of Airship
B = Buoyance Of Gas
C.B. = Center Of Buoyance
C.M. = Center Of Mass
Q.C. = Quarter Chord
D = Drag
L = Lift
S = Side Force
M = Moment About Y Axis
N = Moment About Z Axis
ν = Velocity
ℓ = Length
a = Hull (Airship)
H = Horizontal Fin
V = Vertical Fin
t = Tail
G = Gimbal

CURVILINEAR FLIGHT IN HORIZONTAL, $\overline{XY}$, PLANE

Figure 5.24 Geometry and nomenclature used for airship flight stability analysis.

Sum of moments about y axis equal moment of inertia times angular acceleration about the y axis:

$$M_a + M_t - L_a h \sin\alpha + D_a h \cos\alpha - L_H (\ell_t \cos\alpha + h \sin\alpha)$$

$$+ D_H (h \cos\alpha - L_t \sin\alpha) - T \cos\tau (h \cos\delta + \ell_G \sin\delta)$$

$$- B\, h \sin\Theta = I_{yy}\ddot{\Theta}$$

Sum of moments about z axis equal moment of inertia times angular acceleration about the z axis:

$$-N_a - N_t + \ell_t (L_V \cos\beta + D_V \sin\beta) - T\ell_G \cos\delta \sin\tau = I_{zz}\ddot{\psi}$$

These equations are used in conjunction with the basic autopilot/gimbal performance defined with the following equation:

$$\delta = G_{PE}(\Theta - A) + G_{PR}\dot{\Theta}$$

and

$$\tau = G_{YE}(\psi - B) + G_{YR}\dot{\psi}$$

where G is the autopilot amplifier gain, (P denotes pitch, Y denotes yaw, E denotes angular error, and R denotes angular rate), A is the pitch correction, and B is the heading correction factor. When these equations demand that the gimbal respond outside of realistic capabilities, it is limited to its actual rate and limit stop capabilities. Also, each of the major terms in the aerodynamic equation needs to be expanded upon in terms of aerodynamic derivations, and coefficients dependent upon angular displacements or velocities. The result is that the equations in their more complex form allow for the solving of ν, Φ, γ, Θ, and ψ if all other angles, their time derivatives, and the velocity have known values.

To start the simulation calculation, initial conditions are assumed for these other angles, time derivatives, and velocity. The autopilot/gimbal system will react to this initial condition by its electromechanical response which can be calculated. By using short time intervals it is valid to assume that all accelerations are constant over each time interval. New values of each of the initial conditions can be recalculated using equations in the forms:

$$\Theta_1 = \Theta_0 + \frac{\dot{\Theta}_0+\dot{\Theta}_1}{2}(\Delta)$$

or

$$\dot{\Theta}_1 = \dot{\Theta}_0 + \frac{\ddot{\Theta}_0+\ddot{\Theta}_1}{2}(\Delta)$$

where Δ denotes the time increment.

The procedure is repeated in an iterative manner to calculate values of θ, α, δ, ψ, β, τ, and ν at discrete time intervals. The computer output then shows how the system is predicted to respond to a specific situation defined by the initial conditions. Examples of the system response are shown in Figure 5.25. The computer program, POSIM, and examples of its output are listed in Appendix D.

5.3.4 Heading Control System

For station keeping demonstration purposes it has been determined that a fairly crude navigation technique used in conjunction with a heading control capability would be sufficient. Also, for the purposes of this effort, station keeping has been defined as remaining within 200 nautical miles of the ground command center. To accomplish this it is recommended that course heading changes be made from the ground station based upon flight vectors determined by radar positioning. These heading changes would be made by the heading control unit diagrammed in Figure 5.26.

The autopilot is designed to operate by actuating the gimbal to cause the airship to hold the heading programmed as a reference. The same magnetometer which is used for yaw stability control is also used for heading control. The reference heading is derived from a tapped potentiometer driven by a reversible stepping motor. The station operator can steer the airship by sending only "turn left" or "turn right" commands to the stepping motor. The program heading can then be changed in increments of less than one degree and verified by telemetry.

The heading command output is a linear voltage whose magnitude represents the deviation from north and whose polarity indicates the direction of deviation. The motor and driver provide .031 rad (1.8 deg) increments. A gear type speed reducer would reduce the step size to .016 rad (0.9 deg). The power converter output is approximately 1 W and

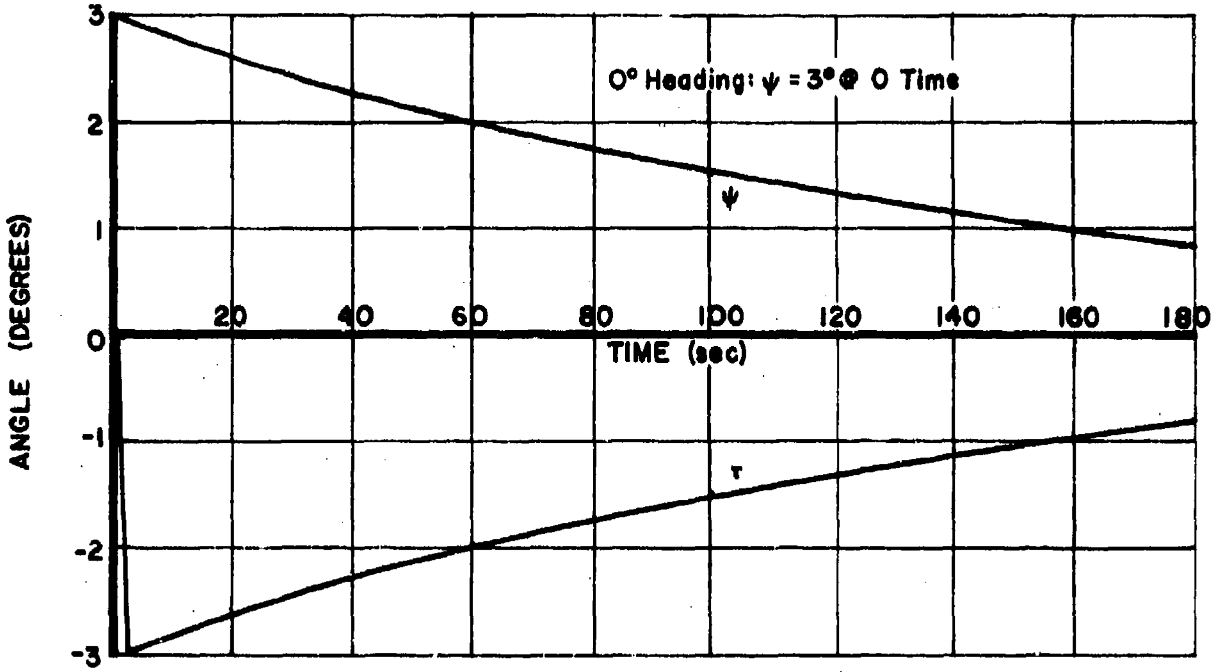

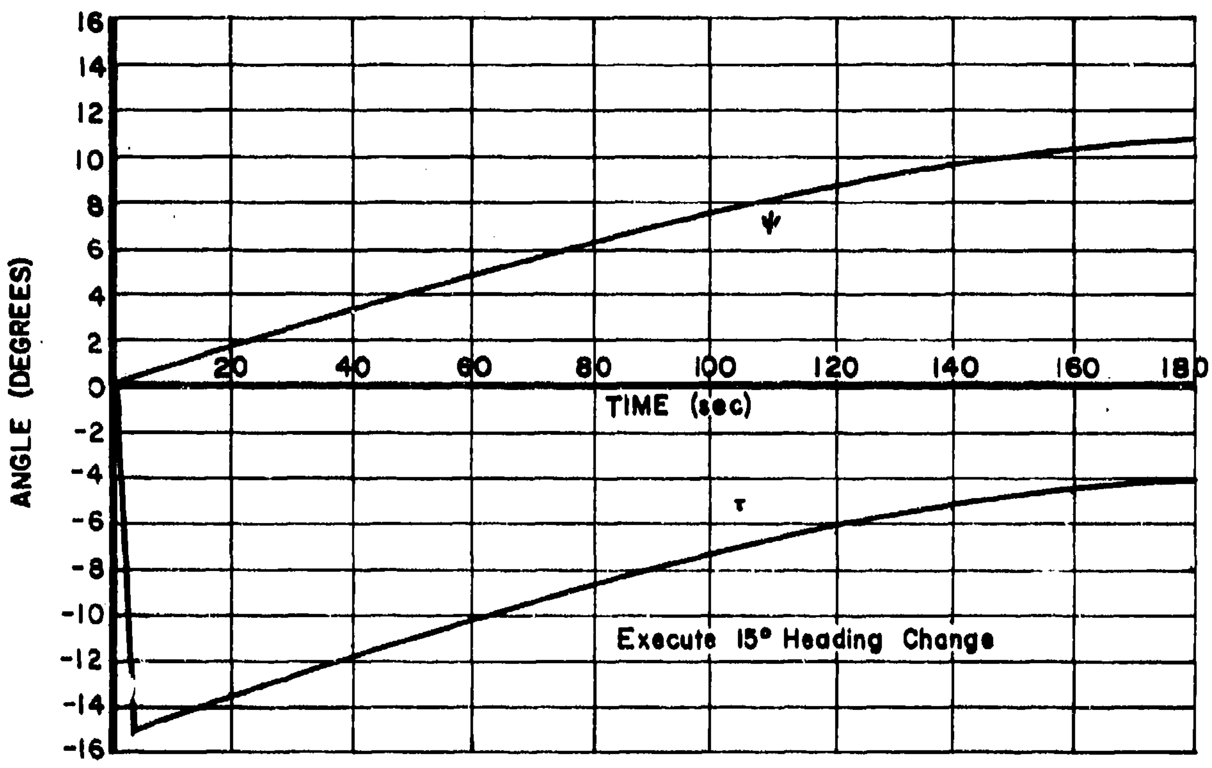

Figure 5.25 Two examples of airship performance for lateral control.

the efficiency of this type supply is typically about 65%. Input power requirements are approximately 15 W peak. Assuming the heading would seldom be changed, the average power is estimated to be 1.5 W. Weight of this unit is estimated to be 5 N (1.1 lb).

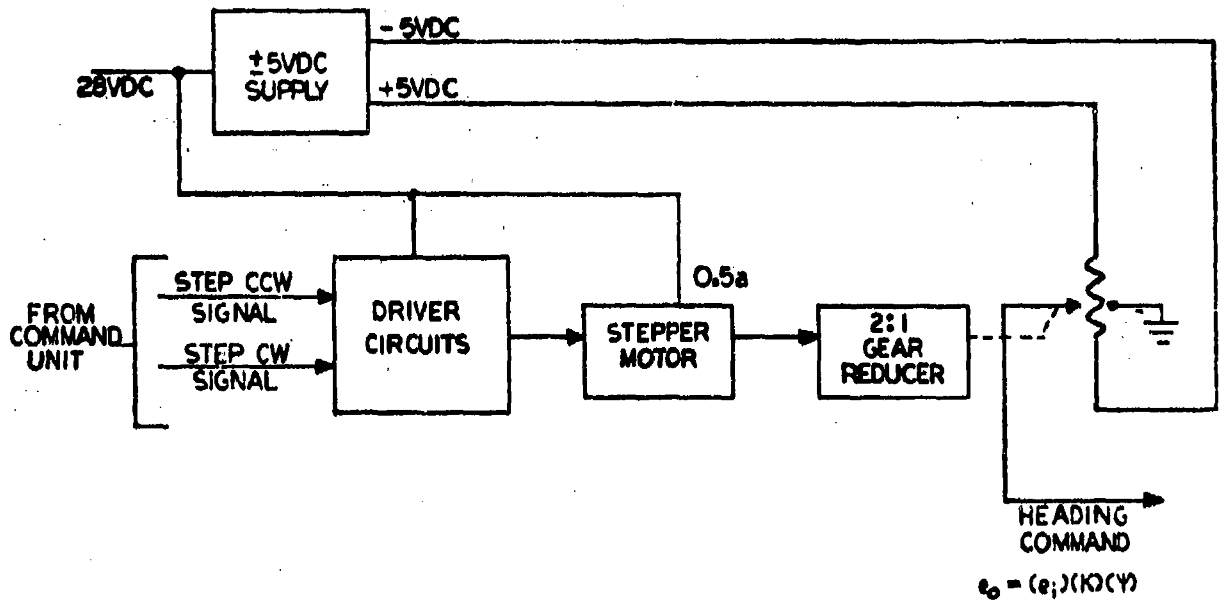

Figure 5.26 Heading control block diagram.

As seen from the above description, the heading control is simple and somewhat crude by spacecraft standards. As the winds may exceed twice the airspeed capability of the airship, and the area of station keeping made much smaller, it may be desirable to design an on-board, station-keeping, navigation system at a later date for such applications. For the present, this system will allow evaluation of airship performance and variations in the wind field at this altitude.

5.3.5 Command and Telemetry System

The command system for the early stages of this project shall consist of a VHF, Narrow Band, FM radio link. The transmitter is located at the ground control station and the receiver is aboard the airship. A block diagram of the radio command unit is shown in Figure 5.27. This unit is composed of building blocks found within the Raven TRAC system. The command system described herein has been in use by Raven Industries for balloon-borne applications since 1968 with an excellent history and proven operation to the radio horizon as found in balloon applications.

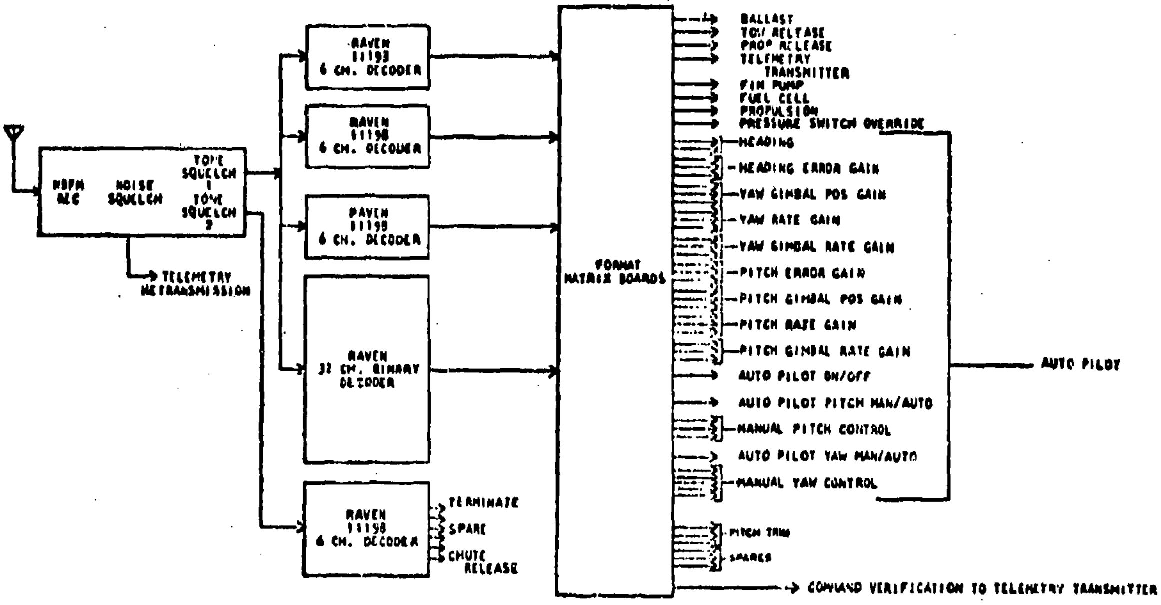

Figure 5.27 Radio command system block diagram.

The commands required are presented in Figure 5.27. To provide maximum reliability, the termination commands have a "private line" (tone squelch) independent from the airship command squelch. This command system contains a binary decoder which allows the transmission of up to 32 commands by utilizing only 5 command tones from the ground station. To verify command reception, a command verification signal is available to modulate the telemetry transmitter. This gives the ground station operator an audio tone upon command execution.

The switch closures provided by the format matrix boards must be heavy duty contacts (2-3 A) to permit control with a minimum of complexity. The estimated power consumption is 1 W. The approximate physical dimensions of this unit are 18 x 24 x 15 cm (7.1 x 9.4 x 5.9 in) and the weight is estimated to be 23 N (5.2 lb).

During the first flights many parameters must be telemetered for real time evaluation. This will allow the ground crew to evaluate performance and make appropriate adjustments. Analog chart recordings are ideally suited for this application. The analog recordings, as opposed to digital, give a history of operation at a glance. This is ideal where signals are continuously changing and real time evaluation is required.

An FM-FM telemetry system operating in the L or S band is proposed. The components that make up a system such as this are off-the-shelf items. The system can easily be tailored to suit system needs and meet IRIG (inter-range instrumentation group) requirements.

The airborne electronics will consist of appropriate commutators feeding IRIG ± 7-1/2% proportional subcarrier oscillators. The standard IRIG format will allow up to 11 channels of data. (Due to possible ranging data interference and the limited data bandwidth, channels 1-10 have not been considered.) These subcarriers than modulate an L or S band transmitter as required. The advantage of L or S band telemetry over lower bands is the ability to utilize subcarrier channels 20 and 21. Figure 5.28 is a block diagram showing the on-board telemetry system. The telemetry unit will require approximately 35 W of power including the transmitter. The estimated weight is 10N (2.2 lb) including signal conditioning requirements and case. A space allowance of 15 x 15 x 15 cm (5.9 x 5.9 x 5.9 in) should be made available for the telemetry unit.

5.4 Power Supply System

POBAL-S requires electrical power to operate the power train, gimbal mechanism, autopilot, on-board telemetry/command system, housekeeping functions, payload, and internal electrical functions. The power supply system to accomplish this consists of the fuel cell, the interfacing control unit, and an emergency power supply to operate the telemetry/command system.

5.4.1 Fuel Cell System

Design of the hydrogen-oxygen fuel cell system was furnished by Pratt & Whitney in conjunction with a concurrent contract.[20] An output voltage of 30 V was selected early in the program to expedite the fuel cell design. The voltage choice was based on three factors: 1) a similar system designed at 30 V had previously been developed by Pratt & Whitney, 2)

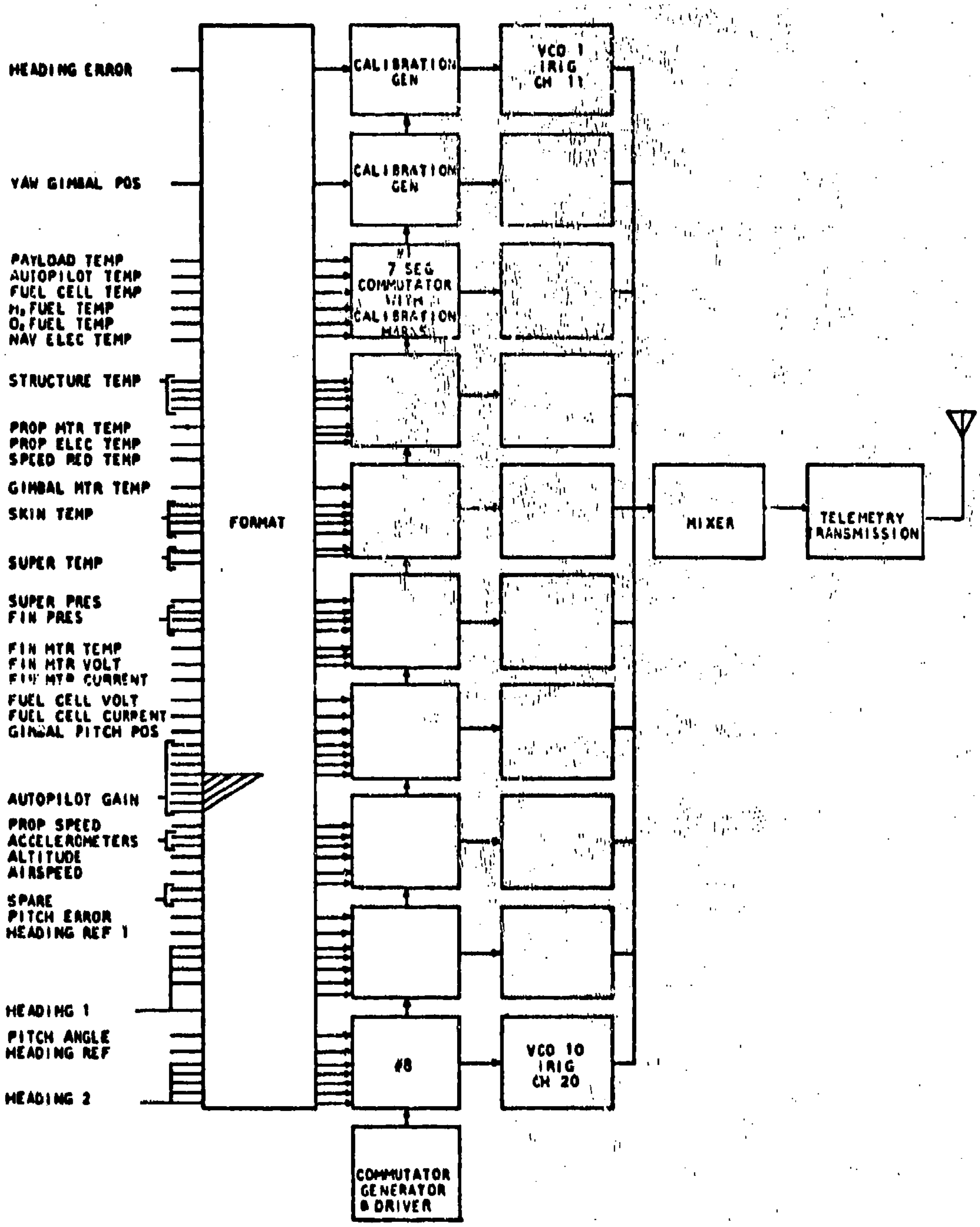

Figure 5.28 Telemetry system block diagram.

voltages needed to be limited to prevent any arcing problems during operation at 21 km (70,000 ft), and 3) by using components from existing fuel cell designs the airship size was minimized at a fuel cell voltage of approximately 30 V.

The fuel cell is to furnish 2.52 kW net terminal power for 7 days continuously. The characteristic curves are shown in Figure 5.29. The heat rejection rate of the fuel cell is 1170 W which is accomplished with a radiator/coolant unit operating at 93°C. The fuel cell can be started from its own residual power in approximately 14 minutes and can withstand a 100% overload for a short time without permanent damage.

Basically, the fuel cell system components include the fuel cell (consisting of the cell stack, valves, coolant, pumps, condenser, heaters, piping, etc.), the liquid H_2 and O_2 in their respective storage tanks, the radiator, and the H_2O storage bag. Section 5.1.3 discusses how these components are contained within the gondola. The weight breakdown is as follows:

Fuel cell		636.1 N
H_2 tank (empty		467.0
O_2 tank (empty)		244.6
H_2		218.0
O_2		1405.6
H_2O storage bag		22.2
Radiator		97.9
Piping and wiring		66.7
	Total	3158.1 N (710 lb)

5.4.2 Power Distribution and Control System

Power from the fuel cell is allocated as follows:

Payload		500 W
Autopilot, telemetry, gimbal, etc.		220 W
Motor		1800 W
	Total	2520 W

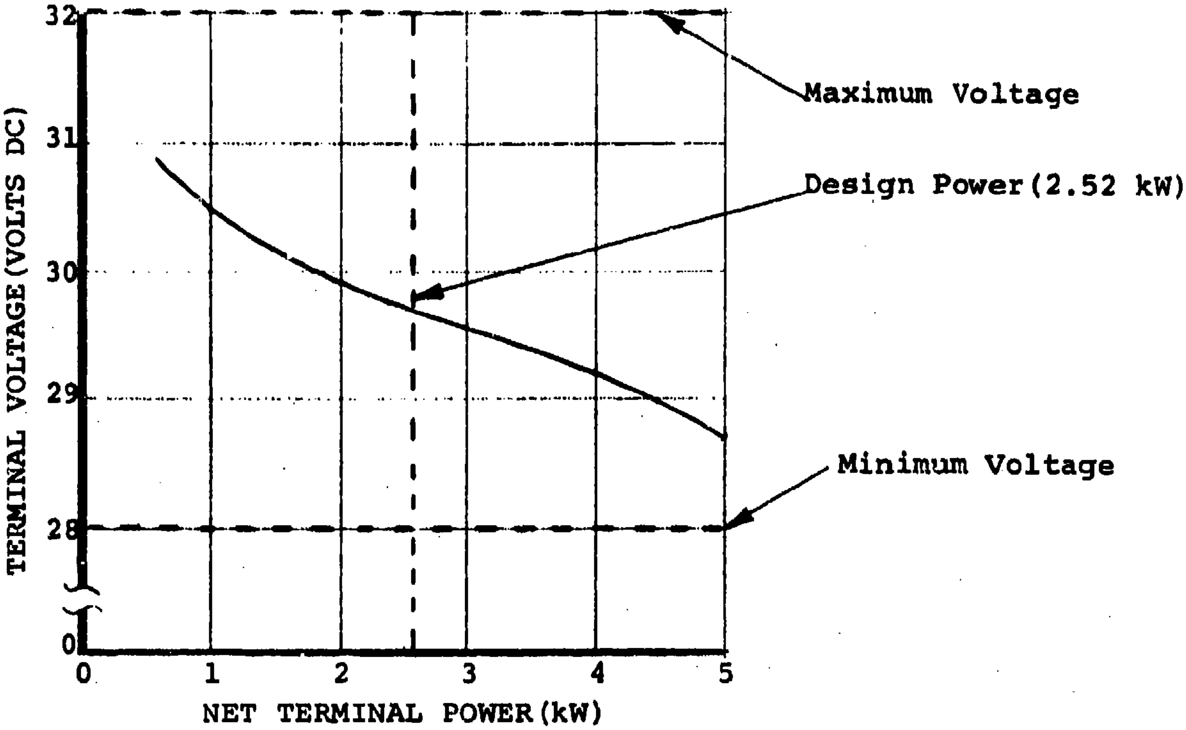

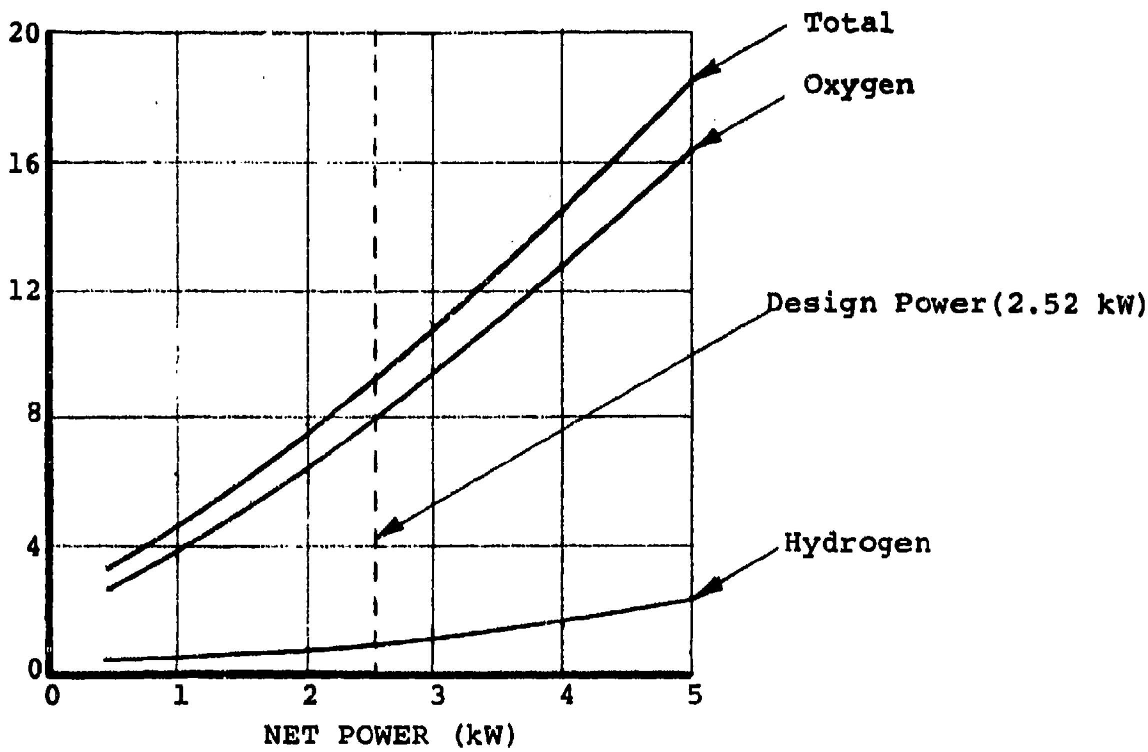

Figure 5.29 Fuel cell characteristics.

The control system provides the interface between the heavy duty power circuitry and sensitive electronic circuitry to provide proper power allocation. Referring to Figure 5.30 the power control and switching is located within the control system. All control functions are depicted as switches for clarity; however, solid state devices are desirable and should be incorporated in most areas.

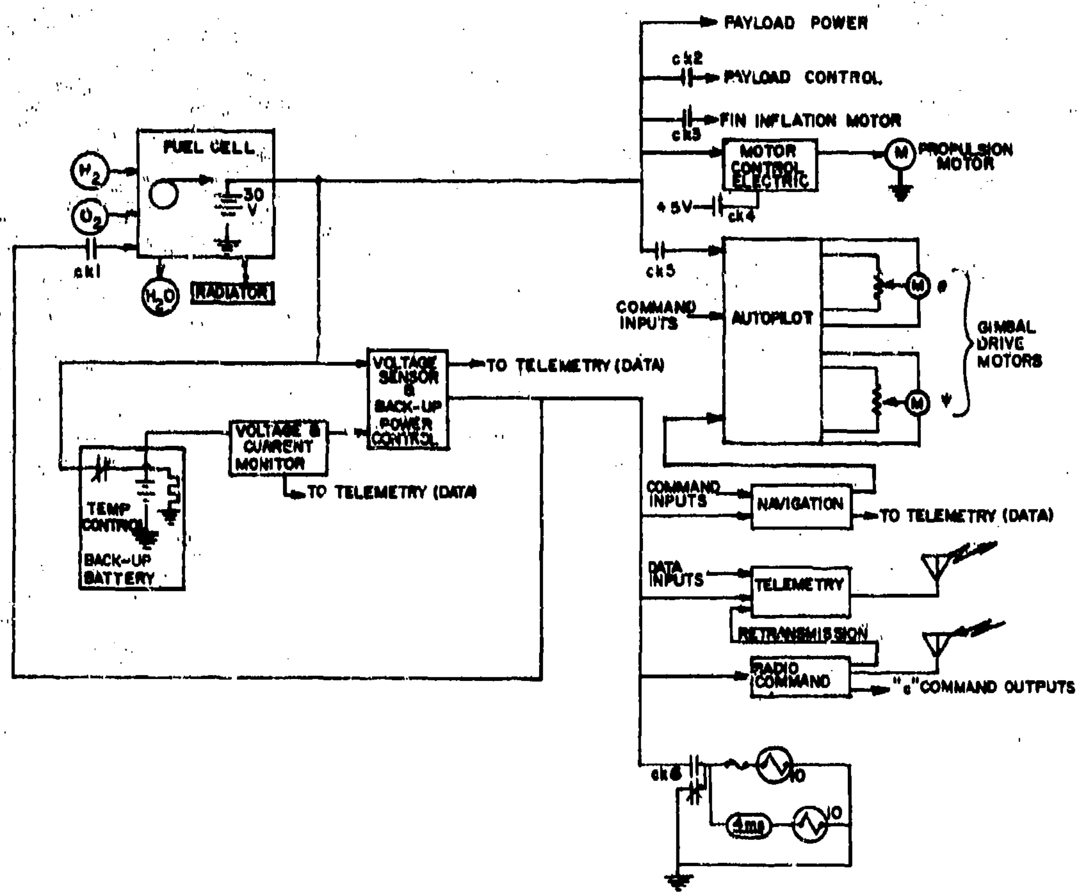

Figure 5.30 Power distribution and control system block diagram.

The payload power was specified to be 500 W and furnished by the fuel cell. A TTL-compatible logic signal is furnished to the payload which is assumed to contain a switching device capable of controlling its 16.7 A current.

The voltage sensor and back-up power control shown performs an automatic switching function. This circuit connects the largest of the two voltages to the telemetry, command, and navigation systems. Therefore, if the fuel cell voltage should drop below the battery voltage, indicating fuel cell failure, the back-up battery will automatically supply the required current. The voltage output of the fuel cell and current drain of the back-up battery are continuously monitored and coupled to the telemetry to alert the ground station operator should the back-up battery come "on-line" By using small regulators at each load, instead of one large regulator, improved filtering of switching transients and noise is achieved. By using sealed relays and solid state devices the control unit need not be pressurized. The volume of the control unit is 11 x 11 x 11 cm (4.3 x 4.3 x 4.3 in). The estimated total weight is 26 N (5.7 lb).

5.4.3 Emergency Power Supply

A back-up battery as shown in Figure 5.30 provides back-up power for the command, telemetry, heading control, and termination devices. This power supply is to provide minimum tracking, control, and telemetry for a 24 hour period in case of a propulsion system malfunction or a fuel cell failure. Should a failure occur, this can be extended to 48 hours by commanding the telemetry transmitter on and off as required. The average current to operate the telemetry unit, command unit, and attitude sensors is estimated to be 1.55 A.

The battery must also furnish power to fire the squibs at flight termination, energize relays, energize transducers, etc. These short pulses will not occur at any predictable frequency, nor at any particular time during the flight. In an attempt to insure that the required peak power is available for these intermittent loads, an additional 1 A of current was added to the battery requirement.

For high reliability it was decided to use a primary type battery. Acceptable solutions for the primary battery requirements were received from only two sources. The pertinent details are:

Vendor	Yardney	Chromalloy
Type	Silver-Zinc	Lithium-Organic
Size	29.2 x 19.7 x 17.8 cm	34.8 x 31.8 x 30.2 cm
Weight	222 N	167 N
Heater power	12.4 W	9 W
Shelf Line	1 month	1 year

Silver-zinc batteries are proven and offer the best reliability. Lithium-organic production experience is not well established at this time, but it is expected to improve in the future. The final battery choice should be made when a complete control unit design is accomplished.

5.5 Launch and Recovery

The POBAL-S vehicle as described above is a complex balloon system. The launch and recovery operation will be a difficult task and eventually must be considered a major task item.

5.5.1 Launch

The recommended launch technique for this vehicle is a "tail first" vertical launch utilizing a tow balloon under which the airship will ascend tail first. The primary reasons for this type of launch are to prevent damage to the propeller during lift-off and keep the heaviest weight concentration (gondola) near the bottom of the balloon to prevent surging of helium during ascent. A subtask of some future effort should be to demonstrate the launch concept under an experimental test.

The launch sequence is shown in Figure 5.31. The balloon should be laid out longitudinally with the stern structure positioned over the aft end. Approximately 4.6 m (15 ft) from the tail end the balloon should be clamped off so that only the tail will inflate to facilitate lacing the stern structure to the balloon. A crane would position and lift the stern structure as the inflation and lacing proceeds. The clamp would be released when lacing is completed.

The crane would have to raise the structure until the tow balloon is inflated and can support the airship tail. The tow balloon would have a buoyancy of approximately 1,480 N (333 lb). As the crane is released from the stern structure the tow balloon would hold the aft end of the airship vertical while inflation of the airship continues.

At approximately 30.5 m (100 ft) from the tail a tri-roller will have been clamped to the airship hull. The tri-roller is attached to two winches that will control the lift-off until the length of the airship is in the vertical position. In this manner, the gondola can be lifted slowly from the ground to avoid any snatch forces which would otherwise be encountered. When the entire balloon is clear of the ground and in the vertical position, the tri-roller clamp would be released.

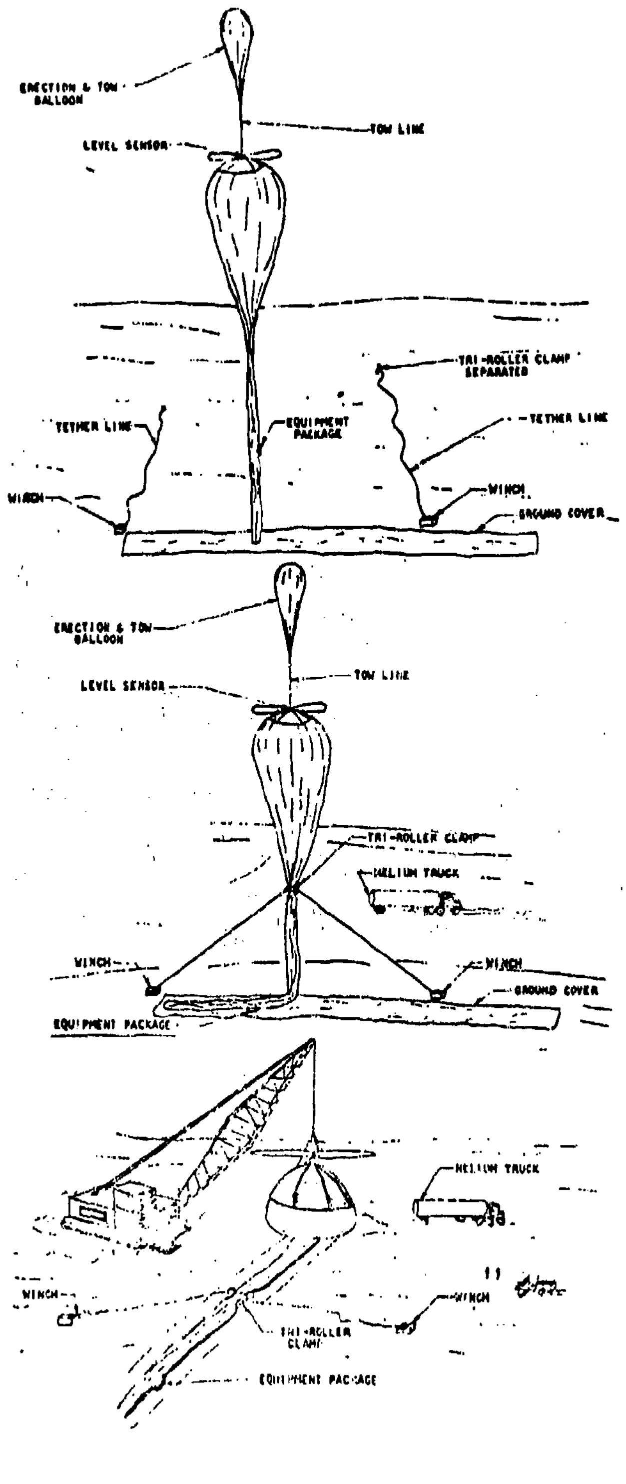

Figure 5.31 Launch sequence.

This launch technique requires two inflation valves. A valve would be located between the stern structure and the "tie off". The purpose of this valve is to inflate the aft cone for lacing of the battens to the airship. As the crane is released and the tow balloon begins to pick up the tail of the airship, a second valve which is located near the tri-roller would be opened. This valve is used to fill the balloon to its gross inflation.

The airship gross inflation would be 22,000 N (4,950 lb). This is the airship gross weight plus 20% free lift. The inflation gas is to be helium. The 20% free lift would be counteracted by 18% or 3,290 N (740 lb) of ballast which would leave 2% free lift in the system. The ballast and tow balloon would be released by a pressure sensing switch. The rate of ballast release would be adjusted to assure that the airship eases into final pressurization.

A total of 10% free lift would be required to launch this vehicle. Since the airship has 2% free lift remaining after accounting for the ballast, the tow balloon would require a buoyancy of 8% of the gross system weight or 1,480 N (333 lb). Thus, the two balloon serves two purposes; it holds the stern structure and tail of the airship in the vertical position during the initial states of inflation and ascent, and it provides the required free lift for ascent.

A level sensor would be attached to the stern structure as a safety device so that when the tow-line reaches a 70^0 lean-over angle (from the vertical), a time delayed squib and cannon assembly would release the tow balloon. This is redundant to the pressure switch. Since the tow balloon is not used to vent gas to the airship, its buoyancy is retained and it would continue to rise and clear the propeller once it is released. The airship will level out and ease into its float altitude of 21 km (70,000 ft) as ballast is released.

Figure 5.32 shows the gondola and load patches going through the complete ascent deployment sequence from the vertical to the horizontal position. In the initial stages of launch, as the gondola is vertical, the three launch patches directly over the gondola support the entire load. The load lines from these patches are secured on the plane of the center of gravity of the gondola. As the balloon begins to tip to the .79 rad (45 deg) position all seven of the launch patches, two on either side and three directly above the gondola, would share the weight of the gondola.

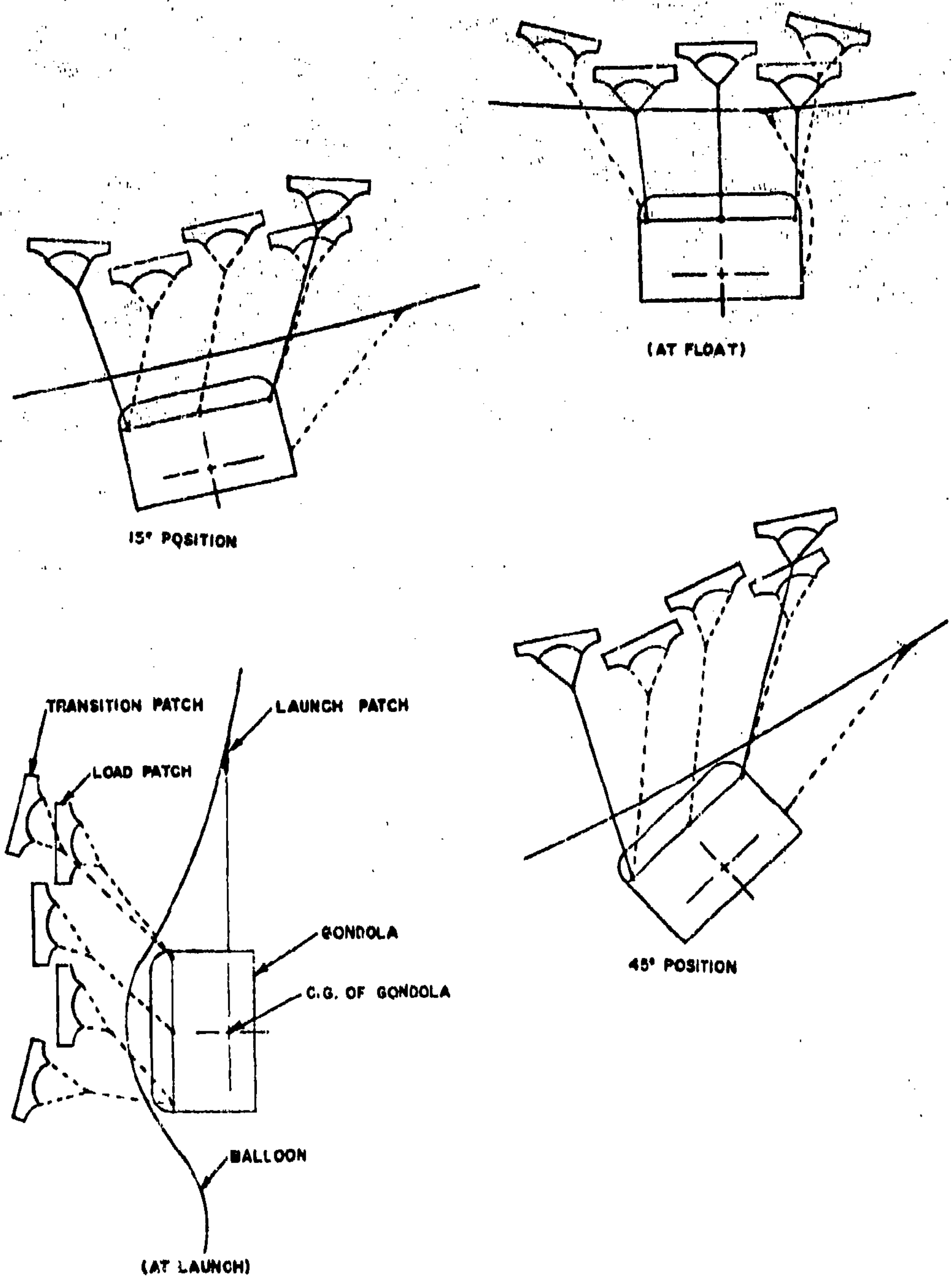

Figure 5.32 Gondola/load patch deployment sequence.

Then as the balloon continues to tip into its final horizontal flight position the load is transferred from the launch patches to the six load patches, three on either side of the gondola; and the launch patch lines become slack.

5.5.2 Recovery

The POBAL-S gondola contains expensive equipment. The items within the gondola can be reused if a method of recovery is provided. The most reliable and least expensive method of accomplishing recovery is with the use of a parachute which would be actuated upon release of the gondola from the balloon. The gondola termination circuitry consists of a relay, fuse, and time delay. The termination would be accomplished by cutting the support lines with cutters containing two Dupont S-68, four grain squibs which are energized independently. By energizing the second squib shortly after the first, the reliability can be doubled. The recommended firing current is 0.6 A for 4 ms for each squib. If the second squib pulse is delayed for 4 ms, the current required would be 0.6 A for 8 ms per line cutter. Occasionally the terminals of the squibs will be shorted together by the detonation. Therefore, a fuse is used in the line to the primary squibs such that if one should short it would not jeopardize the firing of the back-up squibs. In order to prevent static build-up an SPDT relay should be used for the control interface so that the squib power lines are shorted together until actuated.

The decelerator system selected must limit the shock forces experienced by the gondola at parachute opening and at ground impact to an acceptable value. The parachute selected for use in this application must posses an "effective drag area" of 264 m^2 (2,840 ft^2) to provide a 6.1 m/s (20 ft/s) impact velocity. A parachute of this size will weigh approximately 310 N (70 lb) and require a packing volume of 0.059 m^3 (2.1 ft^3).

The parachute utilized for this application must inflate reliably at the low dynamic pressure which would be experienced at the parachute deployment altitude, and it must provide stable descent. An unstable trajectory would result in a less predictable and usually higher rate of descent. In addition, if the parachute is oscillating, the possibility exists that the payload would not impact with the base in a horizontal orientation. If the payload impacts the ground at an angle, the shock attenuation material on the base of the package is less efficient and impact loads are increased.

The existence of surface wind increases the importance of using a stable, oscillation free recovery system. Surface winds impart a horizontal velocity to the descending gondola; and, if strong enough, these winds will cause the gondola to tumble or roll after ground impact. Impact loads can better be controlled if the package can be maintained upright during recovery. Preliminary analysis shows that if the recoverable load impacts the ground with its base horizontal, the upright orientation of the gondola can be maintained with winds up to 10.5 m/s (20.4 kn). However, if the payload and parachute are oscillating so that the base of the gondola impacts the ground at an angle of .35 rad (20 deg), the payload may overturn with winds above 5.1 m/s (10 kn).

Parachute designs such as the cross, disk-gap-band, and ringslot all provide stable descent. These designs will maintain an oscillation angle from the vertical of less than .17 rad (10 deg).

The parachute should be folded and packed in the gondola with the apex of the canopy to the top or open end. Parachute packing and rigging is then completed by attaching one one end of the lanyard (cord) to the apex of the canopy and the other end of the lanyard to a support structure in the airship. When recovery is initiated, the gondola and airship separate. As this separation occurs the lanyard would extract and deploy the parachute. When the complete parachute is deployed the lanyard would break, separating the gondola from the airship. The parachute is then free to inflate and support the vehicle to impact.

The length of the lanyard should be long enough to extend approximately 3 m (10 ft) below the airship to avoid canopy-with-airship contact during the deployment. Lanyard strength should be approximately 890 N (200 lb). This is sufficiently strong to insure extraction of the 310 N (70 lb) parachute without adding unnecessary weight to the airship for lanyard structural support.

The parachute can best be attached to the gondola using a four-legged bridle with one leg of the bridle attached near each corner of the gondola. This method of parachute attachment provides the most stable gondola orientation at ground impact.

Upon impact with the ground, a line cutter will be activated to cut the parachute from the gondola to preclude the possibility of the gondola being dragged.

The stern structure is not designed for a parachute recovery and will be returned with the airship. Since there are no shock attenuators attached to the structure, nearly as much damage would be imparted upon impact using a parachute recovery as would be by remaining with the balloon. The additional design effort to salvage the stern assembly is not warranted as the salvageable hardware is a small part of the system cost.

As the gondola is released from the airship a rip panel would be opened. The rip cord used to open the panel would be attached to the top of the parachute. The cord would be long enough so that the parachute is fully deployed before the cord opens the panel. The rip panel would be located near the nose of the airship. As the gondola is released, the airship will tip nose up due to the weight of the stern structure assembly. This would allow the helium to vent rapidly as the airship descends with the stern assembly down.

6. SUMMARY AND CONCLUSIONS

The task reported on in this text primarily consisted of a parametric analysis which resulted in a system concept definition for POBAL-S (a high altitude, superpressure airship) and the design of the airship. Also included was a brief historical discussion of powered balloons applicable to POBAL-S. The parametric analysis was presented in enough detail so that future extensions of the work performed here could be readily accomplished. The design was presented in enough detail so that it was shown to be feasible to fabricate, launch, and operate the POBAL-S system.

The types of systems analyzed included propeller driven superpressure airships powered by a solar cell array, a fuel cell, a battery, a gas turbine engine, and internal combustion engines. For mission durations of less than one week there are definite cost and design advantages of using a fuel cell powered vehicle. Combustion engine vehicles may also be applicable to the one week mission but a significant development effort to demonstrate feasibility would be required. Also, because of fuel consumption the engine concept presents design complications. For mission durations of two to three weeks the combustion engine should definitely be considered and an effort should be expended in developing such a concept. The fuel cell concept may have cost advantages for these durations, as compared to the solar cell array powered airship, but it is doubtful that such a system is feasible to launch because of its large size. For missions of extended duration (longer than one month) the solar cell array powered airship presents the only feasible alternative. However, in spite of its obviously high cost, such a vehicle could be developed under a single effort and fulfill all mission requirements. The primary disadvantage is that the solar cells are not recoverable. The cost per flight of this vehicle is then highly dependent on solar cell costs.

The analysis section of this report discussed the sensitivity of the system design to all design parameters. Also, the parametric curves indicate the dependency of system feasibility on various parameters. These analyses indicate that one of the major future efforts required leading to vehicle development is that of envelope material development. Other system design parameters such as film design stress limit, maximum supertemperature, required free lift, coefficient of drag, etc., must also be accurately determined. To minimize design complications, system size, and system costs and to maximize reliability any future development efforts should place great emphasis on accurate determination of these parameters.

The chosen concept was for a vehicle capable of supporting an 880 N (200 lb) payload requiring 500 W continuous power at an altitude of 21 km (70,000 ft) for a 7 day duration. The airship to meet this mission requirement is to be fuel cell powered and operate at an 8.18 m/s (15.9 kn) airspeed. In the design it was assumed that a new biaxially oriented nylon film would be used as the envelope material; however, at the present time this film is not a proven superpressure balloon material. Other new materials should also be considered since conventional polyester film, even though it exhibits near minimum excursions in supertemperature extremes, does not have an acceptable strength-to-weight ratio.

---

*Appendix B reports test results of experimentation with biaxially oriented Nylon 6.

REFERENCES

[1]Winker, J. A., High Altitude Relay Platform System, Report No. 0669011, Raven Industries, Inc. Final report, Contract 4691, Task Order 18. 15 May 1969.

[2]Bourke, Edgan R.. II, "Addenum to Presentation on a Unique Approach to Balloon Station Keeping", Ratheon Company. Presented at Earth Observations from Balloons Symposium, American Society of Photogrammetry. Published by Raytheon Company. 7 February 1969.

[3]Nolan, George F., High Altitude Minimum Wind Fields and Balloon Applications, AFCRL 64-843, Air Force Cambridge Research Laboratories. 1964.

[4]Nolan, George F., A Study of Mesoscale Features of Summertime Wind Fields in the Lower Stratosphere, AFCRL 67-0601. Air Force Cambridge Research Laboratories. 1967.

[5]Nolan, George F., "Meteorological Considerations for Tethered and Hovering Free Balloons, Air Force Cambridge Research Laboratories. Symposium Proceedings, Earth Observations From Balloons, American Society of Photogrammetry. February 1969.

[6]Beemer, Jack D., et al., POBAL-S R & D Design Evaluation Report, Part I, System Concept Choice, Report No. 0273001, Raven Industries, Inc., Air Force Cambridge Research Laboratories Contract No. F19628-73-C-0076. 23 February 1973.

[7]Anderson, A. A., et al., Lighter-Than-Air Concepts Study, Report No. 1765, General Mills, Inc. Final Report, Contract 1589(07). 1 September 1957. Revised, March 1960.

[8]Vorachek, Jerome J., Investigation of Powered Lighter-Than-Air Vehicles, GER 14076, Goodyear Aerpspace Corporation. AFCRL-68-0626, Final Report, Air Force Cambridge Research Laboratories, Contract No. F19628-67-C-0047. 27 November 1968.

[9]High Altitude Powered Balloon Test Program, Report No. BB-2304, Goodyear Aerospace Corporation. November 1968.

[10]Beemer, Jack D., et al., High Platform II, Report No. R-0870025, Raven Industries, Inc., Final Report, Contract 4691, Task Order 22. 14 August 1970.

[11]Beemer, J. D., et al., High Platform III Design Study,

PEFERENCES

Report No. 0871005, Raven Industries, Inc., Final report, Contract 5831. 31 August 1971.

[12]Vorachek, Jerome J., Edward W. McGraw, John W. Bezbatchenko, Development of a Free Balloon Propulsion System, Goodyear Aerospace Corporation. AFCRL TR-73-0128, Final Report, Air Force Cambridge Research Laboratories, Contract No. F19628-72-C-0072. April 1973.

[13]Beemer, Jack D., et al., Study of High Altitude Station Keeping Vehicles, Report No. 0373003, Raven Industries, Inc., Final Report, ARPA Order No. 1983. 15 March 1973.

[14]Rueter, Loren L., "Drag Analysis for POBAL-S & HASKV High Altitude Airships", informal paper, Raven Industries, Inc., 10 October 1972.

[15]McLemore, Clyde H., Wind-Tunnel Tests of a 1/20-Scale Airship Model with Stern Propellers, NASA TN D-1026, Langley Research Center, National Aeronautics and Space Administration. January 1962.

[16]Roark, Raymond J., Formulas for Stress and Strain, McGraw-Hill. 1965.

[17]Hoerner, Sighard F., Fluid-Dynamic Drag. 1958.

[18]Bruhn, E. F., Analysis and Design of Flight Vehicle Structures, Tri-State Offset Co., Cincinnati. 1965.

[19]Soudry, J. G., Structural Analysis Report, Silent Joe II Program, GER 14356, Goodyear Aerospace Corporation, Advanced REsearch Projects Agency Order No. 1255. 29 April 1969.

[20]Handley, L.M., Study of Fuel Cell System for Powered Balloon, PWA-4792, Pratt & Whitney Aircraft. Air Force Cambridge Research Laboratories, AFCRL-TR-73-0447. September 1973.

[21]Van Vliet, Robert M., Passive Temperature Control in the Space Environment, MacMillan & Co. 1965.

[22]Beemer, Jack D., et al., POBAL-S R & D Design Evaluation Report, Part II, Report No. 0673006, Raven Industries, Inc. Air Force Cambridge Research Laboratories, Contract No. F19628-73-C-0076. 6 July 1973.

REFERENCES

[2,3] Handbook of Geophysics and Space Environments, Shea L. Valley, ed., Air Force Cambridge Research Laboratories. 1965.

BIBLIOGRAPHY

Beemer, Jack D., "POBAL-S, Superpressure Powered Balloon", Raven Industries, Inc. Proceedings, (Supplemental Volume), Eighth AFCRL Scientific Balloon Symposium 30 September to 3 October 1974, A. Carten, Jr., ed., AFCRL-TR-74-0596, Air Force Cambridge Research Laboratories, March 1975.

Carten, Andrew S., An Investigation of the Applicability of High Altitude, Lighter-Than-Air (LTA) Vehicles to the Tactical Communications Relay Problem, AFCRL-TR-74-0399, Air Force Cambridge Research Laboratories. 20 August 1974.

Conley, William F., "High-Altitude Tethered Balloon Design", Goodyear Aerospace Corporation. Proceedings, AFCRL Tethered Balloon Workshop, 1967, AFCRL-68-0097, Thomas W. Kelly, ed., Air Force Cambridge Research Laboratories. March 1968.

Doyle, George R., Jr., "Mathematical Model for the Ascent and Descent of a High-Altitude Tethered Balloon", Goodyear Aerospace Corporation. Presented at the Fifth AFCRL Scientific Balloon Symposium. Abstract only published in Proceedings Fifth AFCRL Scientific Balloon Symposium, AFCRL-68-066, Lewis A. Grass, ed., Air Force Cambridge Research Laboratories. December 1968.

Free Balloon Propulsion Payload, GER-15488, Goodyear Aerospace Corporation. Air Force Cambridge Resea ch Laboratories R & D Design Evaluation Report, Contract No. F19628-72-C-0072. 14 January 1972.

Graham, John C., "A Survey of the Potential of Beamed Microwave Power for Balloons". Raytheon Company. Symposium Proceedings, Earth Observations From Balloons, American Society of Photogrammetry. February 1969.

Hamilton, Robert C., Performance, Analysis and Selection of Balloon Electrical Power Systems, Research Paper P-455, IDA Log. No. HQ68-9345, Institute for Defense Analysis. December 1968. Also published in Proceedings, Fifth AFCRL Scientific Balloon Symposium, Grass, Lewis A., ed., AFCRL-68-0661 Air Force Cambridge Research Laboratories. December 1968.

Korn, Arthur O., et al., LDF Powered Balloon Program, AFCRL-TR-73-0424, Air Force Cambridge Research Laboratories. 18 July 1973.

Korn, A. O. and R. Leclaire, "The Powered Balloon System", Air Force Cambridge Research Laboratories. Proceedings, Seventh

BIBLIOGRAPHY

AFCRL Scientific Balloon Symposium, George F. Nolan, ed., Air Force Cambridge Research Laboratories. September 1972.

Lally, Vincent E., Superpressure Balloons for Horizontal Soundings of the Atmosphere, NCAR-TN-28, National Center for Atmospheric Research. June 1967.

Mayer, Norman J., "The Influence of Fineness Ratio on Powered Ellipsoidal Balloon Weight and Other Characteristics", NASA Headquarters. Proceedings, Eighth AFCRL Scientific Balloon Symposium, 30 September to 3 October 1974, Andrew S. Carten, Jr., ed., AFCRL-TR-74-0393, Air Force Cambridge Research Laboratories. 21 August 1974.

Mayer, Norman J., "Advanced Airship Concept for Antenna Platform", NASA Headquarters. Proceedings, Seventh AFCRL Scientific Balloon Symposium, George F. Nolan, ed., Air Force Cambridge Research Laboratories. September 1972.

Menke, James A., High-Altitude Tethered Balloon Systems Study, GER 13260, Goodyear Aerospace Corporation. Sponsored by Advance Research Projects Agency. Monitored by Air Force Cambridge Research Laboratories, Contract F-19628-67-C-0145. 10 May 1967.

Petrone, F. J and P. R. Wessel, "Regenerative Fuel Cell Power System for Aerostats", Naval Ordnance Laboratory. Proceedings, Eighth AFCRL Scientific Balloon Symposium, 30 September to 3 October 1974, A. Carten, Jr., ed., AFCRL-TR-74-0596, Air Force Cambridge Research Laboratories, March 1975.

Report on High Altitude Airship (and Feasibility Model), Report No. 5490-2, General Mills, Inc. 30 June 1959.

Rice, Catherine B., Annotated Bibliography for Scientific Ballooning, AFCRL-TR-0040, Air Force Cambridge Research Laboratories. 16 January 1974.

Rice, Catherine B., "Power Sources for Powered Balloons", Wentworth Institute. Presented at the Seventh AFCRL Scientific Balloon Symposium. Proceedings, Seventh AFCRL Scientific Balloon Symposium, George F. Nolan, ed., Air Force Cambridge Research Laboratories. September 1972.

Ross, R. S. "Advanced Balloon Systems as Photographic Platforms, Goodyear Aerospace Corporation. Symposium Proceedings,

BIBLIOGRAPHY

Earth Observations from Balloons, American Society of Photogrammetry. February 1969.

Ross, R. S., "A New Material Capability for the Balloon Field", Goodyear Aerospace Corporation. Proceedings, 1964 AFCRL Scientific Balloon Symposium, AFCRL-65-486, Arthur O. Korn, Jr., ed., Air Force Cambridge Research Laboratories. July 1965.

"RPVs - An Emerging Technology", Special Report, Aviation Week and Space Technology, Vol. 98, No. 4, 22 January 1973.

Vorachek, J. J. "A Comparison of Several Very High Altitude Station Keeping Balloon Concepts", Goodyear Aerospace Corporation. Proceedings, Sixth AFCRL Scientific Balloon Symposium, AFCRL-70-0543, Lewis A. Grass, ed., Air Force Cambridge Research Laboratories. 27 October 1970.

Vorachek, Jerome J., "Concept for an Extremely High Altitude Tethered Balloon System", Goodyear Aerospace Corporation. Proceedings, Fifth AFCRL Scientific Balloon Symposium, AFCRL-68-0661, Lewis A. Grass, ed., Air Force Cambridge Research Laboratories. December 1968.

APPENDIX A

```
// READ DEVICE-MFCU1
// PRINT DEVICE-5203
   1          PROGRAM HASKV
          C -- DEVELOPED BY RAVEN INDUSTRIES, INC.  --   MARCH 1973
          C** PROGRAM HASKV SIZES HIGH ALTITUDE STATION KEEPING VEHICLES
          C** DIMENSION ARRAYS FOR ALTITUDE DEPENDENT PARAMETERS AND HEADING
   2          DIMENSION RHO(10),HLIFT(10),PRESR(10),HEAD(20)
          C** STORE BALLOON DESIGN PARAMETERS IN COMMON STORAGE
   3          GLOBAL SKIND,SMAT,ADHE,FIN,GLC,FINMR,SKINR,DELTAP,ENVM,BALNR,VOL,
             1TSKIN,ALENG,DAYS,XLIFT,BASTM
          C** STORE POWER SOURCE AND POWER CHAIN PARAMETERS IN COMMON STORAGE
   4          COMMON BCHEF,BAT1,BAT2,BATCC,BATCY,ECPB,ECPPS,ECPSS,ESPR,SPR,
             1UMM1,CMM1,UMM2,CMM2,EM,WIRE1,WIRE2,WIRE3,WIRE4,WIRE5,BENGY,VOLTFC,
             2CELL2,CELL1,CFCM,RAD,TMR1,TMR2,SFC1,SFC2,STRMR,CSTRM,UFLM,ADDM1,
             3ADDM2,ADDM3,SA,GEOF,TURBOR,SUBPOW,PNBYPD,VOLTSA,DUTY
          C** ESTABLISH COMPUTED COMPONENT MASSES IN COMMON STORAGE
   5          COMMON SPRM,TMM,TBATM,TFCM,FUELM,TANKM,STRM,TWIRM,TSAM,REQM,PROPM,
             1HRS,HRN,TS
          C** INITILIZE STANDARD SEA LEVEL PRESSURE AND DENSITY
   6          DATA SPRES/101325.0/,SRHO/1.225/
          C** INITILIZE ALTITUDE DEPENDENT ARRAYS
   7          DATA RHO/.15287,.12067,.095256,.074873,.058809,.046268,.036459,.02
             18777,.022748,.018012/
   8          DATA HLIFT/.13164,.10393,.082092,.064527,.050686,.039880,.031425,.
             1024807,.019614,.015535/
   9          DATA PRESR/.0938315,.0740668,.0584654,.0461670,.0365115,.0289216,.
             10229457,.0182329,.0145104,.0115654/
          C** READ ALPHANUMERIC HEADING. IF END OF DATA, PROGRAM TERMINATES.
  10        1 READ(1,302,END=99) HEAD
  11      302 FORMAT(20A4)
          C** READ UNFORMATTED INPUTS (CONSTANTS FOR PARAMETRIC EQUATIONS)
  12          READ (1,*)BCHEF,BAT1,BAT2,BATCC,BATCY,ECPB,ECPPS,ECPSS,EPROP,PROP,
             1ESPR,SPR,UMM1,CMM1,UMM2,CMM2,EM,WIRE1,WIRE2,WIRE3,WIRE4,WIRE5,
             2BENGY,VOLTFC,CELL2,CELL1,CFCM,RAD,TMR1,TMR2,SFC1,SFC2,STRMR,CSTRM,
             3UFLM,ADDM1,ADDM2,ADDM3,SA,GEOF,SKIND,SMAT,ADHE,FIN,GLC,FINMR,SKINR
             4,CD,SUPERT,F,AUTOM,TERMM,PAYM,TURBOR,SUBPOW,PNBYPD,VOLTSA,DUTY
          C** READ CONTROL CARD.  IF END OF DATA, READ NEW HEADING.
  13      200 READ(1,290,END=1) K,IIA,MIA,NIA,IWD,MWD,NWD,IIT,MIT,NIT,IAC
  14      290 FORMAT(11(2X,I3))
          C** IIA,MIA,NIA = INITIAL,MAX,AND INCREMENT OF ALTITUDE LOOP COUNTER
          C** IWD,MWD,NIA = INITIAL,MAX,AND INCREMENT OF WIND LOOP COUNTER
          C** IIT,MIT,NIT = INITIAL,MAX,AND INCREMENT OF TIME LOOP COUNTER
          C** IAC = 0,1,2 = NO ALTITUDE CONTROL, 1500 M. A/C, 3000 M. A/C
  15          WRITE(3,302)HEAD
          C** WRITE NAMES OF INPUT PARAMETERS IN 8 COLUMN ROWS
  16          WRITE(3,305)
  17      305 FORMAT('0'///21X,5HBCHEF,5X,4HBAT1,6X,4HBAT2,6X,5HBATCC,5X,5HBATCY
             A,5X,4HECPB,6X,5HECPPS,5X,5HECPSS/21X,5HEPROP,5X,4HPROP,6X,4HESPR,
             B6X,3HSPR,7X,4HUMM1,6X,4HCMM1,6X,4HUMM2,6X,4HCMM2/21X,2HEM,8X,
             C5HWIRE1,5X,5HWIRE2,5X,5HWIRE3,5X,5HWIRE4,5X,5HWIRE5,5X,5HBENGY,5X,
             D6HVOLTFC/21X,5HCELL2,5X,5HCELL1,5X,4HCFCM,6X,3HRAD,7X,4HTMR1,6X,
             E4HTMR2,6X,4HSFC1,6X,4HSFC2/21X,5HSTRMR,5X,5HCSTRM,5X,4HUFLM,6X,
             F5HADDM1,5X,5HADDM2,5X,5HADDM3,5X,2HSA,8X,4HGEOF/21X,5HSKIND,5X,
             G4HSMAT,6X,4HADHE,6X,3HFIN,7X,3HGLC,7X,5HFINMR,5X,5HSKINR,5X,2HCD/
             H21X,6HSUPERT,4X,1HF,9X,5HAUTOM,5X,5HTERMM,5X,4HPAYM,6X,6HTURBOR,
             I4X,6HSUBPOW,4X,6HPNBYPD/21X,6HVOLTSA,4X,4HDUTY///)
          C** WRITE VALUE OF INPUT PARAMETERS IN 8 COLUMN ROWS
```

```
      WRITE(3,*)BCHEF,BAT1,BAT2,BATCC,BATCY,ECPB.ECPPS,ECPSS,EPROP,PROP,
     1ESPR,SPR,UMM1,CMM1,UMM2,CMM2,EM,WIRE1,WIRE2,WIRE3,WIRE4,WIRE5,
     2BENGY,VOLTFC,CELL2,CELL1,CFCM,RAD,TMR1,TMR2,SFC1,SFC2,STRMR,CSTRM,
     3UFLM,ADDM1,ADDM2,ADDM3,SA,GEOF,SKIND,SMAT,ADHE,FIN,GLC,FINMR,SKINR
     4,CD,SUPERT,F,AUTOM,TERMM,PAYM,TURBOR,SUBPOW,PNBYPD,VOLTSA,DUTY
      CALL INFO1(K)
C** INFO1 LISTS TYPE OF POWER SOURCE SPECIFIED
C** EXECUTE ALTITUDE LOOP
      DO 88 IA=IIA,MIA,NIA
      ALT=15000.+1500.*IA
      XLIFT=HLIFT(IA)
C** COMPUTE ALTITUDE,BALLONET RATIO, AND DELTAP FOR A/C SPECIFIED
      IF(IAC-1)15,16,17
   15 ALPHA=1.0
      BALNR=0.0
      HRHO=RHO(IA)
      PRESS=SPRES*PRESR(IA)
      GO TO 19
   16 ALPHA=HLIFT(IA)/HLIFT(IA-1)
      PRESS=SPRES*PRESR(IA-1)
      HRHO=RHO(IA-1)
      GO TO 18
   17 ALPHA=HLIFT(IA)/HLIFT(IA-2)
      PRESS=SPRES*PRESR(IA-2)
      HRHO=RHO(IA-2)
   18 BALNR=1.-(.27*EXP(1.19*ALPHA))
   19 DELTAP=(.862*F*ALPHA+(1.+F)*SUPERT)/((1.-.862*ALPHA)*F+1)*PRESS
C** WRITE ALTITUDE AND CORESPONDING HELIUM LIFT, PRESSURE, AIR DENSITY,
C   AND BALLOON DIFFERENTIAL PRESSURE
      WRITE(3,313)ALT,HLIFT(IA),PRESS,HRHO,DELTAP
  313 FORMAT(//4X,9HALTITUDE=,F7.0,7H METERS,3X,6HHLIFT=,F5.4,6H KG/M3,
     13X,6HPRESS=,F6.0,10H NEWTON/M2,3X,4HRHO=,F6.5,6H KG/M3,3X,
     27HDELTAP=,F6.0,10H NEWTON/M2)
C** EXECUTE WIND LOOP
      DO 88 KWD=IWD,MWD,NWD
      VWIND = 2.574 * KWD
      Q=VWIND**2*HRHO*.5
C** WRITE WIND VELOCITY AND DYNAMIC PRESSURE
      WRITE(3,315)VWIND,Q
  315 FORMAT(//7X,5HWIND=,F6.3,6H M/SEC,6X,2HQ=,F6.2,12H NEWTON/SQ.M/)
      CALL INFO2(K)
C** INFO2 PRINTS OUTPUT HEADING FOR POWER SOURCE SPECIFIED
C** EXECUTE TIME LOOP
      DO 77 IT=IIT,MIT,NIT
      DAYS=IT
      TS=24.*IT
      IF(FIN-1.)23,23,24
   23 HRN=12.0
      GO TO 25
   24 HRN=IT
C** FIRST SIZING USES BALLOON RADIUS = 100 M.
   25 RENV=100.
      RI=0
      J=0
      IS=1
    2 CALL SHAPE (RENV)
C** SHAPE COMPUTES BALLOON PARAMETERS
```

```
      ALIFT=VOL*HLIFT(IA)-ENVM
C** ALIFT = NET LIFT OF BALLOON
      DRAG=Q*CD*VOL**.6666667
      PREQ=DRAG*VWIND*.001
      PUP=PREQ
      PREQ=PREQ/EPROP
      RP=RENV*.45
      PROPM=PROP*RP
      CALL POWER (PREQ,ALENG,K,SRHO,HRHO)
C** POWER COMPUTES COMPONENT MASSES OF POWER SOURCE
      REQM=REQM+PROPM+TMM+STRM+TWIRM+TBATM+PAYM+AUTOM+TERMM+BASTM
C** REQUIRED MASS = MASS OF ALL COMPONENTS REQUIRED TO POWER AND OPERATE
C   BALLOON SYSTEM. FOR SOLUTION, REQM MUST = NET LIFT = ALIFT
      SYSM=REQM+ENVM
      DIFF=ALIFT-REQM
      IF(ABS(DIFF).LE.1.0) GO TO 37
      IF(DIFF)45,37,50
C** IF ALIFT IS LESS THAN REQM FOR 100 M. R, NO ITERATION TAKES PLACE,
C   A MESSAGE IS PRINTED, AND THE PRESENT TIME LOOP IS COMPLETED.
   45 IF(J.EQ.0)GO TO 61
      IF(IS.GT.0) IS=-1
      R1=RENV
      GO TO 59
   50 J=1
      IF(IS.LT.0) IS=1
      R2=RENV
C** R1= LAST R WITH NEG. DIFF, R2= LAST R WITH POS. DIFF
   59 RENV=R1+(R2-R1)*.5
C** NEW RADIUS IS MID-POINT BETWEEN R1 AND R2. LOOP BACK (2) AND COMPUTE
C   ALIFT AND REQM FOR NEW RADIUS.
      GO TO 2
   61 WRITE(3,330)ALIFT,REQM
  330 FORMAT('0*** MAX SIZE CONSIDERED ***'/7H ALIFT=,F8.2,6X,5HREQM=,
     AF8.2//)
      GO TO 88
   37 GO TO (39,39,39,41,42,43),K
C** SOLUTION FOUND - WRITE PROPER OUTPUT FOR POWER SOURCE
   39 WRITE(3,350)DAYS,ALENG,SYSM,PREQ,TSKIN,ENVM,RP,TMM,FUELM,TANKM,
     2STRM,TWIRM,POP,DRAG
      GO TO 77
   41 WRITE(3,350)DAYS,ALENG,SYSM,PREQ,TSKIN,ENVM,RP,TMM,FUELM,TFCM,
     2STRM,TWIRM,POP,DRAG
      GO TO 77
   42 WRITE(3,350) HRS,ALENG,SYSM,PREQ,TSKIN,ENVM,RP,TMM,TBATM,TSAM,
     2STRM,TWIRM,POP,DRAG
      GO TO 77
   43 WRITE(3,350)DAYS,ALENG,SYSM,PREQ,TSKIN,ENVM,RP,TMM,TBATM,TSAM,
     2STRM,TWIRM,POP,DRAG
  350 FORMAT(F5.0,F8.2,F10.2,F8.3,F7.4,F10.2,2F7.2,F9.2,F8.2,2F7.2,F8.4,
     AF8.2)
   77 CONTINUE
   88 CONTINUE
      GO TO 200
C** ALL LOOPS COMPLETED. STM. NO. 200 READS NEW CONTROL CARD
   99 CONTINUE
      STOP
      END
```

```
   000 TOTAL ERRORS FOR THIS COMPILATION
 0L100 I  THE TOTAL CORE USED BY HASKV  IS 13312 DECIMAL.
 0L101 I  THE START CONTROL ADDRESS OF THIS MODULE IS 0E00.
 0L102 I  THE NON-OVERLAY CORE SIZE IS    16244 DECIMAL
 0L104 I  TOTAL NUMBER OF LIBRARY SECTORS REQUIRED IS   76
          NAME-HASKV ,PACK-FORTR2,UNIT-R1,RETAIN-T,LIBRARY-0
```

```
FORTRAN IV VER01/MOD01                                          02/25/75 PAGE 001

      SUBROUTINE INFO1 (K)
C** SUBROUTINE INFO1 PRINTS TYPE OF POWER SOURCE SPECIFIED
      GO TO (1,2,3,4,5,6),K
    1 WRITE(3,308)
  308 FORMAT('ONREC GAS TURBINE AS POWER SOURCE'/)
      RETURN
    2 WRITE(3,309)
  309 FORMAT('OTURBOCHARGED WANKEL AS POWER SOURCE'/)
      RETURN
    3 WRITE(3,310)
  310 FORMAT('OTURBOCHARGED DIESEL AS POWER SOURCE'/)
      RETURN
    4 WRITE(3,311)
  311 FORMAT('OFUEL CELL AS POWER SOURCE'/)
      RETURN
    5 WRITE(3,312)
  312 FORMAT('OSOLAR CELLS AS POWER SOURCE'/)
      RETURN
    6 WRITE(3,313)
  313 FORMAT('OBATTERIES AS POWER SOURCE'/)
      RETURN
      END

  000 TOTAL ERRORS FOR THIS COMPILATION
OLIG3 I  TOTAL NUMBER OF LIBRARY SECTORS REQUIRED IS     5
         NAME-INFO1 ,PACK-FORTR2,UNIT-R1,RETAIN-T,LIBRARY-R,CATEGORY-020
```

```
 1          SUBROUTINE INFO2 (K)
       C** SUBROUTINE INFO2 PRINTS COLUMN HEADINGS FOR OUTPUT DATA
 2          GO TO (1,1,1,2,3,4),K
       C** WRITE COLUMN HEADS FOR IC ENGINE OUTPUT
 3        1 WRITE(3,320)
 4      320 FORMAT(2X,4HDAYS,1X,6HLENGTH,6X,4HMASS,4X,4HPREQ,2X,5HTSKIN,6X,
          14HHULL,4X,2HRP,2X,6HENGINE,5X,4HFUEL,4X,4HTANK,4X,3HSTR,3X,4HWIRE,
          25X,3HPOP,2X,6HTHRUST)
 5          RETURN
       C** WRITE COLUMN HEADS FOR FUEL CELL OUTPUT
 6        2 WRITE(3,322)
 7      322 FORMAT(2X,4HDAYS,1X,6HLENGTH,6X,4HMASS,4X,4HPREQ,2X,5HTSKIN,6X,
          14HHULL,4X,2HRP,3X,5HMOTOR,5X,4HFUEL,3X,4HTFCM,5X,3HSTR,3X,4HWIRE,
          25X,3HPOP,2X,6HTHRUST)
 8          RETURN
       C** WRITE COLUMN HEADS FOR SOLAR ARRAY OUTPUT
 9        3 WRITE(3,324)
10      324 FORMAT (6H HOURS,1X,6HLENGTH,6X,4HMASS,4X,4HPREQ,2X,5HTSKIN,6X,
          14HHULL,4X,2HRP,3X,5HMOTOR,4X,5HTBATM,5X,2HSA,5X,3HSTR,3X,4HWIRE,
          25X,3HPOP,2X,6HTHRUST)
11          RETURN
       C** WRITE COLUMN HEADS FOR ALL BATTERY OUTPUT
12        4 WRITE(3,326)
13      326 FORMAT(2X,4HDAYS,1X,6HLENGTH,6X,4HMASS,4X,4HPREQ,2X,5HTSKIN,6X,
          A4HHULL,4X,2HRP,3X,5HMOTOR,4X,5HTBATM,5X,2HSA,5X,3HSTR,3X,4HWIRE,
          B5X,3HPOP,2X,6HTHRUST)
14          RETURN
15          END

     000 TOTAL ERRORS FOR THIS COMPILATION
  OL103 I  TOTAL NUMBER OF LIBRARY SECTORS REQUIRED IS     6
           NAME-INFO2 ,PACK-FORTR2,UNIT-R1,RETAIN-T,LIBRARY-R,CATEGORY-020
```

```
FORTRAN IV VER01/MOD01                                                02/25/75 PAGE 001

  1           SUBROUTINE SHAPE (RENV)
        C** SUBROUTINE SHAPE COMPUTES BALLON PARAMETERS
  2           GLOBAL SKIND,SMAT,ADHE,FIN,GLC,FINMR,SKINR,DELTAP,ENVM,BALNR,VOL,
             1TSKIN,ALENG,DAYS,HLIFT,BASTM
        C** IF FINENESS RATIO GREATER THAN 1, USE CLASS C SHAPE.
        C** IF FINENESS RATIO LESS THAN OR EQUAL TO 1, USE NATURAL SHAPE.
  3           IF(FIN-1)13,13,14
        C** ALENG = INFLATED LENGTH OR DIAMETER
        C** VOL = VOLUME
        C** S = SURFACE AREA
        C** TSKIN = SKIN THICKNESS
        C** ENVM = ENVELOPE MASS--FINAL VALUE COMPUTED IS TOTAL HULL MASS
        C** NG = NUMBER OF GORES
        C** GL = GORE LENGTH
        C** TAPEM = MASS OF SEALING TAPES
        C** FINM = MASS OF HORZ. AND VERT. FINS
        C** BALNM = BALLONET MASS
        C** BASTM = BALLAST MASS
  4        13 ALENG=2.*RENV
  5           VOL=3.45*RENV**3.
  6           GROSS=VOL*HLIFT
  7           BASTM=GROSS*(1.-.9**DAYS)
  8           ENVM=.243*GROSS
  9           TSKIN=0.0
 10           RETURN
 11        14 ALENG=2.*RENV*FIN
 12           VOL=4.0584*FIN*RENV**3.
 13           S=10.564*RENV**2.*FIN**.9568
 14           TSKIN=1000.*DELTAP*RENV/SMAT
 15           ENVM=(ADHE+SKIND*TSKIN*SKINR)*S
 16           NG=IFIX(4.27*RENV)+1
 17           GL=GLC*ALENG
 18           TAPEM=SKIND*NG*GL*TSKIN*.127
 19           ENVM=ENVM+TAPEM
 20           FINM=ENVM*FINMR
 21           BALNM=(ADHE+SKIND*TSKIN/2.)*S*BALNR
 22           BASTM=0.0
 23           ENVM=ENVM+FINM+BALNM
 24           RETURN
 25           END

   000 TOTAL ERRORS FOR THIS COMPILATION
 OL103 I  TOTAL NUMBER OF LIBRARY SECTORS REQUIRED IS     5
          NAME-SHAPE ,PACK-FORTR2,UNIT-R1,RETAIN-T,LIBRARY-R,CATEGORY-020
```

```
      SUBROUTINE POWER (PREQ,ALENG,K,SRHO,RHO)
C** SUBROUTINE POWER COMPUTES MASS OF POWER DEPENDENT COMPONENTS
      COMMON BCHEF,BAT1,BAT2,BATCC,BATCY,ECPB,ECPPS,ECPSS,ESPR,SPR,
     1UMM1,CMM1,UMM2,CMM2,EM,WIRE1,WIRE2,WIRE3,WIRE4,WIRE5,BENGY,VOLTFC,
     2CELL2,CELL1,CFCM,RAD,TMR1,TMR2,SFC1,SFC2,STRMR,CSTRM,UFLM,ADDM1,
     3ADDM2,ADDM3,SA,GEOF,TURBOR,SUBPOW,PNBYPD,VOLTSA,DUTY
      COMMON SPRM,TMM,TBATM,TFCM,FUELM,TANKM,STRM,TWIRM,TSAM,REQM,PROPM,
     1HRS,HRN,TS
      IF(K-3)20,20,21
C** COMPUTE COMPONENT MASSES FOR IC ENGINE
   20 TBATM=BAT1*BENGY
      PREQ=PREQ+SUBPOW/ECPSS
      TMM=UMM1*PREQ*SRHO/(RHO*TURBOR)+CMM1
      FUELM=SFC1*PREQ*TS
      TANKM=TMR1*FUELM+UFLM*.6*ALENG
      STRM=STRMR*(TMM+PROPM+ADDM1*.9)+CSTRM
      TWIRM=ALENG*.6*(2.*WIRE1+3.*WIRE2)
      REQM=TANKM+FUELM+ADDM1
      RETURN
C** COMPUTE COMPONENT MASSES COMMON TO ELECTRICAL SYSTEMS
   21 SPRM=SPR*PREQ
      PREQ=PREQ/ESPR
      TMM=UMM2*PREQ+CMM2
      PIM=PREQ/EM
      PREQ=PIM/ECPPS+SUBPOW/ECPSS
      IF(K-5)24,25,30
C** COMPUTE COMPONENT MASSES FOR FUEL CELL
   24 CELLM=CELL2*VOLTFC**2.+CELL1*VOLTFC+CFCM
      FUELM=SFC2*TS*(DUTY*PIM/ECPPS+SUBPOW/ECPSS)
      TANKM=TMR2*FUELM
      RADM=RAD*PREQ
      TFCM=CELLM+TANKM+RADM
      TWIRM=2.*WIRE3*.6*ALENG*PIM/VOLTFC
      STRM=STRMR*(TMM+SPRM+PROPM+ADDM2*.5)+CSTRM
      TBATM=BAT1*BENGY
      REQM=TFCM+FUELM+SPRM+ADDM2
      RETURN
C** COMPUTE COMPONENT MASSES FOR SOLAR CELLS
   25 HRS=24.-HRN
      POB =PIM*PNBYPD+SUBPOW/ECPSS
      BATM =POB *BAT2*HRN/BATCY
      XIC=BATCY/(HRS*BCHEF)
      IF(BATCC-XIC)26,28,28
   26 BATM=BATM*XIC/BATCC
   28 BBATM=BAT1*BENGY
      TBATM=BATM+BBATM
      IF(PNBYPD-1.) 11,12,12
   11 TMM=TMM+PIM*EM*PNBYPD*UMM2+CMM2
   12 PREQ=PREQ+1.22*POB/(ECPB*BCHEF)
      TSAM=PREQ*GEOF*(SA+WIRE4)
      TWIRM=ALENG*(.55*WIRE5*4.+.6*WIRE3*2.*PIM/VOLTSA)
      STRM=STRMR*(TMM+SPRM+PROPM+ADDM3*.5)+CSTRM
      REQM=TSAM+SPRM+ADDM3
      RETURN
C** COMPUTE COMPONENT MASSES FOR ALL BATTERY CASE
   30 TBATM=BAT1*(PREQ*TS+BENGY)
      TSAM=0.0
```

```
      TWIRM=ALENG*(.6*WIRE3*2.*PIM/VOLTSA)
      STRM=STRMR*(THM+SPRM+PHOPM+ADDM3*.5)+CSTRM
      REQM=TSAM+SPKM+ADDM3
      RETURN
      END

 000 TOTAL ERRORS FOR THIS COMPILATION
0L103 I  TOTAL NUMBER OF LIBRARY SECTORS REQUIRED IS    9
         NAME-POWER ,PACK-FORTR2,UNIT-R1,RETAIN-T,LIBRARY-K,CATEGORY-020
```

HASKY RUN 60 4/LR80-2 BATTERY, VN/VG = 10/30 -- USER POWER = 50 WATTS

BCHEF	BAT1	BAT2	BATCC	BATCY	ECPB	ECPPS	ECPSS
EPROP	PROP	ESPR	SPR	UMM1	CMM1	UMM2	CMM2
EM	WIRE1	WIRE2	WIRE3	WIRE4	WIRE5	BENGY	VOLTFC
CELL2	CELL1	CFCM	RAD	TMR1	TMR2	SFC1	SFC2
STRRR	CSTRM	UFLM	ADDM1	ADDM2	ADDM3	SA	GEOF
SKIND	SMAT	ADHE	FIN	GLC	FINMR	SKINR	CD
SUPERT	F	AUTOM	TERMM	PAYM	TURBOK	SUBPOW	PNBYPD
VOLTSA	DUTY						

0.89999998E+00	0.43500004E+01	0.85500002E+00	0.60000010E-02	0.61999999E-01	0.89999998E+00	0.97000003E+00	0.89999998E+00
0.75999999E+00	0.38699999E+01	0.94999999E+00	0.00000000E+00	0.80799997E-01	0.12110000E+02	0.86899996E+01	0.40799999E+01
0.75000000E+00	0.38000001E-02	0.50000008E-03	0.80000001E+00	0.33300000E+00	0.30900000E-02	0.83999997E+00	0.30000000E+02
0.24699999E-02	0.10000000E+01	0.32000000E+02	0.81599998E+01	0.63000023E-01	0.31000000E+00	0.73000002E+00	0.36000001E+00
0.19999999E+00	0.11000004E+01	0.52200001E-01	0.86300001E+01	0.45299997E+01	0.22700005E+01	0.44499998E+01	0.30000000E+01
0.11499996E+01	0.82737088E+08	0.43900013E-02	0.50000000E+01	0.10459995E+01	0.24999999E-01	0.90600002E+00	0.50000001E-01
0.10000002E+00	0.19999999E+00	0.45400000E+01	0.35699997E+01	0.90699997E+02	0.10000000E+01	0.10000002E+00	0.37000000E-01
0.11600000E+03	0.10000000E+01						

SOLAR CELLS AS POWER SOURCE

ALTITUDE= 21000. METERS HLIFT=.0645 KG/M3 PRESS= 4678. NEWTON/M2 RHO=.07487 KG/M3 DELTAP= 1331. NEWTON/M2

WIND=15.444 M/SEC Q= 8.93 NEWTON/SQ.M

HOURS	LENGTH	MASS	PREQ	TSKIN	HULL	RP	MOTOR	TBATM	SA	STR	WIRE	POP	THRUST
16.	115.97	2042.78	14.122	0.1866	1519.45	5.22	94.26	67.92	202.64	24.22	13.02	6.8986	446.69
14.	118.41	2172.94	14.711	0.1905	1616.61	5.33	97.93	86.75	211.09	25.04	13.82	7.1921	465.69
12.	120.61	2296.88	15.252	0.1940	1707.89	5.43	101.29	106.41	218.85	25.79	14.57	7.4615	483.14
10.	125.24	2572.29	16.426	0.2015	1911.29	5.64	108.59	150.16	235.69	27.41	16.25	8.0465	521.01
8.	133.06	3083.89	18.503	0.2141	2287.64	5.99	121.51	235.34	265.50	30.26	19.37	9.0817	588.04

HASKV RUN 60 4/LR80-2 BATTERY, VN/VD = 10/30 -- USER POWER = 100 WATTS

BCHEF	BAT1	BAT2	BATCC	BATCY	ECPB	ECPPS	ECPSS
EPROP	PROP	ESPR	SPR	UMM1	CMM1	UMM2	CMM2
EM	WIRE1	WIRE2	WIRE3	WIRE4	WIRE5	WENGY	VOLTFC
CELL2	CELL1	CFCM	RAD	TMR1	TMR2	SFC1	SFC2
STRMR	CSTRM	UFLM	ADDM1	ADDM2	ADDM3	SA	GEOF
SKIND	SMAT	ADHE	FIX	GLC	FINMR	SKINR	CD
SUPERT	F	AUTUM	TERMM	PAYM	TURBOR	SUBPOW	PNBYPD
VOLTSA	DUTY						

0.89999998E+00	0.43500004E+01	0.85500002E+00	0.60000010E-02	0.61999999E-01	0.89999998E+00	0.97000003E+00	0.89999998E+00
0.75999999E+00	0.38699999E+01	0.94999999E+03	0.00000000E+00	0.80799997E-01	0.12110000E+02	0.86899996E+01	0.40799999E+01
0.75000000E+00	0.38000001E-02	0.50000008E-03	0.80000001E+00	0.33300000E+00	0.30900000E-02	0.83999997E+00	0.30000000E+02
0.24699999E-02	0.10000000E+01	0.32000000E+02	0.81599998E+01	0.63000023E-01	0.31000000E+00	0.73000002E+00	0.36000001E+00
0.19999999E+00	0.11000004E+01	0.52200001E-01	0.86300001E+01	0.45299997E+01	0.22700005E+01	0.44499998E+01	0.30000000E+01
0.11499996E+01	0.82737088E+08	0.43900013E-02	0.50000000E+01	0.10459995E+01	0.24999999E-01	0.90600002E+00	0.50000001E-01
0.10000002E+00	0.19999999E+00	0.45400000E+01	0.35699997E+01	0.90699997E+02	0.10000000E+01	0.14999998E+00	0.37000000E-01
0.11600000E+03	0.10000000E+01						

SOLAR CELLS AS POWER SOURCE

ALTITUDE= 21000. METERS HLIFT=.0645 KG/M3 PRESS= 4678. NEWTON/M2 RHO=.07487 KG/M3 DELTAP= 1331. NEWTON/M2

WIND=15.444 M/SEC Q= 3.93 NEWTON/SQ.M

HOURS	LENGTH	MASS	PREQ	TSKIN	HULL	RP	MOTOR	TBATM	SA	STR	WIRE	POP	THRUST
16.	117.43	2119.90	14.613	0.1889	1578.66	5.28	96.45	75.37	209.69	24.71	13.49	7.0740	458.04
14.	119.87	2254.61	15.210	0.1929	1678.30	5.39	100.16	96.09	218.25	25.53	14.32	7.3712	477.29
12.	122.19	2388.91	15.788	0.1966	1776.95	5.50	103.76	117.84	226.54	26.33	15.13	7.6592	495.93
10.	127.08	2687.04	17.041	0.2044	1996.68	5.72	111.55	166.06	244.52	28.06	16.95	8.2835	536.36
8.	135.25	3239.48	19.249	0.2176	2402.46	6.09	125.29	259.48	276.21	31.10	20.32	9.3841	607.62

HASKV RUN 60 4/LR80-2 BATTERY: VN/VD = 10/30 -- USER POWER = 200 WATTS

BCHEF	BAT1	BAT2	BATCC	BATCY	ECPB	ECPPS	ECPSS
EPRUP	PRUP	ESPR	SPR	UMM1	CMM1	UMM2	CMM2
SM	WIRE1	WIRE2	WIRE3	WIRE4	WIRE5	BENGY	VOLTFC
CELL2	CELL1	CFCM	RAD	TMR1	THR2	SFC1	SFC2
STRMR	CSTRM	UFLM	ADDM1	ADDM2	ADDM3	SA	GEOF
SKIND	SMAT	ADHE	FIN	GLC	FINMR	SKINR	CD
SUPERT	F	AUTOM	TERMM	PAYM	TURBOR	SUBPOW	PNBYPD
VOLTSA	DUTY						

0.89999998E+00	0.43500004E+01	0.85500002E+00	0.60000010E-02	0.61999999E-01	0.89999998E+00	0.97000003E+00	0.89999998E+00
0.75999999E+00	0.38699999E+01	0.94999999E+00	0.00000000E+00	0.80799997E-01	0.12110000E+02	0.86899996E+01	0.40799999E+01
0.75000000E+00	0.38000001E-02	0.50000008E-03	0.80000001E+00	0.33300000E+00	0.20900000E-02	0.83999997E+00	0.30000000E+02
0.24699999E-02	0.10000000E+01	0.32000000E+02	0.81599998E+01	0.63000023E-01	0.31000000E+00	0.73000002E+00	0.36000001E+00
0.19999999E+00	0.11000004E+01	0.52200001E-01	0.86300001E+01	0.45299997E+01	0.22700005E+01	0.44499998E+01	0.30000000E+01
0.11499996E+01	0.82737088E+08	0.43900013E-02	0.50000000E+01	0.10459995E+01	0.24999999E-01	0.90600002E+00	0.50000001E-01
0.10000002E+00	0.19999999E+00	0.45400000E+01	0.35699997E+01	0.90699997E+02	0.10000000E+01	0.25000000E+00	0.37000000E-01
0.11600000E+03	0.10000000E+01						

SOLAR CELLS AS POWER SOURCE

ALTITUDE= 21000. METERS HLIFT=.0645 KG/M3 PRESS= 4678. NEWTON/M2 RHO=.07487 KG/M3 DELTAP= 1331. NEWTON/M2

WIND=15.444 M/SEC Q= 8.93 NEWTON/SQ.M

HOURS	LENGTH	MASS	PREQ	TSKIN	HULL	KP	MOTOR	TBATM	SA	STR	WIRE	PO2	THRUST
16.	119.14	2214.54	15.308	0.1917	1645.48	5.36	99.04	89.19	219.66	25.28	14.07	7.2814	471.47
14.	122.31	2395.18	15.097	0.1968	1792.05	5.50	103.95	114.28	230.98	26.38	15.18	7.6745	496.92
12.	124.88	2549.93	16.749	0.2009	1895.30	5.62	108.01	140.08	240.34	27.28	16.12	7.9996	517.97
10.	130.25	2893.11	18.169	0.2095	2147.52	5.86	116.78	197.04	260.58	29.22	18.21	8.7025	563.49
8.	139.40	3547.42	20.701	0.2243	2630.24	6.27	132.59	307.32	297.04	32.70	22.19	9.9689	645.49

HASKV RUN 60 4/L..0-2 BATTERY, VN/VD = 10/30 -- USER POWER = 500 WATTS

BCHEF	BAT1	BAT2	BATCC	BAT..	ECPB	ECPPS	ECPSS
EPROP	PROP	ESPR	SPR	UMM1	CMM1	UMM2	CMM2
EM	WIRE1	WIRE2	WIRE3	WIRE4	WIRE5	BENGY	VOLTFC
CELL2	CELL1	CFCM	RAD	TMR1	TMR2	SFC1	SFC2
STRMR	CSTRM	UFLX	ADDM1	ADDM2	ADDM3	SA	GEOF
SKIND	SMAT	ADHE	FIN	GLC	FINMR	SKINR	CD
SUPERT	F	AUTUM	TERMM	PAY..	TURBOR	SUBPOW	PNEYPD
VOLTSA	DUTY						

0.89999998E+00	0.43500004E+01	0.85500002E+00	0.60000010E-02	0.61999999E-01	0.89999998E+00	0.97000003E+00	0.89999998E+00
0.75999999E+00	0.38699999E+01	0.94999999E+00	0.00000000E+00	0.80799997E-01	0.12110000E+02	0.86899996E+01	0.40799999E+01
0.75000000E+00	0.38000001E-02	0.50000008E-03	0.80000001E+00	0.33300000E+00	0.30900000E-02	0.83999997E+00	0.30000000E+02
0.24699999E-02	0.10000000E+01	0.32000000E+02	0.81599998E+01	0.63000023E-01	0.31000000E+00	0.73000002E+00	0.36000001E+00
0.19999999E+00	0.11000004E+01	0.52200001E-01	0.86300001E+01	0.45299997E+01	0.22700005E+01	0.44499998E+01	0.30000000E+01
0.11499996E+01	0.82737088E+08	0.43900013E-02	0.50000000E+01	0.10459995E+01	0.24999999E-01	0.90600002E+00	0.50000001E-01
0.10000002E+00	0.19999999E+00	0.45400000E+01	0.35699997E+01	0.70699997E+02	0.10000000E+01	0.55000001E+00	0.37000000E-01
0.11600000E+03	0.10000000E+01						

SOLAR CELLS AS POWER SOURCE

ALTITUDE= 21000. METERS HLIFT=.0645 KG/M3 PRESS= 4678. NEWTON/M2 RHO=.07487 KG/M3 DELTAP= 1331. NEWTON/M2

WIND=15.444 M/SEC Q= 8.93 NEWTON/SQ.M

HOURS	LENGTH	MASS	PREQ	TSKIN	HULL	RP	MOTOR	TBATM	SA	STR	WIRE	POP	THRUST
16.	125.24	2571.84	17.679	0.2015	1911.29	5.64	108.59	131.73	253.68	27.41	16.25	8.0465	521.01
14.	128.91	2804.73	18.637	0.2074	2084.58	5.80	114.55	158.25	267.42	28.73	17.67	8.5240	551.93
12.	132.20	3025.13	19.523	0.2127	2245.71	5.95	120.06	206.16	280.13	29.94	19.01	8.9654	580.51
10.	139.04	3519.08	21.432	0.2237	2610.44	6.26	131.93	289.31	307.52	32.56	22.02	9.9166	642.10
8.	150.15	4431.33	24.738	0.2416	3284.62	6.76	152.50	447.40	354.97	37.06	27.56	11.5644	748.80

HASKV RUN 40 --BASE DATA, ALL SYSTEMS --

BCHEF	BAT1	BAT2	BATCC	BATCY	ECPB	ECPPS	ECPSS
EPROP	PROP	ESPR	SPR	UMM1	CMM1	UMM2	CMM2
EM	WIRE1	WIRE2	WIRE3	WIRE4	WIRE5	BENGY	VOLTFC
CELL2	CELL1	CFCM	RAD	TMR1	TMR2	SFC1	SFC2
STRMR	CSTRM	UFLM	ADDM1	ADDM2	ADDM3	SA	GEOF
SKIND	SMAT	ADHF	FIN	GLC	FINMR	SKINR	CD
SUPFRT	F	AUTOM	TERMM	PAYM	TURBOR	SUBPOW	PNBYPD
VOLTSA							

0.11099997E+01	0.43500004E+01	0.13699999E+01	0.44800005E-02	0.61999999E-01	0.89999998E+00	0.97000003E+00	0.89999998E+00
0.75999999E+00	0.38699999E+01	0.10000000E+01	0.00000000E+00	0.80799997E-01	0.12110000E+02	0.86899996E+01	0.40799999E+01
0.75000000E+00	0.58000001E-02	0.50000003E-03	0.80000001E+00	0.33300000E+00	0.30900000E-02	0.83999997E+00	0.37000000E+02
0.74699999E-02	0.10000000E+01	0.32000000E+02	0.81599998E+01	0.63000023E-01	0.50000000E+00	0.73000002E+00	0.36000001E+00
0.13999999E+00	0.11000004E+01	0.52200001E-01	0.86300001E+01	0.45299997E+01	0.22700005E+01	0.44499998E+01	0.30000000E+01
0.11499996E+01	0.82737088E+06	0.43900013E-02	0.50000000E+01	0.10459995E+01	0.24999999E-01	0.10000000E+01	0.50000001E-01
0.10000002E+00	0.19999999E+00	0.45400000E+01	0.35699997E+01	0.90699997E+07	0.10000000E+01	0.50000001E-01	0.37000000E-01
0.10400000E+03							

FUEL CELL AS POWER SOURCE

ALTITUDE= 21000. METERS   HLIFT=.0645 KG/M3   PRESS= 4678. NEWTON/M2   RHO=.07487 KG/M3   DELTAP= 1331. NEWTON/M2

WIND=10.796 M/SEC   Q= 3.97 NEWTON/SQ.M

DAYS	LENGTH	MASS	PREQ	TSKIN	HULL	RP	MOTOR	FUEL	TFCM	STR	WIRE	POP	THRUST
3.	122.07	2381.93	4.152	0.1964	1931.63	5.49	29.98	107.62	160.07	[illegible]	12.58	2.2649	219.97
6.	146.85	4146.64	5.964	0.2363	3349.12	6.61	41.56	310.20	276.31	[illegible]	21.91	3.2777	318.35
9.	176.88	7245.82	8.656	0.2846	5839.20	7.96	59.45	673.11	479.57	19.40	38.29	4.7553	461.86
12.	210.21	12161.91	12.202	0.3362	9776.48	9.46	80.87	1265.14	804.52	25.05	64.26	6.7159	652.29
15.	246.64	19645.46	16.778	0.3968	15778.79	11.10	109.80	2174.49	1296.54	32.10	103.91	9.2461	898.03
18.	284.18	30050.86	22.256	0.4572	24105.00	12.79	144.43	3461.24	1984.61	40.34	158.78	12.2746	1192.17
21.	322.51	43921.51	28.649	0.5189	35190.54	14.51	184.84	5198.00	2905.15	49.75	232.08	15.8091	1535.45
24.	361.94	62083.58	36.067	0.5823	49708.25	16.29	231.75	7478.90	4106.14	60.51	328.03	19.9109	1933.65
27.	401.70	84875.94	44.415	0.6463	67917.19	18.08	284.52	10361.07	5615.34	72.45	448.47	24.5262	2382.11
30.	441.68	112872.31	53.683	0.7106	90731.06	19.88	343.11	13914.75	7467.81	85.56	596.13	29.6509	2879.85

HCHEF	BAT1	BAT2	BATCC	BATCT	ECPB	ECPPS	ECPSS
EPROP	PROP	ESPR	SPR	UMM1	CMM1	UMM2	CMM2
EM	WIRE1	WIRE2	WIRE3	WIRE4	WIRE5	BENGY	VOLTFC
CELL2	CELL1	CFCM	RAD	TMR1	TMR2	SFC1	SFC2
STRMR	CSTRM	UFLM	ADDM1	ADDM2	ADDM3	SA	GEOF
SKIND	SMAT	ADHE	FIN	GLC	FINMR	SKINR	CD
SUPERT	F	AUTOM	TERMM	PAYM	TURBOM	SUBPOW	PMBYPD
VOLTSA							

0.11099997E+01 0.43500004E+01 0.13699999E+01 0.44800005E-02 0.61999999E-01 0.89999998E+00 0.97000003E+00 0.89999998E+00
0.75999999E+00 0.38699999E+01 0.10000000E+01 0.00000000E+00 0.80799999E-01 0.12110000E+02 0.86899996E+01 0.40799999E+01
0.75000000E+00 0.38000001E-02 0.50000008E-03 0.80000001E+00 0.33300000E+00 0.30900000E-02 0.83999997E+00 0.37000000E+02
0.24699999E-02 0.10000000E+01 0.32000000E+02 0.81599999E+01 0.63000002E-01 0.50000000E+00 0.73000002E+00 0.36000001E+00
0.19999999E+00 0.11000004E+01 0.52200001E-01 0.86300001E+01 0.45299997E+01 0.22700005E+01 0.44499998E+01 0.30000000E+01
0.11499996E+01 0.87737098E+08 0.43900013E-02 0.50000000E+01 0.10459995E+01 0.24999999E-01 0.10000000E+01 0.50000001E-01
0.10000002E+00 0.19999999E+00 0.45400000E+01 0.35699997E+01 0.90699997E+02 0.10000000E+01 0.50000001E-01 0.37000000E-01
0.10400000E+03

FUEL CELL AS POWER SOURCE

ALTITUDE= 21000. METERS   HLIFT=.0645 KG/M3   PRESS= 4678. NEWTON/M2   RHO=.07487 KG/M3   DELTAP= 1331. NEWTON/M2

WIND= 5.148 M/SEC   Q= 0.99 NEWTON/SQ.M

DAYS	LENGTH	MASS	PREQ	TSKIN	HULL	RP	MOTOR	FUEL	TFCM	STR	WIRE	POP	THRUST
3.	97.66	1219.81	0.383	0.1571	992.26	4.39	6.15	9.93	80.48	6.18	0.81	0.1812	35.20
5.	99.37	1284.37	0.395	0.1599	1045.55	4.47	6.22	17.06	84.13	6.26	0.85	0.1876	36.44
7.	100.59	1333.17	0.403	0.1618	1082.93	4.53	6.28	24.39	87.66	6.31	0.88	0.1922	37.34
9.	102.29	1402.06	0.415	0.1646	1139.39	4.60	6.35	32.28	91.91	6.39	0.93	0.1988	38.62
11.	104.00	1473.52	0.427	0.1673	1197.78	4.68	6.43	40.61	96.17	6.46	0.97	0.2055	39.92

WIND= 7.722 M/SEC   Q= 2.23 NEWTON/SQ.M

DAYS	LENGTH	MASS	PREQ	TSKIN	HULL	RP	MOTOR	FUEL	TFCM	STR	WIRE	POP	THRUST
3.	104.98	1514.01	1.334	0.1689	1230.43	4.72	12.16	34.57	100.55	7.64	3.38	0.7067	91.51
5.	110.35	1760.49	1.468	0.1775	1429.88	4.97	13.01	63.41	116.06	8.00	3.97	0.7808	101.12
7.	115.97	2042.59	1.615	0.1866	1656.43	5.22	13.94	97.69	134.41	8.38	4.55	0.8623	111.67
9.	122.31	2396.13	1.791	0.1968	1942.77	5.50	15.05	139.24	156.61	8.82	5.34	0.9593	124.23
11.	128.91	2805.18	1.983	0.2074	2272.72	5.80	16.26	188.43	182.78	9.30	6.25	1.0655	137.98

WIND=10.296 M/SEC   Q= 3.97 NEWTON/SQ.M

DAYS	LENGTH	MASS	PREQ	TSKIN	HULL	RP	MOTOR	FUEL	TFCM	STR	WIRE	POP	THRUST
3.	122.07	2331.93	4.152	0.1964	1931.63	5.49	29.98	107.62	160.07	11.80	12.58	2.2649	219.97
5.	135.31	3454.15	5.314	0.2225	2803.52	6.22	37.32	229.56	230.52	13.83	18.30	2.9074	282.38
7.	156.25	4995.49	6.767	0.2514	4030.59	7.03	46.51	409.27	332.23	16.30	26.39	3.7107	360.41
9.	176.86	7245.82	8.656	0.2846	5839.20	7.96	58.45	673.11	479.57	19.40	38.29	4.7553	461.86
11.	199.72	10353.37	10.966	0.3205	8335.63	8.95	73.05	1047.19	682.96	23.10	54.70	6.0323	585.89

WIND=12.870 M/SEC Q= 6.20 NEWTON/SQ.M

DAYS	LENGTH	MASS	PREQ	TSKIN	HULL	RP	MOTOR	FUEL	TFCM	STR	WIRE	POP	THRUST
3.	158.94	5256.86	13.618	0.2557	4240.08	7.15	89.82	352.99	360.00	25.05	54.25	7.4988	582.66
5.	202.15	10815.73	21.996	0.3252	8704.77	9.10	142.79	950.22	726.98	37.15	111.62	12.1309	942.57
7.	249.63	20369.54	33.514	0.4016	16353.61	11.23	215.61	2026.95	1359.33	53.37	210.21	18.4994	1437.41
9.	300.48	35522.51	48.531	0.4834	28482.68	13.57	310.54	3773.79	2355.29	74.13	366.58	26.8022	2082.53
11.	352.48	57339.84	66.762	0.5671	45920.19	15.86	425.80	6345.06	3789.69	98.99	591.75	36.8820	2865.74

WIND=15.444 M/SEC Q= 8.93 NEWTON/SQ.M

DAYS	LENGTH	MASS	PREQ	TSKIN	HULL	RP	MOTOR	FUEL	TFCM	STR	WIRE	[illegible]	THRUST
3.	234.99	16990.48	51.286	0.3780	13651.42	10.57	327.96	1329.34	1155.54	75.33	302.98	28.3254	1834.07
5.	326.02	45372.72	98.669	0.5245	36362.68	14.67	627.51	4262.48	3008.76	138.41	809.13	54.5232	3530.38
7.	420.65	97462.75	164.227	0.6767	77966.75	18.93	1041.97	9932.45	6378.70	224.80	1738.08	90.7705	5877.40
9.	517.82	181806.06	248.832	0.8331	1[illegible] 328.38	23.30	1576.84	19349.18	11777.43	334.96	3242.13	137.5485	8906.28
11.	614.82	304308.56	350.765	0.9891	243039.69	27.67	2221.26	33336.69	19602.96	467.22	5426.73	195.9073	12555.52

HASKV RUN 40 --BASE DATA, ALL SYSTEMS --

BCHEF	BAT1	BAT2	BATCC	BATCY	ECPB	ECPPS	ECPSS
EPROP	PROP	ESPR	SPR	UMM1	CMM1	UMM2	CMM2
EM	WIRE1	WIRE2	WIRE3	WIRE4	WIRE5	BENGY	VOLTFC
CELL2	CELL1	CFCM	RAD	TMR1	TMR2	SFC1	SFC2
STRMR	CSTRM	UFLM	ADDM1	ADDM2	ADDM3	SA	GEOF
SKIND	SMAT	ADHE	FIN	GLC	FINMR	SKINR	CD
SUPERT	F	AUTOM	TERMM	PAYM	TURBOR	SUBPOW	PNBYPD
VOLTSA							

0.11099997E+01	0.43500004E+01	0.13699999E+01	0.64800006E-02	0.61999999E-01	0.89999998E+00	0.97000003E+00	0.89999998E+00
0.75999999E+00	0.39699999E+01	0.10000000E+01	0.00000000E+00	0.80799997E-01	0.12110000E+02	0.86899996E+01	0.40799999E+01
0.75000000E+00	0.38000001E-02	0.50000008E-03	0.80000001E+00	0.33300000E+00	0.30900000E-02	0.83999997E+00	0.37000000E+02
0.24699999E-02	0.10000000E+01	0.32000000E+02	0.81599999E+01	0.63000023E-01	0.50000000E+00	0.73000002E+00	0.36000001E+00
0.19999999E+00	0.11000004E+01	0.52200001E-01	0.66300001E+01	0.45299997E+01	0.22700005E+01	0.44499998E+01	0.30000000E+01
0.11499996E+01	0.82737088E+08	0.43900013E-02	0.50000000E+01	0.10459995E+01	0.24999999E-01	0.10000000E+01	0.50000001E-01
0.10000002E+00	0.19999999E+00	0.45400000E+01	0.35699997E+01	0.90699997E+02	0.10000000E+01	0.50000001E-01	0.37000000E-01
0.10400000E+03							

FUEL CELL AS POWER SOURCE

ALTITUDE= 18000. METERS HLIFT=.1039 KG/M3 PRESS= 7505. NEWTON/M2 RHO=.12067 KG/M3 DELTAP= 2135. NEWTON/M2

WIND=10.296 M/SEC Q= 6.40 NEWTON/SQ.M

DAYS	LENGTH	MASS	PREQ	TSKIN	HULL	RP	MOTOR	FUEL	TFCM	STR	WIRE	POP	THRUST
3.	106.32	2534.66	5.064	0.2744	2037.[illegible]	4.78	35.74	131.26	179.33	12.40	13.40	2.7692	268.96
5.	122.92	3917.11	6.750	0.3173	3141.60	5.53	46.40	291.61	273.27	15.12	20.71	3.7015	359.51
7.	141.97	6034.45	8.965	0.3664	4830.87	6.39	60.53	543.42	417.41	18.60	31.90	4.9371	479.52
9.	163.15	9158.06	11.848	0.4211	7321.63	7.34	78.63	921.31	629.71	22.96	48.42	6.5201	633.26
11.	186.10	13591.59	15.399	0.4803	10857.68	8.37	101.08	1463.52	929.80	28.25	71.86	8.4834	823.95

ALTITUDE= 19500. METERS HLIFT=.0821 KG/M3 PRESS= 5924. NEWTON/M2 RHO=.09526 KG/M3 DELTAP= 1686. NEWTON/M2

WIND=10.296 M/SEC Q= 5.05 NEWTON/SQ.M

DAYS	LENGTH	MASS	PREQ	TSKIN	HULL	RP	MOTOR	FUEL	TFCM	STR	WIRE	POP	THRUST
3.	113.04	2406.00	4.524	0.2303	1937.12	5.09	37.33	117.27	167.93	11.96	12.71	2.4708	239.97
5.	129.27	3598.56	5.900	0.2634	2891.90	5.82	41.03	254.89	247.97	14.26	19.02	3.2315	313.85
7.	147.34	5327.64	7.648	0.3002	4269.25	6.63	52.[illegible]	462.54	366.06	17.10	28.15	4.1978	407.71
9.	167.97	7894.09	9.923	0.3422	6318.22	7.56	68.4[illegible]	771.60	539.15	20.70	41.71	5.4556	529.88
11.	190.43	11502.98	12.738	0.3880	9200.46	8.57	84.26	1210.64	781.65	25.04	60.78	7.0122	681.07

ALTITUDE= 21000. METERS HLIFT=.0645 KG/M3 PRESS= 4678. NEWTON/M2 RHO=.07487 KG/M3 DELTAP= 1331. NEWTON/M2

WIND=10.296 M/SEC Q= 3.97 NEWTON/SQ.M

DAYS	LENGTH	MASS	PREQ	TSKIN	HULL	RP	MOTOR	FUEL	TFCM	STR	WIRE	POP	THRUST
3.	122.07	2381.93	4.152	0.1964	1931.63	5.49	29.98	107.67	160.07	11.80	12.58	2.2649	219.97
5.	138.31	3464.15	5.314	0.2225	2893.52	6.27	37.32	229.56	230.52	13.83	18.30	2.9076	282.38
7.	156.75	4995.49	6.767	0.2514	4030.59	7.03	46.51	409.27	332.23	16.30	26.39	3.7107	360.41
9.	176.88	7245.32	8.656	0.2846	5839.20	7.96	59.45	673.11	479.57	19.40	38.29	4.7553	461.86
11.	199.72	10353.32	10.966	0.3205	8335.63	8.96	73.05	1042.19	682.96	23.10	54.70	6.0323	585.89

ALTITUDE= 22500. METERS HLIFT=.0507 KG/M3 PRESS= 3700. NEWTON/M2 RHO=.05881 KG/M3 DELTAP= 1053. NEWTON/M2

WIND=10.296 M/SEC Q= 3.12 NEWTON/SQ.M

DAYS	LENGTH	MASS	PREQ	TSKIN	HULL	RP	MOTOR	FUEL	TFCM	STR	WIRE	POP	THRUST
3.	132.57	2396.27	3.850	0.1687	1960.18	5.97	28.07	99.80	153.70	11.78	12.66	2.0981	203.77
5.	148.93	3397.45	4.844	0.1895	2772.77	6.70	34.36	209.28	216.55	13.61	17.95	2.6478	257.16
7.	167.48	4932.70	6.112	0.2131	3936.04	7.54	42.37	369.66	307.08	15.86	25.53	3.3486	325.24
9.	188.23	6859.88	7.706	0.2395	5578.74	8.47	57.45	599.21	434.87	18.60	36.24	4.2299	410.83
11.	210.21	9552.81	9.596	0.2674	7753.86	9.46	64.40	912.03	606.70	21.75	50.47	5.2750	512.34

APPENDIX B

MATERIAL TESTING

A biaxially oriented nylon 6 film was chosen as the candidate material from which the laminated film for hull construction was to be fabricated. This type of film was unproven for balloon use; and consequently, testing of the film was required. Also, tests were required to demonstrate the structural integrity of patches and seal junctions used in the design. Thermoplastic adhesive tapes had previously been developed for this film and it was intended that a significant portion of the tests be conducted on seals and seal junctions using these tapes. However, it was discovered that these tapes did not have sufficient shear strength for the intended use. Two additional procurements of sealing tapes were made, but after extensive testing the adhesive characteristics could not be improved. Consequently, the efforts to perform tests on the thermoplastic adhesive tapes were abandoned.

For the patch tests, a liquid adhesive, Adcote 102A, was successfully used. Patches of the fan and parabolic design, as shown on the following page, were tested both from a straight pull and at an angle of 45°. The fan patches were sealed to laminate with a 1 inch wide seal around the entire patch whereas the parabolic patches utilize a "T" tape with the base of the tape as the seal area. The results of these tests are listed in the table below. Limitations of the test

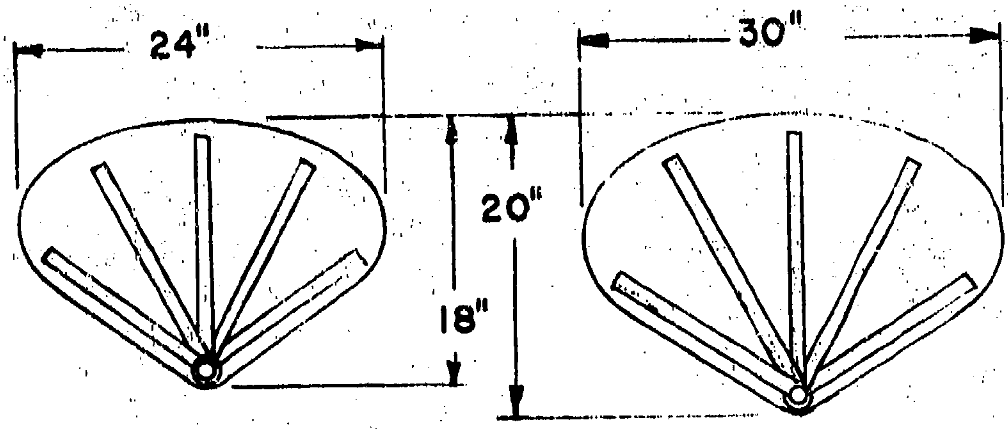

FAN PATCHES

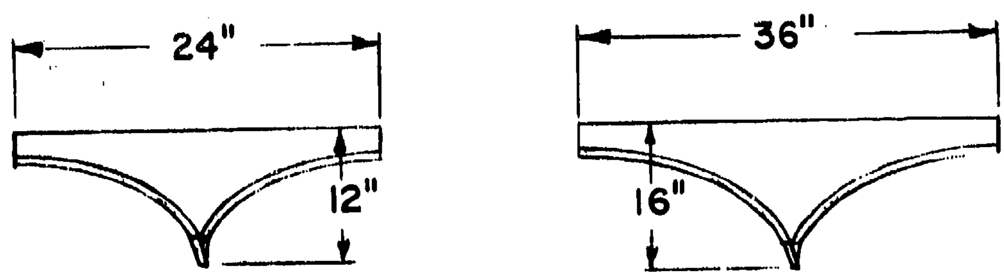

PARABOLIC PATCHES

equipment prevented any of the patches from being tested to ultimate strength. However, the results obtained in most cases are three to four times the actual loading that the patches would encounter in a launch or flight condition.

POBAL-S PATCH TESTS

NO.	PATCH DESCRIPTION	TYPE OF TEST	TENSION-POUNDS	OBSERVATIONS
1	24" FAN PATCH SEALED ON 3 PLY NYLON LAMINATE, 4 WEBBINGS IN PATCH	STRAIGHT PULL	1600	PATCH AND LAMINATE IN-TACT, NO TEARING OF WEBBINGS FROM PATCH FABRIC, DISTRIBUTES LOAD EVENLY.
2	24" FAN PATCH SEALED ON 3 PLY NYLON LAMINATE, 4 WEBBINGS IN PATCH	PULLED AT 45°	1000	TOP HALF OF PATCH TAKES MAJORITY OF LOAD, SLIGHT TEARING OF WEBS FROM FABRIC AT "D" RING ATTACHMENT.
3	24" FAN PATCH SEALED ON 3 PLY NYLON LAMINATE, 4 WEBBINGS IN PATCH	STRAIGHT PULL	1350	NO SIGNS OF PATCH OR LAMINATE FAILURE.
4	30" FAN PATCH SEALED ON 4 PLY NYLON LAMINATE, 5 WEBBINGS IN PATCH	STRAIGHT PULL	1000	PATCH AND LAMINATE IN-TACT.
5	30" FAN PATCH SEALED ON 4 PLY NYLON LAMINATE, 5 WEBBINGS IN PATCH	PULLED AT 45°	1250	PATCH AND LAMINATE IN-TACT.
6	24" PARABOLIC SEALED ON 3 PLY NYLON LAMINATE	STRAIGHT PULL	1350	ENDS OF PATCH CURL TO CENTER DUE TO UNI-AXIAL TEST, LEG OF "T" TAPE STRETCHES APPROX ½" FROM BASE THROUGH MIDDLE 1/3 OF PATCH.
7	24" PARABOLIC SEALED ON 3 PLY NYLON LAMINATE	PULLED AT 45°	1200	REINFORCEMENT WEBBING ALONG SLOPE OF CURVE BEGINS TO TEAR FROM FABRIC AROUND ATTACHMENT POINT.
8	24" PARABOLIC SEALED ON 3 PLY NYLON LAMINATE	STRAIGHT PULL	1250	LEG OF "T" TAPE STRETCHING BASE THROUGH CENTER 1/3 OF PATCH - SLOPE OF CURVE NEEDS TO BE INCREASED TO ALLEVIATE THIS.
9	36" PARABOLIC SEALED ON 4 PLY NYLON LAMINATE	STRAIGHT PULL	800	36" PARABOLIC HAS A GREATER SLOPE AND THUS DISTRIBUTES LOAD INTO LAMINATE MORE EVENLY. TEST TERMINATED AT 800 LBS. DUE TO MAL-FUNCTION OF EQUIPMENT.
10	36" PARABOLIC SEALED ON 4 PLY NYLON LAMINATE	PULLED AT 45°	600	WEBBING TEARS FROM FABRIC AT LOAD ATTACH-MENT - NEED HEAVIER FABRIC & WEBBING.

Both patch designs appear to distribute the load into the laminate, on which it is sealed, quite uniformly considering this was a uniaxial and not a biaxial test. The fan patch exhibited higher loadings than the parabolic at the 45° pull without any tearing of the fabric or webbings in the patch.

The tearing, however, could be alleviated by using heavier fabric and webbing in the patch design.

Earlier ultraviolet radiation exposure tests had shown that the biaxially oriented nylon 6 film exhibits much less degradation in strength and ductility after exposure than does comparable polyester film. Samples were exposed under a GE H12T3, 750 W UV lamp at a nominal distance of 14 inches from the lamp. Exposure times of 9 hours and 16 hours were used. Tensile strengths and ultimate elongations were determined from strip tensile tests performed at -60°C with an initial jaw distance of 2 inches and a separation rate of 2 inches/minute. The results are as follows:

ULTRAVIOLET DEGRADATION TESTS

Material	Orientation	Tensile Strength (lb) After exposure of 0 hr	9 hr	16 hr	Elongation (%) After exposure of 0 hr	9 hr	16 hr
1 mil nylon 6	TD	41.2	33.1	7.3	36.8	21.0	0
½x½ mil polyester	TD	30.6	18.9	6.3	29.5	3.1	0
1 mil nylon 6	MD	42.1	32.5	---	35.8	14.3	---
½x½ mil polyester	MD	36.8	14.3	---	31.0	1.9	---

Tests have consistently shown the nylon film to be superior; but as the table shows after enough exposure the nylon, like the polyester, will degrade to an unusable state.

Water absorption by the nylon film can be an important factor to consider. Tests have been performed to determine the changes in weight, tensile strength, and ultimate elongation of the film as affected by relative humidity. Samples were stored at room temperature at 0, 50, and 100% relative humidities and were tested after 7 days and 30 days. Most of the change occurred after 7 days, but additional change can be detected after 30 days. The 30 day results are summarized below. For the tensile tests the jaw distance was 3 inches with separation rates of 2.0, 0.5, and 0.2 inch/min corresponding to testing temperatures of 21, -25, and -70°C.

EFFECTS OF WATER ABSORPTION TESTS

	0% RH	50% RH	100% RH
Thickness, μm	25.1	26.1	26.0
Weight, g/m²	29.1	31.9	32.0
Specific gravity (calculated)	1.16	1.22	1.23
M.D. Tensile Strengths, lb, @:			
21°C	31.0	29.1	27.1
-25°C	29.6	29.4	30.5
-70°C	34.6	34.5	37.3
T.D. Tensile Strengths, lb, @:			
21°C	34.0	32.0	30.3
-25°C	33.6	31.4	32.9
-70°C	38.2	36.2	35.4

(cont.)

EFFECTS OF WATER ABSORPTION TESTS (cont.)

	0% RH	50% RH	100% RH
M.D. Elongation, %, @:			
21°C	68	69	74
-25°C	48	47	58
-70°C	42	41	46
T.D. Elongation, %, @:			
21°C	72	68	73
-25°C	50	48	57
-70°C	47	39	34

A variety of stress/strain tests were performed using the 25 µm film. During this testing it became obvious that the nylon film exhibited unstable creep characteristics. Further, it was determined that the creep characteristics were very difficult to predict as a result of variations in the film properties and because of the sensitivity of these characteristics to temperature. There were significant differences between identical tests and anomalies between similar tests performed at different temperatures. The following table summarizes the nominal results obtained from the biaxial creep tests.

BIAXIAL CREEP TESTS

Stress lb/in^2	Temperature (°C)	Elongation (%) Initial Value	Elongation (%) After 4 Hours of Creep
12,000	-70	3	4
14,000	-70	---	8
14,000	-33	4	5
8,000	-25	2	4
10,000	-25	5	7
14,000	-25	---	20
8,000	-10	5	25
10,000	-10	2	9
7,000	0	8	725
10,000	21	7	12

The uniaxial dead load tests also showed creep instabilities which are difficult to predict. The following lists are some typical examples:

UNIAXIAL DEAD LOAD CREEP TESTS

Stress	Temperature	Elongation (%)					
(lb/in^2)	(°C)	after test times of					
		0 hr	3 hr	24 hr	51 hr	96 hr	168 hr
10,000	21	10	15	18	25	---	---
14,000	21	18	22	27	33	---	35
14,000	-33	3	---	---	---	10	---
21,000	-33	7	---	---	---	17	---

Except for the creep instability, the biaxially oriented nylon 6 film would function as a good superpressure balloon material. All other characteristics including handling, pinholing, permeability, spectral transmittance and reflectance, etc., are excellent; and this film should be analyzed further for possible use as a fiber reinforced gas barrier.

APPENDIX C

```
// READ DEVICE-MFCU1
// PRINT DEVICE-5203
   1              PROGRAM STABAN
            C     STABILITY ANALYSIS PROGRAM
            C     SOLUTION FOR GAIN AND PHASE ANGLE OF EQUATION OF THE FORM
            C     EO/EI=K1*K2*...*KN*(1+2*S)*...*(1+TM*S)/S*(1+T1*S)...*(1+TJ*S)
   2              DIMENSION      TNUM( 7),TDEN( 8),ZK(8),HEAD(20)
   3              DIMENSION T2DEN( 4),ZETA( 4)
   4              READ(1,10) HEAD
   5         10   FORMAT(20A4)
   6              READ(1,20) (ZK(I), I=1,8)
            C   **READ TAU'S (TNUM) IN NUMERATOR
   7              READ(1,20)(TNUM(I),I=1,7)
            C*****READ INFO FOR DENOMINATOR
            C   **READ EXPONENT OF S
   8              READ(1,20)EXS
            C   **READ TAU'S (TDEN) IN DENOMINATOR
   9              READ(1,20)(TDEN(I),I=1,8)
            C   **READ TAU'S AND ZETA'S FOR EACH TERM
  10              READ(1,20)((T2DEN(I),ZETA(I)),I=1,4)
            C*****READ BEGINNING AND ENDING VALUES FOR OMEGA, ALSO INCREMENT
  11              WRITE(3,11) HEAD
  12         11   FORMAT('1',20A4)
  13              WRITE(3,400)
  14        400   FORMAT(/'  INPUT PROBLEM = EO/EI ='/' (K1)(K2)(K3)(K4)(K5)(K6)(K7)
                 2(K8)(1+T1S)(1+T3S)(1+T5S)(1+T7S)(1+T9S)(1+T11S)(1+T13S)'/' S**N(1+
                 3T2S)(1+T4S)(1+T6S)(1+T8S)(1+T10S)(1+T12S)(1+T14S)(1+T16S)(1+2Z2T18
                 4S+T18**2S**2)(1+2Z4T20S+T20**2S**2)'/61X,'(1+2Z6T22S+T22**2S**2)(1
                 5+2Z8T24S+T24**2S**2)')
  15              WRITE(3,401)(ZK(I),I=1,8)
  16        401   FORMAT(' K1=',F10.5,2X,'K2=',F10.5,2X,'K3=',F10.5,2X,'K4=',F10.5,
                 22X,'K5=',F10.5,2X,'K6=',F10.5,2X,'K7=',F10.5,2X,'K8=',F10.5)
  17              WRITE(3,402)(TNUM(I),I=1,7)
  18        402   FORMAT(' T1=',F8.5,2X,'T3=',F8.5,2X,'T5=',F8.5,2X,'T7=',F8.5,2X,
                 2'T9=',F8.5,2X,'T11=',F8.5,2X,'T13=',F8.5)
  19              WRITE(3,403) EXS,(TDEN(I),I=1,8),(ZETA(I),T2DEN(I),I=1,4)
  20        403   FORMAT(' N=',F3.0,2X,'T2=',F8.5,2X,'T4=',F8.5,2X,'T6=',F8.5,2X,
                 2'T8=',F8.5,2X,'T10=',F8.5,2X,'T12=',F8.5,2X,'T14=',F8.5,2X,'T16',
                 3F8.5 /' ZETA2=',F6.5,2X,'T18=',F8.5,3X,'ZETA4=',F6.5,2X,'T20=',
                 4F8.5,3X,'ZETA6=',F6.5,2X,'T22=',F8.5,3X,'ZETA8=',F6.5,2X,'T24=',
                 5F8.5 ///)
  21              DO 150 I=1,8
  22              IF(ZK(I).EQ.0.0)ZK(I)=1.0
  23        150   CONTINUE
  24        100   READ(1,20,END=500) WBEGIN,WEND,WINCR
  25         20   FORMAT(5F10.0)
  26              IF(WBEGIN.EQ.0.0)GO TO 500
            C*****PERFORM CALCS
  27              W=WBEGIN
  28        105   CONTINUE
            C*****EVALUATE NUMERATOR TERMS
  29              GNUMT=0.0
  30              PHINUM=0.0
  31              DO 160 I=1,7
  32              GNUMT=GNUMT+20.0*ALOG10(SQRT(1.0 +(W*TNUM(I))**2))
  33              PHIN=ATAN(W*TNUM(I))
  34              IF(PHIN.LT.0.0)PHIN=PHIN+3.1416
```

```
160   PHINUM=PHINUM+PHIN
C*****EVALUATE DENOMINATOR TERMS
      GDENT=0.0
      PHIDEN=0.0
      DO 170 I=1,6
      GDENT=GDENT+20.0*ALOG10(SQRT(1.0+(W*TDEN(I))**2))
      PHID=ATAN(W*TDEN(I))
      IF(PHID.LT.0.0)PHID=PHID+3.1416
170   PHIDEN=PHIDEN+PHID
C*****EVALUATE SECOND ORDER DENOMINATOR TERMS
      GDEN2=0.0
      PHIDN2=0.0
      DO 190I=1,4
      T1=(1.0-T2DEN(I)**2*W**2)**2
      T2=(2.0*ZETA(I)*T2DEN(I)*W)**2
      T3=SQRT(T1+T2)
      T4=ALOG10(T3)
      GDEN2=GDEN2+20.0*T4
      CHECK=1.0-T2DEN(I)**2*W**2
      IF(ABS(CHECK).GT..00001)GO TO 188
      IF(CHECK.GT.0.0)GO TO 185
      PHIT=-1.5708
      GO TO 189
185   PHIT=1.5708
      GO TO 189
188   CONTINUE
      PHIT=ATAN(2.0*ZETA(I)*T2DEN(I)*W)/(1.0-T2DEN(I)**2*W**2))
C     IF PHIT IN 4TH QUADRANT, SHIFT TO 2ND QUADRANT
189   CONTINUE
      IF(PHIT.LT.0.0)PHIT=PHIT+3.1416
190   PHIDN2=PHIDN2+PHIT
      GAIN=GNUMT-GDENT
      PHI=PHINUM-PHIDEN
      GAIN=GAIN-GDEN2
      PHI=PHI-PHIDN2
      AK=ZK(1)*ZK(2)*ZK(3)*ZK(4)*ZK(5)*ZK(6)*ZK(7)*ZK(8)
      GAIN=GAIN+20.0*ALOG10(AK )
      GAIN=GAIN-20.0*EXS*ALOG10(W)
      PHI=PHI*360./3.1416/2.0-EXS*90.0
      WRITE(3,300)W,GAIN,PHI
300   FORMAT(' OMEGA=',F8.3,'RAD/S',5X,'GAIN=',F8.1,'DB',5X,'PHI=',F9.2,
     2'DEG')
      W=W+WINCR
      IF(W.GT.WEND)GO TO 100
      GOTO 105
500   STOP
      END

000 TOTAL ERRORS FOR THIS COMPILATION
OL100 I  THE TOTAL CORE USED BY STABAN IS 11452 DECIMAL.
OL101 I  THE START CENTRAL ADDRESS OF THIS MODULE IS 0C00.
OL104 I  TOTAL NUMBER OF LIBRARY SECTORS REQUIRED IS   49
         NAME-STABAN,PACK-FORTR2,UNIT-R1,RETAIN-T,LIBRARY-0
```

BODE PLOT OF TRANSFER FUNCTION RUN 4

INPUT PROBLEM = E3/E1 =

```
(K1)(K2)(K3)(K4)(K5)(K6)(K7)(K8)(1+T1S)(1+T3S)(1+T5S)(1+T7S)(1+T9S)(1+T11S)(1+T13S)
S**3(1+T2S)(1+T4S)(1+T6S)(1+T8S)(1+T10S)(1+T12S)(1+T14S)(1+T16S)(1+2Z2T18S+T18**2S**2)(1+2Z4T20S+T20**2S**2)
(1+2Z6T22S+T22**2S**2)(1+2Z8T24S+T24**2S**2)
```

```
K1= 19.16001  K2= 24.70000  K3= 0.00210  K4= 24.60001  K5= 0.01100  K6= 0.00000  K7= 0.00000  K8= 0.00000
T1= 0.00000  T3= 0.00000  T5= 0.00000  T7= 0.00000  T9= 0.00000  T11= 0.00000  T13= 0.00000
T2= 1.  T2= 1.44000  T4= 0.00000  T6= 0.00000  T8= 0.00000  T10= 0.00031  T12= 0.00000  T14= 0.00000  T16= 0.00000
ZETA2=.00236  T18= 0.00059  ZETA4=.00000  T20= 0.00000  ZETA6=.00000  T22= 0.00000  ZETA8=.00000  T24= 0.00000
```

OMEGA= 0.1000RAD/S	GAIN= 21.108	PHI= -93.559DEG
OMEGA= 0.2000RAD/S	GAIN= 15.108	PHI= -95.070DEG
OMEGA= 0.3000RAD/S	GAIN= 11.598	PHI= -97.530DEG
OMEGA= 0.4000RAD/S	GAIN= 9.013	PHI= -100.330DEG
OMEGA= 0.5000RAD/S	GAIN= 7.308	PHI= -102.540DEG
OMEGA= 0.6000RAD/S	GAIN= 5.303	PHI= -105.450DEG
OMEGA= 0.7000RAD/S	GAIN= 3.[illegible]	PHI= -107.490DEG
OMEGA= 0.8000RAD/S	GAIN= 2.51[illegible]	PHI= -10[illegible]DEG
OMEGA= 0.9000RAD/S	GAIN= 1.403	PHI= -111.830DEG
OMEGA= 1.0000RAD/S	GAIN= 0.603	PHI= -113.900DEG
OMEGA= 2.0000RAD/S	GAIN= -7.5[illegible]	PHI= -131.670DEG
OMEGA= 3.0000RAD/S	GAIN= -12.[illegible]	PHI= -144.140DEG
OMEGA= 4.0000RAD/S	GAIN= -17.101	PHI= -150.670DEG
OMEGA= 5.0000RAD/S	GAIN= -20.603	PHI= -155.[illegible]DEG
OMEGA= 6.0000RAD/S	GAIN= -23.503	PHI= -157.470DEG
OMEGA= 7.0000RAD/S	GAIN= -26.103	PHI= -162.200DEG
OMEGA= 8.0000RAD/S	GAIN= -2[illegible]	PHI= -164.410DEG
OMEGA= 9.0000RAD/S	GAIN= -30.[illegible]	PHI= -165.[illegible]DEG
OMEGA= 10.0000RAD/S	GAIN= -32.603	PHI= -167.[illegible]DEG
OMEGA= 20.0000RAD/S	GAIN= -43.[illegible]	PHI= -173.570DEG
OMEGA= 30.0000RAD/S	GAIN= -50.903	PHI= -175.720DEG
OMEGA= 40.0000RAD/S	GAIN= -55.[illegible]	PHI= -176.[illegible]DEG
OMEGA= 50.0000RAD/S	GAIN= -59.4[illegible]	PHI= -177.410DEG
OMEGA= 60.0000RAD/S	GAIN= -62.[illegible]	PHI= -177.[illegible]DEG
OMEGA= 70.0000RAD/S	GAIN= -65.[illegible]	PHI= -178.[illegible]DEG
OMEGA= 80.0000RAD/S	GAIN= -67.[illegible]	PHI= -178.4[illegible]DEG
OMEGA= 90.0000RAD/S	GAIN= -70.[illegible]	PHI= -178.[illegible]DEG
OMEGA= 100.0000RAD/S	GAIN= -71.[illegible]	PHI= -178.[illegible]DEG
OMEGA= 200.0000RAD/S	GAIN= -83.[illegible]	PHI= -177.510DEG
OMEGA= 300.0000RAD/S	GAIN= -9[illegible]	PHI= -179.[illegible]DEG
OMEGA= 400.0000RAD/S	GAIN= -95.[illegible]	PHI= -177.750DEG
OMEGA= 500.0000RAD/S	GAIN= -9[illegible]	PHI= -179.[illegible]DEG
OMEGA= 600.0000RAD/S	GAIN= -101.[illegible]	PHI= -179.[illegible]DEG
OMEGA= 700.0000RAD/S	GAIN= -104.[illegible]	PHI= -179.[illegible]DEG
OMEGA= 800.0000RAD/S	GAIN= -105.[illegible]	PHI= -1[illegible]DEG
OMEGA= 900.0000RAD/S	GAIN= -107.1[illegible]	PHI= -1[illegible]DEG
OMEGA=1000.0000RAD/S	GAIN= -10[illegible]	PHI= -1[illegible].110DEG
OMEGA=1100.0000RAD/S	GAIN= -1[illegible]	PHI= -1[illegible]DEG
OMEGA=1200.0000RAD/S	GAIN= -10[illegible].0[illegible]	PHI= -1[illegible].770DEG
OMEGA=1300.0000RAD/S	GAIN= -10[illegible]	PHI= -1[illegible].460DEG
OMEGA=1400.0000RAD/S	GAIN= -1[illegible]	PHI= -1[illegible]DEG
OMEGA=1500.0000RAD/S	GAIN= -105.704	PHI= -181.[illegible]DEG
OMEGA=1600.0000RAD/S	GAIN= -101.[illegible]	PHI= -18[illegible]DEG
OMEGA=1700.0000RAD/S	GAIN= -75.704	PHI= -2[illegible]DEG
OMEGA=1800.0000RAD/S	GAIN= -10[illegible]	PHI= -357.[illegible]DEG
OMEGA=1900.0000RAD/S	GAIN= -111.[illegible]	PHI= -35[illegible].7[illegible]DEG
OMEGA=2000.0000RAD/S	GAIN= -115.608	PHI= -35[illegible].11DEG
OMEGA=2100.0000RAD/S	GAIN= -119.208	PHI= -35[illegible].11DEG
OMEGA=2200.0000RAD/S	GAIN= -122.2[illegible]	PHI= -35[illegible].4[illegible]DEG
OMEGA=2300.0000RAD/S	GAIN= -124.709	PHI= -35[illegible].51DEG
OMEGA=2400.0000RAD/S	GAIN= -127.0[illegible]	PHI= -357.56DEG
OMEGA=2500.0000RAD/S	GAIN= -129.108	PHI= -35[illegible].61DEG

```
  1           SUBROUTINE STADER
  2           COMMON AO(8),BO(4),     CDO,CDI,CDOT,CDIT,ELT,ELG,HZ,GSA,GSAM,
             1GSAL,GSALR,GSAMR,GSHT,GSVT,GHTM,GVTM,GHTL,GVTL,SUMFZ,SUMFX,SUMFY,
             2ZMOM,YMOM,THR,VELO,LOOP,B,LINE,L,ITEST
        C** STADER READS STABILITY DERIVATIVES AND CALCULATES NEEDED CONSTANTS.
  3           READ(1,*) CLA,CLQ,CDO,CDI,CMA,CMQ,CLAT,CDOT,CDIT,CMT,VOL,DIA,ELA,
             1ELG,ELT,HZ,SV,SH,CV,CH,RHO
  4           WRITE(3,55)
  5        55 FORMAT('1'////31X,'INPUTS AND OUTPUT CONSTANTS FOR SUBROUTINE STAD
             1ER'///)
  6           WRITE(3,4)
  7         4 FORMAT(21X,3HCLA,7X,3HCLQ,7X,3HCDO,7X,3HCDI,7X,3HCMA,7X,3HCMQ,7X,
             A4HCLAT,6X,4HCDOT/21X,4HCDIT,6X,3HCMT,7X,3HVOL,7X,3HDIA,7X,3HELA,
             B7X,3HELG,7X,3HELT,7X,2HHZ/21X,2HSV,8X,2HSH,8X,2HCV,8X,2HCH,8X,
             C3HRHO///)
  8           WRITE(3,*)CLA,CLQ,CDO,CDI,CMA,CMQ,CLAT,CDOT,CDIT,CMT,VOL,DIA,ELA,
             1ELG,ELT,HZ,SV,SH,CV,CH,RHO
        C** VARIABLE NAMES BEGINING WITH G ARE CONSTANT PARAMETERS
  9           GSA=VOL**0.666667/2.*RHO
 10           GSAM=VOL/2.*RHO*CMA
 11           GSAL=GSA*CLA
 12           GSAR=ELA**2.*DIA*RHO
 13           GSALR=GSAR*CLQ
 14           GSAMR=GSAR*ELA*CMQ
 15           GSHT=SH/2.*RHO
 16           GSVT=SV/2.*RHO
 17           GHTM=GSHT*CH*CMT
 18           GVTM=GSVT*CV*CMT
 19           GHTL=GSHT*CLAT
 20           GVTL=GSVT*CLAT
 21           WRITE(3,44) GSA,GSAM,GSAL,GSAR,GSALR,GSAMR,GSHT,GSVT,GHTM,GVTM,
             1GHTL,GVTL
 22        44 FORMAT(5H0GSA=,E14.7,7X,5HGSAM=,E14.7,6X,5HGSAL=,E14.7,6X,5HGSAR=,
             1E14.7/7H GSALR=,E14.7,5X,6HGSAMR=,E14.7,5X,5HGSHT=,E14.7,6X,5HGSVT
             2=,E14.7/6H GHTM=,E14.7,6X,5HGVTM=,E14.7,6X,5HGHTL=,E14.7,6X,5HGVTL
             3=,E14.7//)
 23           RETURN
 24           END

    000 TOTAL ERRORS FOR THIS COMPILATION
 QL103 I  TOTAL NUMBER OF LIBRARY SECTORS REQUIRED IS     8
          NAME-STADER,PACK-FORTR2,UNIT-R1,RETAIN-T,LIBRARY-R,CATEGORY-020
```

APPENDIX D

```
// READ DEVICE-MFCU1
// PRINT DEVICE-5203
 1          PROGRAM POSIM
 2          COMMON AO(8),BO(4),    CDO,CDI,CDOT,CDIT,ELT,ELG,HZ,GSA,GSAM,
          1GSAL,GSALR,GSAMR,GSHT,GSVT,GHTM,GVTM,GHTL,GVTL,SUMFZ,SUMFX,SUMFY,
          2ZMOM,YMOM,THR,VELO,LOOP,B,LINE,L,ITEST
 3          DIMENSION AX(8),BX(4),CO(2),CX(2),TITLE(20),AN(8)
      C** A ARRAY IS... 1=ALPHA,2=BETA,3=GAMMA,4=PHI,5=PSI,6=TAU,7=THETA,
      C 8=DELTA-- B ARRAY IS FIRST DERIVATIVE WITH TIME... 1=GAMMA,2=PHI,3=PSI
      C 4=THETA-- C ARRAY IS SECOND DERIVATIVE WITH TIME... 1=PSI,2=THETA
      C   ARRAYS WITH X ARE ITERATIONS BASED ON INITIAL ZERO ARRAYS
      C   AN ARRAY IS AO ARRAY IN DEGREES FOR OUTPUT
      C** INITIALIZE FOR STRAIGHT AND LEVEL FLIGHT
 4          DATA RAD,DEG/0.01745329,57.29578/
 5          CALL STADER
 6       99 READ(1,4,END=999)TITLE
 7        4 FORMAT(20A4)
 8          READ (1,3) AO
 9        3 FORMAT(8F10.0)
10          READ(1,2)  VELO,THR,B,TMAX,DIT,LOOP,ITEST
11        2 FORMAT(5F10.0,2I5)
12          READ(1,3) XMASS,YMASS,ZMASS,YYI,ZZI
13          READ(1,3) PEG,PRG,YEG,YRG,HEAD,AY,RATE
      C**        VELO   =    INITIAL VELOCITY-- M/SEC
      C          RATE   =    ANGULAR RATE OF GIMBAL-- DEG/SEC
      C          DIT    =    DIFFERENTIAL INCREMENT OF TIME-- SEC
      C          LOOP   =    NUMBER OF LOOPS BETWEEN PRINT OUTS
      C          PEG    =    AUTOPILOT PITCH ERROR GAIN
      C          PRG    =    AUTOPILOT PITCH RATE GAIN
      C          YEG    =    AUTOPILOT YAW ERROR GAIN
      C          YRG    =    AUTOPILOT YAW RATE GAIN
      C          HEAD   =    INPUT HEADING
      C          AY     =    TRIM PITCH ANGLE
14          TOO= 0.0
15          VELDO = 0.0
16          DO 6 I=1,4
17          BX(I)=0.0
18        6 BO(I)=0.0
19          DO 7 I=1,8
20        7 AX(I)=0.0
21          DO 8 I=1,2
22          CO(I)=0.0
23        8 CX(I)=0.0
24          WRITE(3,4)TITLE
25          WRITE(3,5)HEAD,AY,RATE,PEG,PRG,YEG,YRG
26        5 FORMAT('0',20X,'INPUT HEADING=', F6.2,8X,'TRIM PITCH ANGLE=',F6.2/
          A/   31X,'GIMBAL RATE=',F5.2,8H DEG/SEC/16X,'PITCH ERROR GAIN=',
          BF6.2,6X,'PITCH RATE GAIN=',F6.2/16X,'YAW ERROR GAIN=',F6.2,10X,
          C'YAW RATE GAIN=',F6.2//)
27          WRITE(3,11) DIT,VELO,THR
28       11 FORMAT('0',20X,'DIFFERENTIAL TIME INCREMENT=',F5.2/21X,
          1'INITIAL VELOCITY=',F6.2/21X,'THRUST=',F7.2//)
29          WRITE(3,12) XMASS,YMASS,ZMASS,YYI,ZZI
30       12 FORMAT('0',20X,'BALLON PARAMETERS FOR DYNAMIC EQUATIONS--'/16X,
          A'XMASS= ',E14.7/16X,'YMASS= ',E14.7/16X,'ZMASS= ',E14.7/16X,
          B'IYY= ',E14.7/16X,'IZZ= ',E14.7)
31          RATE=RATE * RAD
```

```
      GARC= RATE* DIT
      GLIMIT = 45. * RAD
      AY=AY * RAD
      BY=HEAD* RAD
   14 WRITE(3,45)
   45 FORMAT('1'///18X,'TIME',8X,'THETA',7X,'ALPHA',7X,'DELTA',7X,'PSI',
     A9X,'BETA',8X,'TAU',9X,'VEL'//)
      LINE = 5
   66 DO 30 L=1,LOOP
      CALL FORCE
      VELDX= SUMFX / XMASS
      BX(1)= SUMFZ /(ZMASS * VELO)
      BX(2)= SUMFY /(YMASS * VELO)
      CX(1)= ZMOM / ZZI
      CX(2)= YMOM / YYI
      HT= DIT/2.
      VELX= VELO + (VELDO +VELDX)*HT
      BX(4)= BO(4) +(CO(2) +CX(2)) *HT
      AX(7)= AO(7)+(BO(4) +BX(4)) *HT
      BX(3)= BO(3) +(CO(1) +CX(1)) *HT
      AX(5)= AO(5) +(BO(3) +BX(3)) *HT
      AX(3)= AO(3) +(BO(1) +BX(1)) *HT
      AX(4)= AO(4) +(BO(2) +BX(2)) *HT
      AX(1)= AX(7) -AX(3)
      AX(2)= AX(4) -AX(5)
      AX(8)= PEG* (AX(7)-AY) + PRG* BX(4)
      AX(6)= YEG* (AX(5)-BY) + YRG *BX(3)
      DO 21 J=6,8,2
      IF(ABS(AX(J)-AO(J)).GT.GARC) AX(J)= AO(J)+ SIGN(GARC,AX(J))
      IF(ABS(AX(J)).GT.GLIMIT) AX(J)= SIGN(GLIMIT,AX(J))
   21 CONTINUE
      VELO=VELX
      DO 23 I=1,8
   23 AO(I)=AX(I)
      DO 24 I=1,4
   24 BO(I)=BX(I)
      DO 25 I=1,2
   25 CO(I)=CX(I)
      TOO=TOO +DIT +0.0000159
      IF(ITEST-1) 30,68,30
   68 IF(LOOP-(L+1)) 30,69,30
   69 WRITE(3,32) TOO,AO(7),AO(1),AO(8),AO(5),AO(2),AO(6),VELO
      WRITE(3,71) BO,CO
   71 FORMAT(' FIRST DERIVATIVE WITH TIME--'/6X,'GAMMA= ',E14.7,5X,
     2'PHI= ',E14.7,5X,'PSI= ',E14.7,5X,'THETA= ',E14.7/' SECOND DERIVAT
     3IVE WITH TIME--',6X,'PSI= ',E14.7,5X,'THETA= ',E14.7)
      LINE=LINE + 4
   30 CONTINUE
      DO 31 I=1,8
   31 AN(I)=AO(I)*DEG
      WRITE(3,32) TOO,AN(7),AN(1),AN(8),AN(5),AN(2),AN(6),VELO
   32 FORMAT(12X,8F12.5)
      LINE=LINE+1
      IF(TMAX-TOO) 99,99,35
   35 IF(LINE-58) 66,14,14
  999 STOP
      END
```

```
   000 TOTAL ERRORS FOR THIS COMPILATION
OL100 I  THE TOTAL CORE USED BY POSIM  IS 13312 DECIMAL.
OL101 I  THE START CONTROL ADDRESS OF THIS MODULE IS 0000.
OL102 I  THE NON-OVERLAY CORE SIZE IS    15375 DECIMAL
OL104 I  TOTAL NUMBER OF LIBRARY SECTORS REQUIRED IS   72
         NAME-POSIM ,PACK-FORTR2,UNIT-R1,RETAIN-T,LIBRARY-O
```

```
 1          SUBROUTINE STADER
 2          COMMON A0(8),B0(4),     CDO,CDI,CDOT,CDIT,ELT,ELG,HZ,GSA,GSAM,
           1GSAL,GSALR,GSAMR,GSHT,GSVT,GHTM,GVTM,GHTL,GVTL,SUMFZ,SUMFX,SUMFY,
           2ZMOM,YMOM,THR,VELO,LOOP,B,LINE,L,ITEST
      C** STADER READS STABILITY DERIVATIVES AND CALCULATES NEEDED CONSTANTS.
 3          READ(1,*) CLA,CLQ,CDO,CDI,CMA,CMQ,CLAT,CDOT,CDIT,CMT,VOL,DIA,ELA,
           1ELG,ELT,HZ,SV,SH,CV,CH,RHO
 4          WRITE(3,55)
 5       55 FORMAT('1'////31X,'INPUTS AND OUTPUT CONSTANTS FOR SUBROUTINE STAD
           1ER'///)
 6          WRITE(3,4)
 7        4 FORMAT(21X,3HCLA,7X,3HCLQ,7X,3HCDO,7X,3HCDI,7X,3HCMA,7X,3HCMQ,7X,
           A4HCLAT,6X,4HCDOT/21X,4HCDIT,6X,3HCMT,7X,3HVOL,7X,3HDIA,7X,3HELA,
           B7X,3HELG,7X,3HELT,7X,2HHZ/21X,2HSV,8X,2HSH,8X,2HCV,8X,2HCH,8X,
           C3HRHO///)
 8          WRITE(3,*)CLA,CLQ,CDO,CDI,CMA,CMQ,CLAT,CDOT,CDIT,CMT,VOL,DIA,ELA,
           1ELG,ELT,HZ,SV,SH,CV,CH,RHO
      C** VARIABLE NAMES BEGINING WITH G ARE CONSTANT PARAMETERS
 9          GSA=VOL**0.666667/2.*RHO
10          GSAM=VOL/2.*RHO*CMA
11          GSAL=GSA*CLA
12          GSAR=ELA**2.*DIA*RHO
13          GSALR=GSAR*CLQ
14          GSAMR=GSAR*ELA*CMQ
15          GSHT=SH/2.*RHO
16          GSVT=SV/2.*RHO
17          GHTM=GSHT*CH*CMT
18          GVTM=GSVT*CV*CMT
19          GHTL=GSHT*CLAT
20          GVTL=GSVT*CLAT
21          WRITE(3,44) GSA,GSAM,GSAL,GSAR,GSALR,GSAMR,GSHT,GSVT,GHTM,GVTM,
           1GHTL,GVTL
22       44 FORMAT(5HGGSA=,E14.7,7X,5HGSAM=,E14.7,6X,5HGSAL=,E14.7,6X,5HGSAR=,
           1E14.7/7H GSALR=,E14.7,5X,6HGSAMR=,E14.7,5X,5HGSHT=,E14.7,6X,5HGSVT
           2=,E14.7/6H GHTM=,E14.7,6X,5HGVTM=,E14.7,6X,5HGHTL=,E14.7,6X,5HGVTL
           3=,E14.7//)
23          RETURN
24          END

   000 TOTAL ERRORS FOR THIS COMPILATION
OL103 I  TOTAL NUMBER OF LIBRARY SECTORS REQUIRED IS     8
         NAME-STADER,PACK-FORTR2,UNIT-K1,RETAIN-T,LIBRARY-R,CATEGORY-020
```

```
      SUBROUTINE FORCE
      COMMON AO(8),BO(4),     CDO,CDI,CDOT,CDIT,ELT,ELG,HZ,GSA,GSAM,
     1GSAL,GSALR,GSAMR,GSHT,GSVT,GHTM,GVTM,GHTL,GVTL,SUMFZ,SUMFX,SUMFY,
     2ZMOM,YMOM,THR,VELO,LOOP,B,LINE,L,ITEST
      VV= VELO ** 2.
      ANG2= AO(1)**2.+AO(2)**2.
      ANG= SQRT(ANG2)
      ALA=GSAL * AO(1) * VV
      ALQ= GSALR * BO(4) * VELO
      ADF= VV * GSA * (CDO + CDI * ANG2)
      APMA= VV * GSAM * AO(1)
      APMQ= VELO * GSAMR * BO(4)
      ASB= GSAL * VV *(-AO(2))
      ASR= GSALR * VELO * BO(3)
      AYMB= VV * GSAM *(-AO(2))
      AYMR= VELO * GSAMR * BO(3)
      HTL= VV * GHTL * AO(1)
      VTL= VV * GVTL *(-AO(2))
      HTD= VV * GSHT * (CDOT + CDIT * AO(1)**2.)
      VTD= VV * GSVT * (CDOT + CDIT * AO(2)**2.)
      HTM= VV * GHTM * AO(1)
      VTM= VV * GVTM *(-AO(2))
      TAUCOS= COS(AO(6))
      DELCOS= COS(AO(8))
      BETCOS= COS(AO(2))
      ALPCOS= COS(AO(1))
      ALPSIN= SIN(AO(1))
      BETSIN= SIN(AO(2))
      SUMFZ= ALA+ALQ+HTL+THR* TAUCOS   *SIN(AO(8)+AO(1))
      SUMFX= THR*COS(AO(6)-AO(2))*COS(AO(8)+AO(1))-ADF-HTD-VTD
      SUMFY= ASR+ASB+VTL+THR* DELCOS   *SIN(AO(6)-AO(2))
      FPM= HTM+(HTD+VTD* BETCOS ) * (HZ* ALPCOS   -ELT* ALPSIN ) -HTL*
     A(ELT * ALPCOS  +HZ* ALPSIN )
      FYM= ELT*(-VTL* BETCOS +(HTD * ALPCOS + VTD)* BETSIN) + VTM
      ZMOM= AYMR+AYMB+FYM-THR* DELCOS * SIN(AO(6)) * ELG
      YMOM= FPM + APMA +APMQ -HZ* ALPSIN *(ALA+ALQ) -B*HZ*SIN(AO(7))
     1+ADF*  HZ* ALPCOS -THR* TAUCOS*( HZ* DELCOS + ELG*SIN(AO(8)))
      IF(ITEST-1) 17,14,17
   14 IF(LOOP-L) 17,15,17
   15 WRITE(3,16)
   16 FORMAT (//21X,3HALA,7X,3HALQ,7X,3HADF,7X,4HAPMA,6X,4HAPMQ,6X,3HASB
     1,7X,3HASR,7X,4HAYMB/21X,4HAYMR,6X,3HHTL,7X,3HVTL,7X,3HHTD,7X,3HVTD
     2,7X,3HHTM,7X,3HVTM,7X,5HSUMFZ/21X,5HSUMFX,5X,5HSUMFY,5X,3HFPM,7X,
     3 3HFYM,7X,4HZMOM,6X,4HYMOM/)
      WRITE(3,*) ALA,ALQ,ADF,APMA,APMQ,ASB,ASR,AYMB,AYMR,HTL,VTL,HTD,VTD
     1,HTM,VTM,SUMFZ,SUMFX,SUMFY,FPM,FYM,ZMOM,YMOM
      LINE= LINE + 9
   17 RETURN
      END
```

000 TOTAL ERRORS FOR THIS COMPILATION
OL103 I TOTAL NUMBER OF LIBRARY SECTORS REQUIRED IS 13
NAME-FORCE ,PACK-FORTR2,UNIT-RI,RETAIN-T,LIBRARY-R,CATEGORY-020

CONDITION 6,RUN 1 -- INITAL YAW ANGLE = 3 DEG ** FEEDBACK CONTROL

INPUT HEADING= 0.00 TRIM PITCH ANGLE= 0.00

GIMBAL RATE= 3.00 DEG/SEC

PITCH ERROR GAIN= 1.00 PITCH RATE GAIN= 1.00
YAW ERROR GAIN= 1.00 YAW RATE GAIN= 1.00

DIFFERENTIAL TIME INCREMENT= 0.20

INITIAL VELOCITY= 7.78
THRUST= 122.70

BALLON PARAMETERS FOR DYNAMIC EQUATIONS--

XMASS= 0.2407300E+04
YMASS= 0.4121102E+04
ZMASS= 0.4121102E+04
IYY= 0.2680000E+07
IZZ= 0.2680000E+07

TIME	THETA	ALPHA	DELTA	PSI	BETA	TAU	VEL
2.00015	0.00053	-0.00195	0.00098	2.99177	-2.71953	2.98094	7.77785
4.00030	0.00152	-0.00614	0.00202	2.96170	-2.47816	2.94371	7.77616
6.00045	0.00243	-0.00957	0.00283	2.92292	-2.31244	2.90259	7.77481
8.00061	0.00312	-0.01161	0.00341	2.88150	-2.18200	2.86059	7.77369
10.00076	0.00359	-0.01238	0.00378	2.83965	-2.07121	2.81878	7.77275
12.00091	0.00388	-0.01220	0.00398	2.79815	-1.97359	2.77754	7.77196
14.00106	0.00401	-0.01133	0.00404	2.75725	-1.88610	2.73697	7.77129
16.00121	0.00402	-0.01001	0.00400	2.71704	-1.80704	2.69711	7.77073
18.00133	0.00394	-0.00843	0.00388	2.67752	-1.73526	2.65793	7.77026
20.00145	0.00379	-0.00673	0.00370	2.63868	-1.66988	2.61942	7.76988
22.00157	0.00359	-0.00500	0.00347	2.60050	-1.61014	2.58157	7.76957
24.00169	0.00335	-0.00332	0.00322	2.56296	-1.55543	2.54434	7.76932
26.00182	0.00308	-0.00173	0.00294	2.52603	-1.50519	2.50773	7.76912
28.00194	0.00280	-0.00027	0.00266	2.48971	-1.45891	2.47170	7.76898
30.00206	0.00251	0.00105	0.00237	2.45397	-1.41618	2.43625	7.76888
32.00218	0.00222	0.00221	0.00208	2.41880	-1.37660	2.40136	7.76881
34.00230	0.00193	0.00322	0.00179	2.38413	-1.33984	2.36701	7.76879
36.00243	0.00165	0.00408	0.00151	2.35010	-1.30559	2.33319	7.76879
38.00255	0.00138	0.00479	0.00124	2.31654	-1.27359	2.29989	7.76882
40.00267	0.00111	0.00536	0.00098	2.28349	-1.24361	2.26709	7.76888
42.00279	0.00086	0.00581	0.00074	2.25094	-1.21543	2.23479	7.76897
44.00291	0.00062	0.00615	0.00050	2.21839	-1.18887	2.20298	7.76907
46.00304	0.00039	0.00639	0.00028	2.18731	-1.16376	2.17164	7.76919
48.00316	0.00018	0.00655	0.00008	2.15620	-1.13996	2.14077	7.76933
50.00328	-0.00002	0.00662	-0.00012	2.12556	-1.11734	2.11035	7.76949
52.00340	-0.00021	0.00663	-0.00030	2.09536	-1.09578	2.08038	7.76966
54.00352	-0.00038	0.00658	-0.00047	2.06561	-1.07519	2.05084	7.76984
56.00365	-0.00055	0.00649	-0.00062	2.03629	-1.05547	2.02174	7.77004
58.00377	-0.00070	0.00635	-0.00077	2.00741	-1.03655	1.99307	7.77025
60.00389	-0.00084	0.00619	-0.00091	1.97494	-1.01835	1.96481	7.77047
62.00401	-0.00097	0.00600	-0.00103	1.95038	-1.00081	1.93696	7.77069
64.00414	-0.00109	0.00579	-0.00115	1.92323	-0.98387	1.90951	7.77093
66.00426	-0.00120	0.00556	-0.00126	1.89598	-0.96749	1.88246	7.77118
68.00438	-0.00130	0.00533	-0.00135	1.86913	-0.95162	1.85579	7.77143
70.00450	-0.00140	0.00509	-0.00145	1.84265	-0.93622	1.82952	7.77169
72.00462	-0.00149	0.00485	-0.00153	1.81656	-0.92125	1.80361	7.77196
74.00475	-0.00157	0.00461	-0.00161	1.79085	-0.90669	1.77808	7.77223
76.00487	-0.00164	0.00437	-0.00168	1.76550	-0.89251	1.75292	7.77251
78.00499	-0.00171	0.00413	-0.00174	1.74052	-0.87867	1.72812	7.77279
80.00511	-0.00177	0.00390	-0.00180	1.71589	-0.86517	1.70367	7.77308

TIME	THETA	ALPHA	DELTA	PSI	BETA	TAU	VEL
82.00523	-0.00183	0.00368	-0.00186	1.69162	-0.85197	1.67957	7.77337
84.00536	-0.00188	0.00346	-0.00191	1.66769	-0.83907	1.65581	7.77367
86.00548	-0.00193	0.00325	-0.00195	1.64410	-0.82644	1.63239	7.77397
88.00560	-0.00197	0.00305	-0.00199	1.62085	-0.81407	1.60931	7.77428
90.00572	-0.00201	0.00285	-0.00203	1.59793	-0.80195	1.58656	7.77458
92.00584	-0.00205	0.00267	-0.00207	1.57534	-0.79006	1.56413	7.77489
94.00597	-0.00208	0.00250	-0.00210	1.55307	-0.77840	1.54201	7.77520
96.00609	-0.00211	0.00233	-0.00213	1.53111	-0.76695	1.52022	7.77552
98.00621	-0.00214	0.00217	-0.00215	1.50947	-0.75571	1.49873	7.77583
100.00633	-0.00217	0.00202	-0.00218	1.48814	-0.74467	1.47755	7.77615
102.00645	-0.00219	0.00188	-0.00220	1.46711	-0.73382	1.45667	7.77647
104.00658	-0.00221	0.00175	-0.00222	1.44633	-0.72315	1.43608	7.77680
106.00670	-0.00223	0.00162	-0.00223	1.42594	-0.71266	1.41579	7.77712
108.00682	-0.00224	0.00150	-0.00225	1.40579	-0.70235	1.39579	7.77744
110.00694	-0.00226	0.00139	-0.00226	1.38593	-0.69220	1.37607	7.77777
112.00706	-0.00227	0.00128	-0.00227	1.36635	-0.68222	1.35663	7.77809
114.00719	-0.00228	0.00118	-0.00228	1.34705	-0.67239	1.33747	7.77842
116.00731	-0.00229	0.00109	-0.00229	1.32802	-0.66272	1.31858	7.77874
118.00743	-0.00229	0.00100	-0.00230	1.30927	-0.65320	1.29995	7.77907
120.00755	-0.00230	0.00092	-0.00230	1.29077	-0.64383	1.28159	7.77939
122.00768	-0.00231	0.00084	-0.00231	1.27254	-0.63460	1.26349	7.77971
124.00780	-0.00231	0.00077	-0.00231	1.25457	-0.62551	1.24565	7.78004
126.00792	-0.00231	0.00070	-0.00231	1.23685	-0.61656	1.22806	7.78036
128.00804	-0.00231	0.00064	-0.00232	1.21939	-0.60774	1.21072	7.78069
130.00816	-0.00232	0.00058	-0.00232	1.20218	-0.59905	1.19363	7.78101
132.00829	-0.00232	0.00052	-0.00231	1.18520	-0.59050	1.17678	7.78134
134.00841	-0.00231	0.00046	-0.00231	1.16847	-0.58207	1.16016	7.78166
136.00853	-0.00231	0.00041	-0.00231	1.15197	-0.57376	1.14379	7.78198
138.00865	-0.00231	0.00037	-0.00231	1.13571	-0.56558	1.12764	7.78231
140.00877	-0.00231	0.00032	-0.00230	1.11968	-0.55752	1.11172	7.78263
142.00890	-0.00230	0.00028	-0.00230	1.10388	-0.54957	1.09603	7.78296
144.00902	-0.00230	0.00024	-0.00229	1.08829	-0.54174	1.08056	7.78328
146.00914	-0.00229	0.00020	-0.00229	1.07294	-0.53403	1.06531	7.78360
148.00926	-0.00228	0.00016	-0.00228	1.05779	-0.52643	1.05028	7.78391
150.00938	-0.00228	0.00013	-0.00227	1.04286	-0.51894	1.03545	7.78423
152.00951	-0.00227	0.00009	-0.00227	1.02815	-0.51155	1.02084	7.78454
154.00963	-0.00226	0.00006	-0.00226	1.01364	-0.50427	1.00644	7.78486
156.00975	-0.00225	0.00003	-0.00225	0.99934	-0.49710	0.99224	7.78517
158.00987	-0.00225	0.00000	-0.00224	0.98524	-0.49003	0.97824	7.78549
160.00999	-0.00224	-0.00002	-0.00223	0.97134	-0.48307	0.96444	7.78579

TIME	THETA	ALPHA	DELTA	PSI	BETA	TAU	VEL
162.01012	-0.00223	-0.00005	-0.00222	0.95763	-0.47620	0.95083	7.78610
164.01024	-0.00222	-0.00007	-0.00221	0.94412	-0.46943	0.93742	7.78640
166.01036	-0.00221	-0.00009	-0.00220	0.93080	-0.46276	0.92419	7.78671
168.01048	-0.00219	-0.00011	-0.00219	0.91767	-0.45619	0.91115	7.78701
170.01060	-0.00218	-0.00014	-0.00218	0.90475	-0.44971	0.89830	7.78731
172.01073	-0.00217	-0.00015	-0.00217	0.89197	-0.44332	0.88563	7.78761
174.01085	-0.00216	-0.00017	-0.00215	0.87939	-0.43702	0.87314	7.78791
176.01097	-0.00215	-0.00019	-0.00214	0.86693	-0.43082	0.86083	7.78820
178.01109	-0.00213	-0.00021	-0.00213	0.85475	-0.42470	0.84868	7.78850
180.01122	-0.00212	-0.00022	-0.00212	0.84270	-0.41867	0.83672	7.78879

CONDITION 10,RUN 1 -- 15 DEGREE HEADING CHANGE

INPUT HEADING= 15.00   TRIM PITCH ANGLE= 0.00

GIMBAL RATE= 3.00 DEG/SEC

PITCH ERROR GAIN= 1.00   PITCH RATE GAIN= 1.00
YAW ERROR GAIN= 1.00   YAW RATE GAIN= 1.00

DIFFERENTIAL TIME INCREMENT= 0.20

INITIAL VELOCITY= 7.78
THRUST= 122.70

BALLON PARAMETERS FOR DYNAMIC EQUATIONS--

XMASS= 0.24073000E+04
YMASS= 0.41211102E+04
ZMASS= 0.41211102E+04
IYY= 0.26800000E+07
IZZ= 0.26800000E+07

TIME	THETA	ALPHA	DELTA	PSI	BETA	TAU	VEL
2.00015	-0.00011	0.00042	-0.00020	0.00757	0.00533	-5.99999	7.78039
4.00030	-0.00022	0.00095	-0.00021	0.05339	0.14480	-11.99997	7.78023
6.00045	0.00007	-0.00022	0.00035	0.17312	0.51280	-14.75432	7.77909
8.00061	0.00078	-0.00327	0.00120	0.33507	1.05834	-14.57794	7.77757
10.00076	0.00171	-0.00696	0.00272	0.51494	1.62624	-14.39306	7.77565
12.00091	0.00283	-0.01104	0.00344	0.70078	2.15353	-14.20571	7.77316
14.00106	0.00418	-0.01564	0.00492	0.86813	2.62304	-14.01815	7.77001
16.00121	0.00580	-0.02086	0.00668	1.07530	3.03371	-13.83129	7.76620
18.00133	0.00768	-0.02663	0.00869	1.26162	3.36979	-13.64548	7.76172
20.00145	0.00981	-0.03279	0.01092	1.44631	3.69687	-13.46091	7.75663
22.00157	0.01213	-0.03908	0.01333	1.63070	3.96054	-13.27769	7.75098
24.00169	0.01458	-0.04525	0.01584	1.81320	4.18591	-13.09590	7.74485
26.00182	0.01712	-0.05104	0.01840	1.99423	4.37757	-12.91562	7.73829
28.00194	0.01968	-0.05624	0.02095	2.17373	4.53954	-12.73691	7.73140
30.00206	0.02220	-0.06068	0.02345	2.35163	4.67537	-12.55981	7.72422
32.00218	0.02465	-0.06423	0.02584	2.52789	4.78816	-12.38440	7.71683
34.00230	0.02697	-0.06683	0.02809	2.70244	4.88062	-12.21072	7.70929
36.00243	0.02914	-0.06843	0.03018	2.87524	4.95515	-12.03880	7.70166
38.00255	0.03112	-0.06905	0.03206	3.04625	5.01383	-11.86869	7.69397
40.00267	0.03291	-0.06870	0.03375	3.21544	5.05853	-11.70042	7.68628
42.00279	0.03448	-0.06746	0.03521	3.38277	5.09085	-11.53402	7.67862
44.00291	0.03583	-0.06540	0.03645	3.54822	5.11224	-11.36952	7.67103
46.00304	0.03695	-0.06260	0.03746	3.71175	5.12398	-11.20695	7.66355
48.00316	0.03786	-0.05916	0.03825	3.87336	5.12716	-11.04631	7.65619
50.00328	0.03854	-0.05517	0.03883	4.03303	5.12280	-10.88761	7.64897
52.00340	0.03901	-0.05074	0.03920	4.19075	5.11177	-10.73086	7.64192
54.00352	0.03929	-0.04596	0.03937	4.34651	5.09485	-10.57608	7.63506
56.00365	0.03937	-0.04093	0.03936	4.50032	5.07273	-10.42325	7.62839
58.00377	0.03927	-0.03572	0.03918	4.65216	5.04604	-10.27239	7.62193
60.00389	0.03901	-0.03041	0.03884	4.80205	5.01532	-10.12348	7.61568
62.00401	0.03860	-0.02509	0.03836	4.94998	4.98106	-9.97653	7.60965
64.00414	0.03805	-0.01980	0.03774	5.09596	4.94370	-9.83153	7.60385
66.00426	0.03738	-0.01461	0.03701	5.23999	4.90362	-9.68846	7.59827
68.00438	0.03660	-0.00956	0.03618	5.38209	4.86119	-9.54732	7.59293
70.00450	0.03572	-0.00469	0.03526	5.52227	4.81670	-9.40811	7.58782
72.00462	0.03475	-0.00004	0.03425	5.66054	4.77044	-9.27079	7.58294
74.00475	0.03372	0.00437	0.03318	5.79691	4.72266	-9.13537	7.57829
76.00487	0.03262	0.00853	0.03205	5.93139	4.67357	-9.00182	7.57387
78.00499	0.03146	0.01241	0.03088	6.06401	4.62338	-8.87013	7.56968
80.00511	0.03027	0.01601	0.02967	6.19478	4.57227	-8.74028	7.56571

TIME	THETA	ALPHA	DELTA	PSI	BETA	TAU	VEL
82.00523	0.02905	0.01933	0.02443	6.32371	4.52040	-8.61227	7.56196
84.00536	0.02779	0.02235	0.02716	6.45032	4.46790	-8.48606	7.55842
86.00548	0.02652	0.02510	0.02589	6.57613	4.41493	-8.36164	7.55510
88.00560	0.02524	0.02756	0.02460	6.69966	4.36158	-8.23900	7.55199
90.00572	0.02396	0.02976	0.02332	6.82143	4.30796	-8.11810	7.54907
92.00584	0.02267	0.03169	0.02203	6.94146	4.25417	-7.99895	7.54636
94.00597	0.02139	0.03337	0.02075	7.05976	4.20028	-7.88150	7.54384
96.00609	0.02012	0.03481	0.01949	7.17637	4.14636	-7.76574	7.54151
98.00621	0.01886	0.03603	0.01824	7.29128	4.09251	-7.65167	7.53936
100.00633	0.01762	0.03703	0.01701	7.40452	4.03878	-7.53925	7.53739
102.00645	0.01640	0.03784	0.01579	7.51612	3.98521	-7.42847	7.53559
104.00658	0.01520	0.03845	0.01460	7.62610	3.93185	-7.31929	7.53396
106.00670	0.01402	0.03890	0.01343	7.73447	3.87875	-7.21172	7.53249
108.00682	0.01286	0.03919	0.01229	7.84127	3.82594	-7.10571	7.53117
110.00694	0.01174	0.03933	0.01118	7.94650	3.77346	-7.00126	7.53001
112.00706	0.01064	0.03934	0.01009	8.05018	3.72135	-6.89834	7.52900
114.00719	0.00957	0.03923	0.00904	8.15235	3.66963	-6.79694	7.52813
116.00731	0.00852	0.03901	0.00801	8.25301	3.61832	-6.69702	7.52740
118.00743	0.00751	0.03870	0.00701	8.35219	3.56744	-6.59858	7.52680
120.00755	0.00653	0.03829	0.00604	8.44990	3.51703	-6.50158	7.52633
122.00768	0.00557	0.03781	0.00510	8.54618	3.46708	-6.40603	7.52598
124.00780	0.00465	0.03726	0.00419	8.64103	3.41762	-6.31188	7.52575
126.00792	0.00376	0.03665	0.00332	8.73448	3.36867	-6.21913	7.52564
128.00804	0.00289	0.03598	0.00247	8.82655	3.32021	-6.12775	7.52563
130.00816	0.00206	0.03528	0.00165	8.91725	3.27228	-6.03772	7.52574
132.00829	0.00125	0.03453	0.00086	9.00661	3.22488	-5.94903	7.52594
134.00841	0.00048	0.03375	0.00009	9.09464	3.17802	-5.86166	7.52624
136.00853	-0.00027	0.03295	-0.00064	9.18136	3.13169	-5.77559	7.52664
138.00865	-0.00099	0.03213	-0.00135	9.26680	3.08591	-5.69079	7.52712
140.00877	-0.00169	0.03129	-0.00203	9.35097	3.04068	-5.60725	7.52769
142.00890	-0.00235	0.03044	-0.00268	9.43388	2.99602	-5.52496	7.52835
144.00902	-0.00299	0.02958	-0.00331	9.51556	2.95190	-5.44389	7.52908
146.00914	-0.00361	0.02871	-0.00391	9.59602	2.90834	-5.36404	7.52989
148.00926	-0.00420	0.02785	-0.00449	9.67528	2.86532	-5.28537	7.53078
150.00938	-0.00476	0.02698	-0.00504	9.75337	2.82287	-5.20787	7.53173
152.00951	-0.00531	0.02612	-0.00557	9.83029	2.78096	-5.13152	7.53275
154.00963	-0.00582	0.02527	-0.00608	9.90606	2.73962	-5.05632	7.53383
156.00975	-0.00632	0.02442	-0.00656	9.98071	2.69882	-4.98224	7.53497
158.00987	-0.00679	0.02358	-0.00703	10.05424	2.65857	-4.90926	7.53617
160.00999	-0.00725	0.02275	-0.00747	10.12657	2.61836	-4.83736	7.53742

TIME	THETA	ALPHA	DELTA	PSI	BETA	TAU	VEL
162.01012	-0.00768	0.02194	-0.00789	10.19803	2.57970	-4.76655	7.53873
164.01024	-0.00809	0.02114	-0.00879	10.26832	2.54108	-4.69678	7.54008
166.01036	-0.00849	0.02035	-0.00868	10.33756	2.50300	-4.62806	7.54148
168.01048	-0.00886	0.01958	-0.00904	10.40578	2.46544	-4.56036	7.54293
170.01060	-0.00922	0.01883	-0.00939	10.47297	2.42843	-4.49367	7.54442
172.01073	-0.00955	0.01809	-0.00972	10.53916	2.39193	-4.42798	7.54595
174.01085	-0.00988	0.01736	-0.01003	10.60436	2.35595	-4.36326	7.54751
176.01097	-0.01018	0.01666	-0.01033	10.66860	2.32049	-4.29951	7.54912
178.01109	-0.01047	0.01597	-0.01061	10.73187	2.28554	-4.23671	7.55075
180.01122	-0.01074	0.01530	-0.01087	10.79420	2.25109	-4.17485	7.55242